REPUBLIQUE DU CAMEROUN
****
UNIVERSITE DE YAOUNDE I
****
FACULTE DES SCIENCES
****
CENTRE DE RECHERCHE ET DE FORMATION DOCTORALE EN SCIENCES TECHNOLOGIE ET GEOSCIENCES
****
UNITE DE RECHERCHE ET DE FORMATION DOCTORALE EN PHYSIQUES ET APPLICATIONS
****
DEPARTEMENT DE PHYSIQUE

REPUBLIC OF CAMEROON
****
THE UNIVERSITY OF YAOUNDE I
****
FACULTY OF SCIENCES
****
POSTGRADUATE SCHOOL OF SCIENCE, TECHNOLOGY AND GEOSCIENCES
****
RESEARCH AND POSTGRADUATE TRAINING UNIT FOR PHYSICS AND APPLICATIONS
****
DEPARTMENT OF PHYSICS

LABORATOIRE DE MECANIQUE, MATERIAUX ET STRUCTURES
LABORATORY OF MECHANICS, MATERIALS AND STRUCTURES

ON VIBRATION ANALYSIS AND CONTROL OF STRUCTURES SUBJECTED TO COMBINED ACTION OF THERMAL AND MECHANICAL LOADS

Thesis submitted and defended in partial fulfillment of the requirements for the award of degree of Doctor of Philosophy (Ph.D.) in Physics.

Specialty: **Mechanics, Materials and Structures**

By

DJUITCHOU YALEU Thomas Bell
Registration number: ***08W0138***
Master of Science in Physics
Option: **Fundamental Mechanics and Complex Systems**

Supervised by :

NANA NBENDJO Blaise Roméo
Professor
University of Yaoundé I

WOAFO Paul
Professor
University of Yaoundé I

UNIVERSITE DE YAOUNDE I
UNIVERSITY OF YAOUNDE I

FACULTE DES SCIENCES
FACULTY OF SCIENCE

DEPARTEMENT DE PHYSIQUE
DEPARTMENT OF PHYSICS

ATTESTATION DE CORRECTION DE LA THESE DE DOCTORAT/Ph.D

Nous, Professeur **DJUIDJE KENMOE Germaine** et Professeur **TCHAWOUA Clément**, respectivement Examinateur et Président du jury de la thèse de Doctorat/Ph.D de Monsieur **DJUITCHOU YALEU Thomas Bell,** Matricule **08W0138**, préparée sous la Co-direction du Professeur **NANA NBENDJO Blaise Roméo** et du Professeur **WOAFO Paul,** intitulée : «**ON VIBRATION ANALYSIS AND CONTROL OF STRUCTURES SUBJECTED TO COMBINED ACTION OF THERMAL AND MECHANICAL LOADS**», soutenue le **Mercredi, 31 Mai 2023**, en vue de l'obtention du grade de Docteur/Ph.D en Physique, Spécialité **Mécanique, Matériaux et Structures**, option **Mécanique Fondamentale et Systèmes Complexes** attestons que toutes les corrections demandées par le Jury de soutenance ont été effectuées.

En foi de quoi, la présente attestation lui est délivrée pour servir et valoir ce que de droit.

Fait à Yaoundé, le ...13 JUIN 2023.....

Examinateur	Président du jury	Le Chef du Département de Physique
Pr. DJUIDJE KENMOE Germaine	Pr. TCHAWOUA Clément	Pr. NDJAKA Jean-Marie Bienvenu

UNIVERSITE DE YAOUNDE I * FACULTE DES SCIENCES * Le Chef de Département DEPARTEMENT DE PHYSIQUE

DEPARTMENT OF PHYSICS

On vibration analysis and control of structures subjected to combined action of thermal and mechanical loads

Thesis

Submitted and defended for the award of

Doctorat/ PhD in Physics

Specialty: **Mechanics, materials and structures**

Option: **Fundamental mechanics and complex systems**

DJUITCHOU YALEU Thomas Bell

Registration Number: **08W0138**

Email adress: thomasbelld@yahoo.fr

Master degree in Physics

Supervised by:

NANA NBENDJO Blaise Roméo
Professor

WOAFO Paul
Professor

Year 2023

Contents

List of Figures

List of Tables

List of abbreviations

PVC: Passive vibration control

AVC: Active vibration control

HVC: Hybrid vibration control

SAVC: Semi-Active vibration control

HSLDS: High Static Low Dynamic Stiffness

HSLDS-AS: High Static Low Dynamic Stiffness with Auxiliary system

QZS: Quasi Zero Stiffness

PDE(s): Partial Differential Equation(s)

SDE(s): System of Differential Equation(s)

ODE(s): Ordinary Differential Equation(s)

HBM: Harmonic Balance Method

RK4: Fourth order Runge Kutta

ABM: Adam Baschford Method

dB: decibel

Dedications

I dedicate this work:

To the **Almighty God**, the Father of Beauties, the Beloved Son and the Holy One, always loving, living and laboring.

To my lovely mother **Yaleu Pauline, my wife and children** whose unconditional loves, supports, payers, encouragements and patience have permitted me to end these research works.

To my "Father" **Reverend Pastor NGASSAM Jérémie**, my sisters and brothers **DAPET Edith**, **NGASSAM Sara**, **MBAKOP Jean** and **KAMCHUMEN Luc**. Thanks for your al time encouragement, support, sincere kindness and prayers.

"I can do all things through who strengthens me". **Philipians 4: 13**

In the memory of:

- My late father, **Mr YALEU David**. Daddy, you founded a family but did not have the opportunity to watch it grow on Earth. Besides God, keep looking after us.
- My late elder brothers and sister, **CHOUKWI YALEU Bérard**, **MBATCHOU YALEU Françis** and , **KOUNDJOU YALEU Christine** who left us early without strength when we were in moments of weakness; your courage and determination in work are a strength for me. May the Almighty allows us to keep a memory of you in our heart.

Acknowledgements

This thesis is the fruit of several supports of special persons, and I will take this occasion to give them few words. I would like to address my very king gratitude:

- To Prof. **NANA NBENDJO Blaise Roméo**, Director of this thesis, whose vigor in work, know-how and cordiality have inspired me throughout this work, for his multiform support scientifically, materially and morally. Dear Prof receive the expression of my deep and sincere gratitude and proof that your efforts have not been in vain since the Master degree up till to now.

- To Prof. **WOAFO Paul** for his urging follow-up during my research studies with this other work as fruit that adds to the Master degree of few years ago.

- To Prof. **NDJAKA Jean-Marie Bienvenu**, the Head of Department of Physics, for the teachings, advices and encouragements that he gave to me during the academic cycles of Master and Doctorate/PhD.

- To All the jury members for the time that they give to evaluate this work and for all their remarks to render it.
  -Prof. **TCHAWOUA Clément**
  -Prof. **WOAFO Paul**
  -Prof. **NANA NBENDJO Blaise Roméo**
  -Prof. **DJUIDJE KENMOE Germaine**
  -Prof. **YAMAPI Réné**
  -Prof. **VONDOU Derbetini Appolinaire**
  -Prof. **EYEBE FOUDA Jean Sire**

- To Prof. **KOFANE Timoléon Crépin** whose the fruitful advices and valuable teaching during courses in nonlinear physics and in the research has been very beneficial for me in my work.

- To Prof. **TCHAWOUA Clément** for his quite beneficial courses in vibration and elasticity .

- To All the teaching staff and personnel of the Department of Physics, Faculty of Science, University of Yaoundé I, for their valuable teaching and their fruitful advices.

- To my elders and mates **Dr NANA Bonaventure**, the late **Dr MBOUSSI Aïssatou**, **Dr ABOBDA Lejuste**, **Dr METSEBO Jules**, **Dr TCHAKUI Murielle**, **Dr NDEMANOU Peggy**, **Dr ANAGUE Merveil**, **Dr MBA Clori-ant**, **Dr SONFACK Hervé**, **Dr KOUNGAN Willy Magloire**, **Dr FANKEM Eliane Raïssa**, **Dr PIEDJOU Alex**, **Dr YOUTHA Octave**, **Dr NGOUNOU Armel**, **MOKOLA Dalahaï**, **KENTSA Bill Steven**, **AZEGHAP SIMO Ibrahim**, and all the others, thank for your inspiring life experiences.

- To My "parents" **LIADJI Bibiane** and **LIADJI Thomas** for their full love.

- To Rev. **Pastor FETZEU Henock**, Rev. **Pastor DJOMO Christian**, **Miss and Mrs TCHATCHOUA**, **Mrs TOUKAM Roland**, **Mrs ARREY Valentine**, **Mrs MAKALA Maxime**, and **Mrs NGANKONG Ulrich**, thanks for their love and trust.

- To the General Director of MaKo industries M. **KOUATCHOU Gide**, for his full love, trust and support.

- To that particular group of special persons on which I am extremely happy to be a member of. I think of **YMCA Oyom-Abang, YMCA Mbalmayo, Groupe Unité, AARUO Oyom-ABang, LA RELEVE**, thank you for your support.

- To all my parents, uncles, aunts, brothers, sisters, nephews, nieces, friends those whose names have not been mentioned here, those reading this work for their active support.

Please, receive all of you moreover, my gratefulness for this achievement, your achievement for you guide me unconditionally with love and I will respond also with unconditional and pure love.

Abstract

This thesis describes the analysis of the dynamic response of structures, when they are subjected to the combined action of thermal loads (resulting from temperature variations) and mobile loads or turbulent wind.

The structures studied in this work are bridge models modeled as simply supported Euler Bernoulli beams. Appropriate numerical and analytical tools are used to analyze and characterize the response of these structures. For a good understanding, analysis and explanation of the combined effect of thermal and mechanical loads, two assumptions are taken into account, namely: nonlinear and linear temperature variations.

In the first assumption, we studied a beam simply supported and suspended by inextensible cables. The modeled structure is subjected to the action of a convoy of moving loads and turbulent wind loads. The material constituting the structure is viscoelastic possessing the memory effect modeled by means of fractional derivative orders. Then, the conditions of stability and appearance of various types of bifurcation are clearly established according to the properties of the material, the thermal conditions and the parameters of the mechanical loads.

In the second assumption, a structure modeled by a beam controlled by the isolator HSLDS-AS, is considered. This structure is subjected to the action of a moving force and the thermal loads resulting from temperature variations. Optimal performance conditions (based on the study of frequencies, transmissibility and vibration amplitude) of the system are established. Similarly, the effects of temperature variations on the dynamic behavior of the structure are clearly established.

Keywords: Temperature, thermal loads, wind, turbulence, beam, moving loads, fractional derivative order, bifurcation, transmissibility and vibration control.

Résumé

Cette thèse décrit l'analyse de la réponse dynamique des structures, lorsqu'elles sont soumises à l'action combinée, des charges thermiques (résultantes des variations de la température) et des charges mobiles ou du vent turbulent. Les structures étudiées dans ce travail, sont des modèles de pont modélisés comme des poutres d'Euler Bernoulli simplement supportée. Les outils numériques et analytiques appropriés sont utilisés pour analyser et caractériser la réponse de ces structures. Pour une bonne compréhension, analyse et explication de l'effet combiné des charges thermiques et mécaniques, deux suppositions sont prises en compte, à savoir : les variations non linéaires et linéaires de la température.

Dans la première supposition, nous avons étudié une poutre simplement supportée et suspendue par des câbles inextensibles. La structure modélisée est soumise à l'action d'un convoi de charges mobiles et des charges du vent turbulent. Le matériau constituant la structure est viscoélastique possédant l'effet mémoire, et modélisé par le biais des dérivées d'ordres fractionnaires. Alors, les conditions de stabilité et d'apparition de divers types de bifurcation sont clairement établies en fonction des propriétés du matériau, des conditions thermiques et des paramètres des charges mécaniques.

Dans la deuxième supposition, une structure modélisée par une poutre simplement supportée et contrôlée par l'isolateur HSLDS-AS, est considérée. Cette structure est soumise à l'action d'une force mobile et des charges thermiques résultantes des variations de la température. Les conditions de performance optimale (basées sur l'étude de la fréquences, de la transmissibilité et de l'amplitude de vibration) du système sont établies. De même, les effets des variations de la température sur le comportement dynamique de la structure sont clairement établis.

Mots-clés: Température, charges thermiques, vent, turbulence, poutre, charges mobiles, dérivation d'ordre fractionnaire, bifurcation, transmissibilité et contrôle des vibrations

General Introduction

Nowadays, spectacular industrial revolution and construction of infrastructures are the ways for developing countries. Civil and mechanical engineering are main disciplines to achieve these objectives. Many researches have been devoted to these fields of research and some of their results have improved the technology used today. In past decades, we met with new phenomenon related to environmental changes called global warming; then, it is observed rise in the average temperature of the climate system and its related effect. The primary effects as higher wind as well as secondary effects as deterioration and corrosion, the changes in type of load at structures induced by rising sea level or variation of temperature through cross section. Researcher and engineers play a major role in the mitigation and adaptation to climate change in terms of research. Development of improved practices and standards, and education of future engineers is very urgent [1–3].
Follow above mentioned assumption, it is well known that materials behaviour changes with temperature variations. The increase of temperature creates an expansion of material and in the same manner the decrease of temperature creates contraction. Daily and seasonal changes in shade air temperature, solar radiation, re-radiation, wind speed, longwave radiation will result in variations of the temperature distribution within individual elements of a structure [4]. The temperature effect will cause strain (expansion or/and contraction) and therefore stresses into the structure which are dependent on geometry, boundary conditions and on physical properties of the material. This effect is also important when material with different coefficient of expansion are used compositely, which can leads to transversal growth of the stresses. In other part, the rapid advances in the field of high performance materials and construction techniques, the bridges are evolving towards long and flexible structures as those of the high-rise buildings. The inclusion of modern materials (heditary material, composite materials,Traffic, etc.) also results in a new generation of lightweight structures which are utterly susceptible to the action of wind. During the last two centuries, major structural failures due to the wind action has occurred and has provoked much interest in wind loadings by engineers. Long-span bridges have often produced the most dramatic failures, such as the Brighton Chain Pier Bridge in England in 1836, the Tay Bridge in Scotland in 1879, and the Tacoma Narrows Bridge in Washington State in 1940. In particular, the failure of the Tacoma Bridge has pushed engineers to conduct various scientific investigations on bridge aerodynamics [4,5]. While flutter may result in dynamic instability and the collapse of the whole structures, large buffeting amplitude may cause serious fatigue damage to structural members or noticeable serviceability problems. Moreover, there are not only loads dues to climate

change, structures are often subjected to another significant mechanical loads as dead, service loads and other accidental loads. These previous major loads (service loads and accidental loads) may cause global failure of the structure, thus control system sis required. Nevertheless the control of vibrations can also be done by looking the interaction between the parts of the system, the external excitation and the structure to be control or the interaction between the external sources [6–9]. Some precautions are taken upstream, during the construction of some mechanical structure precisely in seismic regions in order to prevent catastrophe [10]. Recently, some works treating the problem of vibration control have been published in order to ameliorate the previous ones. They usually focus on some situations faced in agriculture [6, 7], in civil engineering [8], and all the external excitations are often assumed to be sinusoidal.

From above explanations, concurrent action of thermal and mechanicals loads are often neglected in vibratory analysis of structures, although this topic is a fascinating subject as well for scientists than for engineers. Nowadays thermomechanical analysis become more important and research in this research field are intensive. Thus, the present thesis is an extension of the previous ones [11] to the case of thermomechanical structures coupled through it environment. The case of interest in this thesis is to consider the combined action of thermal loads, of moving loads or turbulent wind loads on the dynamics behaviour of controlled or uncontrolled structures. We attempt to solve the following problems :

• The modelling of structures under thermal ad mechanical loadings;

• The analysing of thermal effects on the dynamical response of non controlled or controlled structure subjected to diverse externals loads;

• The analysing taking into account the materials properties, the influence of thermal changes on structural stability.

Thus, the thesis is structure as follow : Chapter 1 presents a brief literature review of the most important aspects related to modelling of the dynamics of structures, mechanical actions on structures and Overviews on structural control systems. This includes specifically the notions on passive base isolation systems modelling. chapter 2 focuses on the different methods used along the thesis to solve the problems presented in chapter 1. Moreover this part present methods for Performance evaluation of isolators. In chapter 3, the results of the mathematical analysis and numerical simulations are presented. Discussion and extension to applications are made. The thesis ends with a general conclusion where the main results obtained are reminded in summary and perspectives for future investigations are suggested.

Chapter I

Literature review

1.1 Introduction

In the fields of mechanical engineering (civil engineering, aerospace, etc.), the world faces a frantic race towards the development and construction of spectacular structures. We often note the remarkable vulnerability of these structures to environmental phenomena and operating loads (wind load, moving loads, thermal loads, earthquakes, etc.). To guarantee their safety, and that of humans, control systems are intensively developed and used to improve the performance of these structures and protect them from accidental phenomena. It is therefore imperative to maintain a technological watch to intensify both analytical and numerical studies in order to assess the response of these structures to the various stresses, and to assess the performance of the control systems used.

In this chapter, a brief review of the literature on the modelling of structures, dynamic loads, control systems and performance evaluation strategic of base isolator are given. In addition, the problems solved in this thesis are presented after which a conclusion is made.

1.2 Dynamics modelling of the structures.

The dynamics of structures, is a recent discipline, which is developing to meet the needs of construction, design and industrial maintenance, it is based on the use of simple models to allow analysis in a fast. These models are three-dimensional deformable solids, with dimensions that are not of the same order of magnitude and that are classified into two main categories :

− Thin structures of which, one dimension (the thickness) is very small compared to the other two(plates or shells);

− Slender structures of which, one dimension (the length) is very large in front of the other two (beam or arch).

In the context of this thesis, the second category is the one that catches our attention, more particularly beams.

1.2.1 Beam model for flexible structure modelling

Beams are very common elements in industrial, civil engineering and mechanical engineering structures. In addition, they can be raw wood, planed wood, cut wood, reinforced concrete, prestressed concrete or steel. For a good understanding of the dynamics, beam theories have been developed in order to facilitate an understanding of the dynamics of

structures (bridges, railroads, tall buildings, etc.). There are four beam modelling theories in the literature, namely [12] : theory of Euler Bernoulli, Rayleigh, with Shear and Timoshenko.

1.2.1.1 Euler Bernoulli Beam model

The Euler-Bernoulli theory for beams, due to its simplicity, and the reasonable results provides, is the most widely used theory in the approximation of beam vibrations [13,14]. However, the Euler or Euler-Bernoulli model tends to slightly overestimate the natural frequencies, a problem which becomes important for the frequencies of higher order modes or when the thickness of the beam is important. This model is therefore suitable for modelling structures so the length is very large in thickness and has been widely used in more engineering problems [6,15]. There are several approaches to derive the equation of the dynamics, in this section the Newtonian approach is used [16]. For this purpose, let us consider a beam of length L, of section A of moment of inertia I. The constituent material of this beam is characterized by a material of Young's modulus E and the mass density ρ. Figure 1.1 gives the diagram of the forces of a beam element in bending.
$V = V(x,t)$ is the shear effort, $M = M(x,t)$ the bending moment, x the coordinate measured along the length of the beam, t the time in second, $W = W(x,t)$ is the transverse displacement of the beam and $f(x,t)$ the external force par unit of length. Considering a

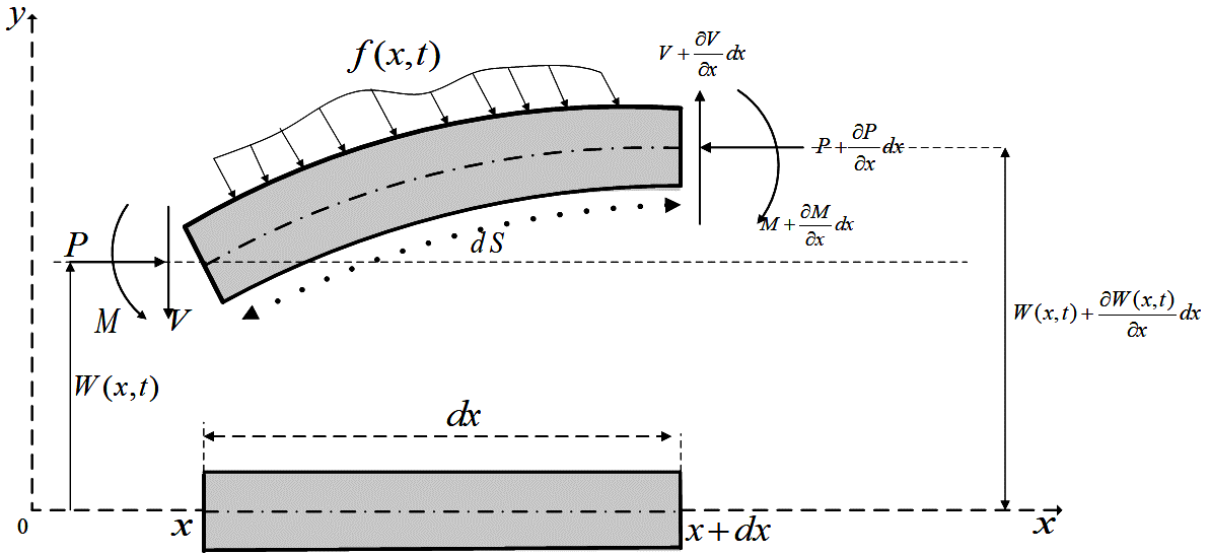

Figure 1.1: Free-body diagram of beam

beam element dx , the balance of moments is translated by

$$M - (M + \frac{\partial M}{\partial x}dx) + V\frac{dx}{2} + (V + \frac{\partial V}{\partial x}dx)\frac{dx}{2} = 0 \tag{1.1}$$

After some manipulations we obtain

$$-\frac{\partial M}{\partial x}dx + Vdx = 0, \tag{1.2}$$

where

$$M = EI\frac{\partial^2 W(x,t)}{\partial x^2}. \tag{1.3}$$

On the other hand,

$$V = \frac{\partial M}{\partial x} = \frac{\partial}{\partial x}\left(EI\frac{\partial^2 W(x,t)}{\partial x^2}\right). \tag{1.4}$$

The balance in the transverse direction is written

$$\rho A\frac{\partial^2 W}{\partial T^2}dX = f(x,t)dx + V - \left(V + \frac{\partial V}{\partial t}dx\right). \tag{1.5}$$

From Eq.1.4 and Eq.1.5 we obtain the equation of the dynamics of Euler Bernoulli derived as

$$\rho A\frac{\partial^2 W(x,t)}{\partial t^2} + EI\frac{\partial^4 W(x,t)}{\partial x^4} = f(x,t). \tag{1.6}$$

Without external load we have

$$\rho A\frac{\partial^2 W(x,t)}{\partial t^2} + EI\frac{\partial^4 W(x,t)}{\partial x^4} = 0. \tag{1.7}$$

The above Eq.1.6 don't take into account many effects whose can appears for certain structures. There are other performed mathematical models.

1.2.1.2 Rayleigh beam model

Lord Rayleigh (1877) brings a first improvement to the classical theory vibration of the beams and achieves, by introducing the effect of the rotation of the sections straight lines (rotational inertia) [17], to partially correct the problem of overestimation of natural frequencies, which despite everything remain overestimated. Taking into account these considerations, the dynamics of the beam is described by

$$\rho A\frac{\partial^2 W(x,t)}{\partial t^2} + EI\frac{\partial^4 W(x,t)}{\partial x^4} - \rho I\frac{\partial^4 W(x,t)}{\partial x^2 \partial t^2} = 0. \tag{1.8}$$

This equation brings up a new term which represents the effect of the rotation of inertia.

1.2.1.3 Shear beam model

Another alternative to the problem of overestimating the natural frequencies of the Euler's beam model was the consideration of the effect of transverse shear. With the emergence of this model, the estimation of the natural frequencies of vibration of a beam has been significantly improved. In this modelling, the equation of motion of the beam become

$$\rho A\frac{\partial^2 W(x,t)}{\partial T^2} - k_s GA\left(\frac{\partial^2 W(x,t)}{\partial x^2} - \frac{\partial \alpha(x,t)}{\partial x}\right) = 0 \tag{1.9a}$$

$$EI\frac{\partial^2 \alpha(x,t)}{\partial x^2} + k_s GA\left(\frac{\partial W(x,t)}{\partial x} - \alpha(x,t)\right) = 0, \tag{1.9b}$$

where $G = \frac{E}{2(1+\nu)}$ is the shear modulus, k_s is the shape factor depends on the geometric of the cross section of the beam and α is the angle of rotation of the section due to the bending moment.

1.2.1.4 Timoshenko beam model

In 1921 Timoshenko [18], proposed a more complete model of the beam by combining the effect of rotational inertia and transverse shear with Euler's model beam ; in this consideration, the equation of motion becomes

$$\rho A\frac{\partial^2 W(x,t)}{\partial t^2} - k_s GA\left(\frac{\partial^2 W(x,t)}{\partial x^2} - \frac{\partial \alpha(x,t)}{\partial x}\right) = 0 \tag{1.10a}$$

$$\rho A\frac{\partial^2 \alpha(x,t)}{\partial t^2} = EI\frac{\partial^2 \alpha(x,t)}{\partial x^2} + k_s GA\left(\frac{\partial W(x,t)}{\partial x} - \alpha(x,t)\right) = 0 \tag{1.10b}$$

By eliminating α that the equations of dynamics become

$$\rho A\frac{\partial^2 W(x,t)}{\partial t^2} + EI\frac{\partial^4 W(x,t)}{\partial x^4} - \rho I(1+\frac{E}{k_s G})\frac{\partial^4 W(x,t)}{\partial x^2 \partial T^2} + \frac{\rho^2 I}{k_s G}\frac{\partial^4 W(x,t)}{\partial t^4} = 0 \tag{1.11}$$

It can be seen that the Timoshenko model constitutes the major improvement of Euler Bernoulli's theory of beams for high rank frequencies, or when the thickness of the beam becomes important, that is to say when the rotational inertia of straight sections and the effect of transverse shear can no longer be neglected.
In the context of this work, the Euler Bernoulli model is used, taking into account the dimensions of the structures studied.

1.2.2 Boundary conditions

In their various applications, the beams can have various configurations. Each of these configurations are characterized by the boundary conditions which make it possible to solve

the equations of the dynamics of the beam. These conditions give a dynamic behavior specific to each structure. There are several identified boundary conditions [12] among which : free-free, hinged-hinged (or simply supported), clamped-clamped, clamped-free, sliding-sliding, free-hinged, free-sliding, clamped-hinged, clamped-sliding and hinged-sliding supports. The work of this thesis is particularly interested in simply supported beams whose boundary conditions are given by the relations.

$$W(0,t) = W(L,t) = 0 \tag{1.12a}$$

$$\frac{\partial^2 W(0,t)}{\partial x^2} = \frac{\partial^2 W(L,t)}{\partial x^2} = 0 \tag{1.12b}$$

The well-defined boundary conditions allow a modal analysis of the dynamics of the structure to be performed.

1.3 Modelling of mechanical actions on structures

Most civil engineering structures are often subject to adverse environmental events, their operating loads and disasters [19–24]. The most important loads to consider when sizing a structure are : (a) Self-weight ; (b) Permanent loads ; (c) Earthquake ; (d) Thermal load ; (e) Traffic ; (f) Wind flow. Nowadays, more and more slender and slightly thick structures are built with new materials more or less noticeably with different dynamic loads. These advances imply the emergence of new dynamic features of these structures which are often little or poorly known, resulting in the destruction or ruin of the structures. In the context of this research work, only thermal loads, traffic loads and wind loads are studied, which will be presented in the remainder of this section.

1.3.1 Thermal loads

The thermomechanical analysis of mechanical structures is an old problem that is coming back very much in the field of engineering, civil, aeronautics, etc. In fact, some studies have found that changes in structural vibration properties because of temperature variations could be more significant than those caused by a medium degree of structural damage [25] or under normal operational loads [26]. Understanding the behaviour of structures under thermal effects is therefore essential, but this topic remains controversial in the field of structural engineering. Although advances in analytical modelling have enabled

structural designers to develop sophisticated models, but actual structural behaviour under thermal effects still requires further investigation. Temperature distributions in the structure are often caused by: fire, Air temperature, wind, humidity, intensity of solar radiation, and type of material. There are several research activities in the field of thermomechanical vibrations. The published books [27–29] related on basis of thermo-elastic vibrations. Formulating theory of thermo-elasticity and practical applications, the importance of thermal variation in rods, beams, and plates was investigated. The dynamics of a beam subjected to a magnetic field and thermal loads with the nonlinear deformation has been studied by Wu [30, 31]. Influences of the magnetic field parameters and temperature changes on the vibration characteristics of the beam have been discussed. The non-linear vibrations of moderately thick, curved and axially moving beams subjected to thermomechanical loads have been examined [32–34]. A spring mass-beam system on the thermomechanical loading were investigated analytically [35]; the mass, spring and thermal effects on a hinged-hinged Euler Bernoulli beam have been analyzed. Non-linear dynamics of a beam under the influence of thermal and mechanical loadings were analysed and discussed by Warminska *et al.* [36, 37]. Analytical analysis of the thermal effect on vibrations of a damped Timoshenko beam have beam made by Lili [38]. Response of steel beam submitted to fire exposure have been investigated [39]. So, there have been shown that thermal strain is present without stress if the material is free to expand and Thermal stresses are present without strain if the material is completely restrained from movement. A combination of strain and stress is usually present because the materials are never completely free to move or completely restrained. Complicating the study of thermal strains is the presence of strain due to creep, shrinkage, humidity, moisture swelling, and change loading. Specially, technical reviewed articles [40–42] presents an overview of current research and development activities in the field of thermal load in civil structures. Followed this, there are many way to establish the thermal load model : theoretical structural dynamics analysis, numerical analysis, field measurement and laboratory test. As our work is intended on the first one, there two cases : coupled thermomechanical models and uncoupled thermomechanical models case.

1.3.1.1 Coupled thermomechanical models

The coupled model considers the displacement field coupling effect in the heat conduction equation. Let $T(x, z, t)$ is the current temperature, T_0 the initial constant temperature, c_p

the thermal conductivity and λ_T the heat capacity per unit volume and $\varepsilon = \varepsilon(x,t)$) the total strain due to the thermomechanical load. From equation 1.6, the system modelling the beam behaviour in such a situation consists of the heat conduction equation coupled with the equation of motion is [39, 45]

$$c_p \frac{\partial T}{\partial t} = \lambda_T \left(\frac{\partial^2 T}{\partial x^2} + \frac{\partial^2 T}{\partial z^2} \right) + Q(x,z,t) - \alpha_T E T_0 \frac{\partial \varepsilon}{\partial t} \tag{1.13a}$$

$$\rho A \frac{\partial^2 W}{\partial t^2} + EI \frac{\partial^4 W}{\partial x^4} + F_T \frac{\partial^2 W}{\partial x^2} - \frac{\partial^2 M_T}{\partial x^2} = f(x,t) \tag{1.13b}$$

Where

$$F_T = EA\alpha_T \int_{-\frac{h}{2}}^{\frac{h}{2}} (T(x,z,t) - T_0) dz \tag{1.14a}$$

$$M_T = EA\alpha_T \int_{-\frac{h}{2}}^{\frac{h}{2}} Z(T(x,z,t) - T_0) dz \tag{1.14b}$$

The term $Q(x,z,t)$ is the applied heat flux source, F_T refers to the internal axial load developed in the member as a result of thermal expansion against ends restraints and M_T the thermal moment. This defined coupled model is employed to analyze the thermoelastic vibrations of thick beams or the beam whose length is not too great. Eqs.1.13 have to be completed with given initial and boundary conditions on displacement.

1.3.1.2 Uncoupled thermomechanical models

For a slender beam (cosidering as thin), studies have shown that the thermoelastic coupling effect is insignificant [41, 44, 45]. We eliminate with this assumption the diffusion equation and work by assuming that the temperature varies uniformly along the beam, Eqs.1.14 becomes

$$F_T = EA\alpha_T \Delta T \tag{1.15}$$

The equation for the dynamics of the structure becomes

$$\rho A \frac{\partial^2 W}{\partial t^2} + EI \frac{\partial^4 W}{\partial x^4} + F_T \frac{\partial^2 W}{\partial x^2} = f(x,t) \tag{1.16}$$

The axial force due to thermal distribution can be linear or nonlinear. When it is linear the expression is given by Eq. 1.15a and when the nonlinear distribution considered, we have [46]

$$F_T = EA\alpha_T \Delta T + \hbar \alpha_T^2 \Delta T^2, \tag{1.17}$$

where

$$\hbar = \hbar_1(1-2\nu) - 2\hbar_2(\nu^2-1) + \hbar_3\nu^2, \tag{1.18}$$

$\hbar_1$,$\hbar_2$ and $\hbar_3$ are Murnaghan's constants and ν is Poisson's ratio that depends on materials properties [46].

The non-linear problem could explain the non homogeneous materials or other input flux ignored in the modelling processus. In the present work, we considered non-linear and the linear uncoupled problem.

1.3.2 Wind loads

Wind plays an important role in designing of large structures because it exerts loads on construction. It is a phenomenon of great complexity due to the many flow situations resulting from the interaction of the wind with the structures. Slender structures or tall buildings are very sensitive to dynamic actions induced by the wind, which causes various phenomena of instability [47–51]. The well-known structural collapse has clearly identified the importance of aeroelastic effects on long span bridge performance and construction. Extensive research has been conducted to better understand the effects of wind on long span bridges, yielding various analytical response prediction techniques.

The instability and bifurcation events can be related to different kinds of excitation. Structures subjected to steady wind are modeled as self-excited autonomous systems, prone to Hopf bifurcations. Structures subjected to turbulent wind are described by parametrically excited non-autonomous systems, therefore potentially suffering divergence, flip or Neimark-Sacker bifurcations. Some attention has been devoted in literature to various interactive aeroelastic phenomena [52–56]. Other papers are specifically devoted to analyze galloping versus parametric excitation [57–59], with particular attention to tall buildings [61–66].

The aerodynamic forces are determined according to the quasi-steady theory, in which data obtained in wind tunnel static tests are exploited. In spite this approximation is rather rough and unrealistic, it is usually accepted to formulate analytical models of complex structures [67–70], in civil as well aeronautical engineering. Followed these researchs, the aerodynamic is related to the wind which blows orthogonally to the beam axis with time-dependent velocity $U(T)$.

In order to model the impact of the wind flow on the structure, a numerical description of the average turbulent wind flow is required to express the fluid force which is applied

to the structure. A turbulent wind flow can be modelled by a drag wind force and a lift wind force [69, 70].

$$P_{\bar{D}} = \frac{1}{2}\rho_a b U_{rel}^2 \left(C_D \cos\theta + C_L \sin\theta\right) \tag{1.19}$$

$$P_{\bar{L}} = -\frac{1}{2}\rho_a b U_{rel}^2 \left(C_L \cos\theta + C_D \sin\theta\right) \tag{1.20}$$

where C_D and C_L are respectively the drift and lift coefficients, ρ_a is the air mass density and b is the projected area of the structure, and

$$U_{rel}^2 = \left(\bar{U} + u\left(x,t\right) - \dot{Y}\right)^2 + \left(\dot{W} + \dot{v}\right)^2,\ \tan\theta = \frac{\dot{y} + \dot{v}}{\bar{U} + u\left(x,t\right) - \dot{W}} \tag{1.21}$$

with Y the displacement of the beam in along wind direction, $\bar{U}$ the steady part of the wind flow, u the unsteady part of the wind flow along Y direction and v the unsteady part of the wind flow along W direction.

Since in our topic we are focus on the vibration of the structure in the across wind direction, we will set $Y = 0$ and we will consider only the lift wind force, this implies that :

$$\tan\theta = \frac{\dot{W} + \dot{v}}{\bar{U} + u\left(x,t\right)} \tag{1.22}$$

We suppose that u is just time dependent, and we set:

$$U\left(t\right) = \bar{U} + u\left(t\right) \tag{1.23}$$

Eq.1.22 becomes, assuming that the speed of the structure along W direction is greater than the unsteady part of the wind flow in the same direction

$$\tan\theta = \frac{\dot{W}}{U\left(t\right)} \tag{1.24}$$

with all the above informations, we can write equation Eq.1.20) as:

$$F_{\bar{L}} = \frac{1}{2}\rho_a b U^2(t) C_W(\theta), \tag{1.25}$$

with $C_W(\theta) = -[C_D(\theta)tan(\theta) + C_L(\theta)]sec(\theta)$, It is showed that $C_W(\theta)$ can be expressed as polynomials of $tan(\theta)$ and F_L can be expressed by:

$$P_L = \frac{1}{2}\rho_a b U^2\left(t\right) \sum_i D_i \tan^i\theta \tag{1.26}$$

The wind force (lift wind force) which blows orthogonally to the structure with time-depending velocity $U(t)$. The general form of the most used fluid force is, taking into account the direction [69, 70]:

$$\vec{F} = \frac{1}{2} b C_W \rho_a \left|U\right| \vec{U} \tag{1.27}$$

Where, C_W is the aerodynamic coefficients relevant to square sections and can be written as $C_W = [A_0 + A_1\left(\frac{\dot{W}}{U}\right) + A_2\left(\frac{\dot{W}}{U}\right)^2 + A_3\left(\frac{\dot{W}}{U}\right)^3]$; W is the longitudinal velocity fluctuations. Wind Force can be rewritten according to it intensity as

$$P_{wind} = \frac{1}{2}\rho_a U^2 b \left[A_0 + A_1\left(\frac{\dot{W}}{U}\right) + A_2\left(\frac{\dot{W}}{U}\right)^2 + A_3\left(\frac{\dot{W}}{U}\right)^3\right] \tag{1.28}$$

1.3.3 Moving loads modelling

Dynamic analysis of beam structures under moving loads have attracted the engineering and scientific community from the middle of the 19^{th} century, with the began of railway construction. Moving-load dynamic problems are very common in engineering and daily life. Any structures or machines subjected to loads which move in space and excite the structures or machines into vibration are such problems. The importance of this problem is manifested in numerous applications in the field of transportation. Bridges, guideways, cranes, cableways, rails, roadways, runways and pipelines are examples of structural elements to be designed to support moving masses. The detailed comprehensive review of previous researches, have been written by Frýba [72] on the subject of moving load. The mains analytical methods are described and explained. An overview of vibration analysis of bridges including the moving oscillator problem between the moving vehicles and the bridge structures is given in [73]. Dynamic stress in the beam structure were firstly solved by Krylov [74] and later by Timoshenko [75]. Transversal vibrations in a simply supported beam traversed by a constant force moving at a constant velocity were presented by Inglis [76], Lowan [77] and later on, other solutions have been given by Koloušek [78]. These works employ mainly modal expansion methods. The first solutions for infinite beams were presented by Timoshenko [18].

Generally, the simplest models are used (see Figure 1.2), namely [72,80–84]: Moving force model, moving mass model, moving sprung mass model and moving harmonic oscillator. The use of these simplified models poses a problem of realism, as structures are most often subjected to several loads simultaneously and apply over a length and not a point. In this sense, Anague *et al.* [70] Model the roads traffic using assume that the sequence of vehicles moving with random or deterministic weights and stochastic velocities; Lu Sun *et al.* [86] Studied a Euler Bernoulli beam resting on a viscoelastic foundation subject to a platoon of moving dynamic loads which represents a physical model to describe railways and high ways under traffic loading. Yang*et al.* [87] obtained the closed form solution for the response of simple beams subjected to the passage of a high-speed train modelled as

a sequence of moving loads with regular non-uniform intervals, in which the conditions of resonance appearance and mittigation were identified. In the study done by Wu *et al.* [88], a bridge containing two railway tracks was considered, with which two trains are allowed to move over the bridge in opposite directions. In this work, we investigated on two types

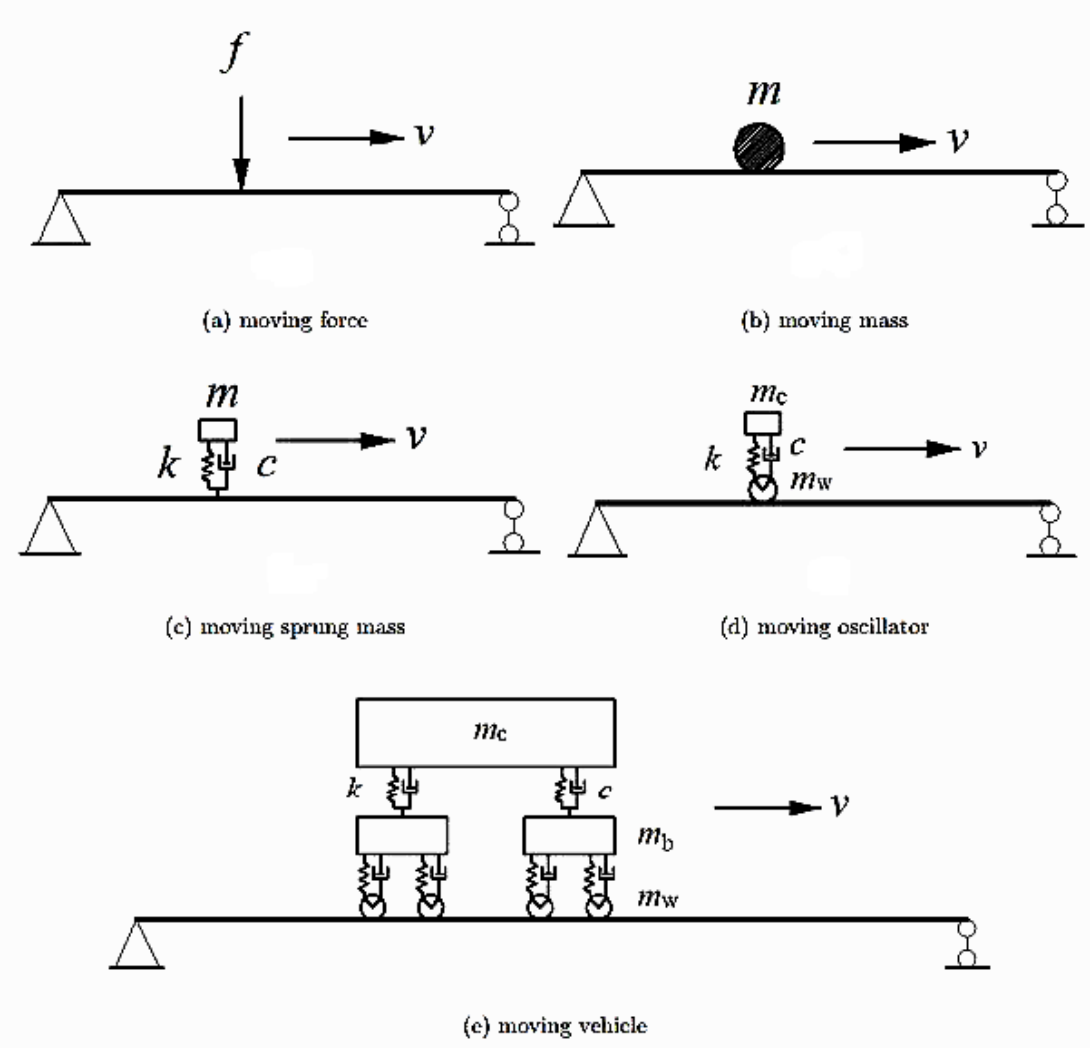

Figure 1.2: Simplest models of moving load [85]

of moving loads,thus a platoon moving oscillator which is a set of many oscillator, and a single moving load.

1.4 Overviews on structural control systems

1.4.1 Vibration control Techniques

In recent years, the attenuation of structural response caused by dynamic loads has become a subject of intensive research. Faced with this, researchers and engineers have therefore carried out research to set up active, semi-active or passive control devices, and many of them have been put into practice. There are a number of motivators for conducting this research. They include : (i) reduction of unwanted vibration levels of flexible structures due to significant and unexpected environmental loads ; (ii) rehabilitation of existing structures against environmental risks; (iii) protection of seismic equipment and major secondary systems; and finally, (iv) provide new concepts for the design of structures against the environmental load. In general, each control system is based on their operating mechanisms.

1.4.1.1 Passive vibration control (PVC)

PVC systems are devices designed to modify structural stiffness or damping appropriately without requiring an external power source to develop the control forces opposing the movement of the structure [90–92] . Passive control may depend on the initial design of the structure, the frictional contact between structural members, or the use of contact dampers at the joints of the structure [93]. Based on the energetical point of view, there are two main classes of passive systems, namely base isolators and energy absorbers.

1.4.1.2 Active vibration control(AVC)

AVC method use an external power device, to change the structural response. The activation of external force is based on the measurement of external disturbance and/or structural response. Sensors are employed for the measurement purposes, and with the help of computers, the digital signal activates the required external forces [91, 98] . The control forces within the framework of an active control system are generated by a wide variety of actuators that can act hydraulic, pneumatic, electromagnetic, piezoelectric or motor driven ball-screw actuation. The controller (e.g. a computer) receives signals from physical sensors (within active control using feedback) and that on basis a pre-determined control algorithm compares the received signals with a desired response and uses the error to generate a proper control signal [97]. The control signal is then sent to actuator.

1.4.1.3 Hybrid vibration control (HVC)

A HVC used the combined of active and passive control system [91, 97]. Such control system consists of employment of an active control device to improve and supplement the performance of passive control system. Alternatively, the passive devices embedded in a structure can decrease the amount of required energy power if an active control system is installed in that structure. For example, a base isolation system can be improved using actuators that act to decrease the displacement of structure or a structure equipped with passive damping devices supplemented upon the its top with an active mass damper in order to enhance reduction efficiency of imputed vibrations. The hybrid method for vibration suppression use synergy between feedforward and feedback control.

1.4.1.4 Semi-Active vibration control (SAVC)

A SAVC system is defined as one that needs energy only to change the mechanical proprieties of the devices and to develop the control forces opposite to the motion of structure. SAVC are a class of active control systems for which the external energy requirements are smaller amounts than those of typical active control. A battery power, for instance, is sufficient to make them operative. Semi-active devices cannot add or remove energy to the structural system, but can control in real time parameters of the structure such as spring stiffness or the viscous damping coefficient. The stability is guaranteed, in the sense that no instability can occur, because semiactive devices use the motion of the structure to develop the control forces. A semiactive device will never destabilize a structural system whereas an active device may destabilize a structural system even though it has a low energy demand. These control devices are often viewed as controllable passive devices.
Every kinds of structural control systems presented above have their own behaviours and importances. Table 1.1 gives comparison between different kinds of structural control systems.

Table 1.1: Comparision between different kinds of structural control systems.

Seismic isolation evices	Passive control Systems	semi-active control systems	Active control systems	Hybrid control devices
-Dissipate part of input energy	-Absorb or diverge part of input energy	-Natural extension of passive devices	-Automatically supply a force into the structure	-Mixture
-Increase horizontal flexibility	-Dependent on relative movement	-Include adaptative systems	-Depends on global response	-Misture
Lengthen fundamental periods of structures	-Related only to local structure response		-Ability to sense exitation and automatically adjust control efforts	
	-No structural response measurements			
Suitable for short to medium heignt	Optimally tuned to specified dynamic loading	-Better than passive systems and less than active systems	-Optimal efficiency compared wit passive control systems	-Suitable for all types of structures
-Efficient against vibrations transmitted through ground	-Not optimal for other types dynamic loadings	-Capable of acting better than passive ones	-Designed for different objective	-Larger capacity than passive system
	-Unable to adapt to excitation and global structural response	Limited control capacity	-No theoretical limits on efficiency	
-Not efficient to resist wind	-limited control capacity		-Wide frequency range	-Greater efficiency tan passinve system
-Safe	-Inherently stable	-fall-safe -reliable	-Detuning may occur	-More reliable
-Economic	-No energy requirement	-Little power requirement	-Dignifiant energy	-Costs less than active system
	-Simpler to design and construct	-Easy to manufacture	-Complicated	
		-Very promising		-Very promising

1.4.2 Passive base isolation systems Modeling

Passive base isolation systems isolator include mitigation of resonance peaks, reduction of transmissibility, enhancement of fatigue life, improvement in ergonomics, etc. in the presence of external or internal sources of dynamic excitation. The design of a vibration isolator requires a close examination of multiple considerations such as the source of dynamic excitation, range of excitation frequency, excitation amplitude, allowable displacement, acceleration limits of the isolated system, available design envelope, etc. Additionally, considerations of environmental conditions, manufacturability, and material choice are also important. Base isolation are widely used in areas such as automotive, rail road, aerospace, manufacturing, heavy machinery, and civil structures. Base isolation exhibit many behaviours which poses several modelling problems such as : Viscoelastic behaviors, Elastomeric behaviors, inertia effect, etc. Most of the passive vibration isolators exhibit viscoelastic behavior as they are designed to provide stiffness and damping characteristics to isolate a system from dynamic forces while allowing for a means of dissipating energy. All these considerations accentuate the importance of a theoretical model that can reasonably predict the performance of the isolation system before finalizing the design and before manufacturing prototypes that can be used for testing. In theoretical modelling we distinguish linear and non-linear isolaor.

1.4.2.1 Viscoelasticity for isolator modelling

The exhibition of a combination of viscous and elastic behavior is defined as viscoelasticity. Viscoelastic behavior is often modeled as a combination of simplest behavior of elastic solids as per Hooke's law and linear behavior of viscous fluids as per Newton's law. The theory of viscoelasticity allows accommodating material behavior that involves storage of mechanical energy as well as dissipation of energy [100]. A typical example is the coil spring isolator, where the spring force is a linear function of the spring deformation. In these isolators, the payload sensitivity to external disturbance is fixed, and is dependent on thestiffness of the supporting structure. A complete review of linear vibration isolation can be found in numerous undergraduate texts, for example, "Passive Vibration Isolation" [101, 102], which contains both theories and extensive examples of the applications of linear vibration isolators. There are many way to modelling linear isolator, we present in this subsections some simplest models. The Voigt or Kelvin-Voigt model is the simplest viscoelastic model that is very commonly used to model a vibration isolator. This model

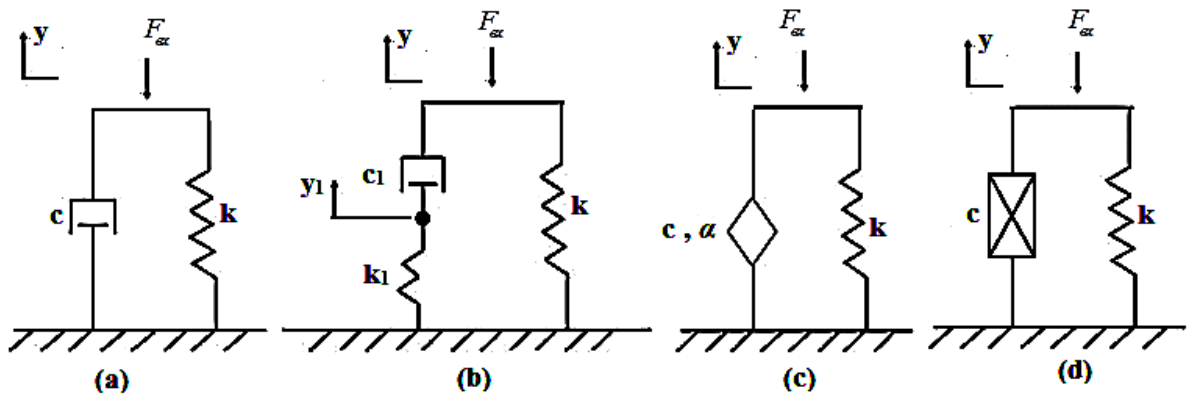

Figure 1.3: Simplest viscoelastic models.

superposes the elastic behaviour and the viscous behaviour of an isolator, a representation of this model is shown in Fig.1.3a. The reaction force of the spring damper element as a result of any perturbation from static equilibrium can be expressed as

$$f(t) = c\dot{y} + ky \tag{1.29}$$

$f(t)$ is the time history of the reaction force in the loading direction, while y is the corresponding displacement about static equilibrium.

The Zener model is a modified form of the Voigt model that introduces a Maxwell element that is parallel to the spring element, instead of the damping element in the Voigt model. A Maxwell element consists of a spring element and a damper in series. This model is shown in Fig.1.3b. The reaction force of the isolator using the Zener model can be expressed as

$$f(t) = c_1(\dot{y} - \dot{y}_1) + k_1 y \tag{1.30}$$

Fractional derivatives have been increasingly used for modeling viscoelastic characteristics [103,104]. A fractional derivative has been defined in multiple forms in the literature [105]. The reaction force of the spring-damper element due to a perturbation of the mass in Fig.1.3c can be expressed as

$$f(t) = c\frac{d^{\alpha}y}{dt^{\alpha}} + ky \tag{1.31}$$

α is the order of the fractional derivative (For $0 < \alpha \leq 1$). If $\alpha = 1$ this model becomes identical to the Voigt model in Figure 1.3(a).

The Hysteresis model considers that, the primary means of damping is due to slippage between internal planes of the isolator material during loading and unloading cycles : this

is hysteresis. Hysteresis is a complex phenomenon that results in input-output relationships that are significantly different during loading as compared to unloading. Although the general modelling of hysteresis is an ongoing area of research, hysteresis damping can be modelled with some adjustment to the viscoelastic models [106, 107]. The damping is given by $c = \frac{k''}{\omega}$ where k'' is the imaginary component of complex stiffness. It can be seen that the damping force is a function of excitation frequency in hysteresis damping. The reaction force from the isolator due to any perturbation of the mass in Fig.1.3d can be expressed as

$$f(t) = \frac{k''}{\omega}\dot{y} + ky \tag{1.32}$$

There are many other models as : Maxwell-Voigt, Generalized Maxwell or Maxwell Ladder, Mawxell-Voigt fractionnal, etc. One can combine all these models to designing many other simplest isolators models. All models provides some of the main characteristics and possible considerations that should be taken into while selecting an appropriate model for isolator design.

However, it is known to bear some limitations, as e.g. its tuning to only one resonant frequency and its sensitivity to the primary structure uncertainty [108, 109]. To overcome these drawbacks, the use of nonlinear vibration absorbers is studied as an alternative to the linear one in order to enhance the range of effectiveness in terms of frequency or vibration amplitude.

1.4.2.2 Review on nonlinear base isolator modelling

As the design of a passive linear vibration isolator involves multiple tradeoffs, a nonlinear vibration isolator can be designed to mitigate some of these tradeoffs. The nonlinear isolator modelling have attract significant attention due to the need of performant vibration isolation. The stiffness and/or damping of the resilient structures used in these designs behave in a nonlinear fashion so that, by combining multiple nonlinear supporting structures, the overall stiffness of the isolator can be more flexibly tuned to suit different applications [96]. Some common applications of nonlinear vibration isolators include : isolation of diesel engines in marine vessels, isolation of space craft, isolation of vehicle passengers from road disturbances, isolation of vibration generated by hand-held tools, and isolation of buildings, bridges, storage tanks and oil pipelines from destructive impacts from earthquakes. The literature reports a considerable number of studies on

nonlinear vibration isolators. A review literature on nonlinear passive vibration isolators have been made by Ibrahim. This covers a wide range mechanisms and mounts. Amont this nonlinear vibration isolators with negative stiffness paid more attention. High static and low dynamics stiffness (HSLDS) are the main properties required to have an effective isolator which requires non-linearity. This principle was used by Shaw *et al.* [110]. and Huang *et al.* [111, 112] to model this type of passive isolator. Recently, the HSLDS model isolators have gained more attention due to their strong conception and outstanding vibration isolation. Carrella *et al.* [113, 114] and Kovacic *et al.* [115] have carried out intensive theoretical work on HSLDS isolators having two horizontal spring providing negative stiffness and another one providing positive stiffness. Using planar springs, Lan et al. [116] have designed and experienced a quasi-zero stiffness (QZS) which is a special type of HSLDS isolator. To overcome the limitations of the HSLDS isolators, Liu et al. [117] modelled an HSLDS-AS by adding a linear auxiliary mass to the HSLDS isolator, to eliminate the jump phenomenon and improve therefore the reduction of the peak of transmissibility. In this later work, only displacement transmissibility has been studied. A passive vibration isolator integrated a dynamic vibration absorber with negative stiffness was developed by Thakaduet al. [118]. The isolator developed bear static load while limiting the static displacement and providing lower-even-zero dynamic stiffness, which are the qualities required for performant isolator. Taking into account various types of uncertainties, Bhowmik *et al.* [119] investigated on stochastic design of negative stiffness integrated tuned mass damper. As a practical application of HSLDS isolators, Abbasi *et al.* [120]used a HSLDS for vibration control of a continuous rotating shaft and Sonfack *et al.* [**?**] investigated the performance of a quasi-zero stiffness isolator in vibration isolation of a multi-span continuous beam bridge under pier base vibrating excitation. HSLDS−AS is used in this thesis for mitigate vibration of a hinged-hinged beam. The mechanism of this kind of isolator will be presented in the next chapter.

1.4.3 Importance and reasons of the thesis

Essential works on vibration control of various mechanical structures have been carried out in our research group and some of those works have been listed above Nowadays, structures face more and more accidental phenomena which require the development of efficient control systems. Furthermore, studies have been shown that the temperature gradient in civil infrastructure environment is in the interval $[-40; +40]^oC$ and the con-

sequence is the appearance of thermal loads in the structure. Thus, one can observe the change on the vibratory characteristics which could rout the monitoring devices responsible for detecting failures in structures, because the changes caused by these thermal loads are most often more significant at the degrees of damage to the structure [25, 26]. Also, the performance of structures under or without control will be strongly affected depending on the type of external loads. Because interaction between thermal loads and other type of excitation need to be scientifically explained, it is important to conduct an complete analysis of thermomechanical structure, depending of environmental complexity (subjected to the combined actions of various loads) before their realization or when designing isolator. Since thermomechanical analysis of structures is an old problem in the field of engineering [40, 42], more investigations and theoretical analysis are still required to clarify thermal effect on controlled and uncontrolled structures.
The present thesis propose firstly a dynamic analysis which aims at developing an enough complete descriptive theoretical analysis of thermomechanical structure subjected to various type of excitation; secondly, the analysis is extend to establishing the effect of thermal variation on performance of isolation of these types of structures.

1.5 Conclusion

In this chapter, we have provided a state of art with as much detail as possible on beams, thermal loads, moving loads, wind loads and vibration control systems. The details on the problems solved in this thesis work have been given. The following chapter is devoted to general background of some analytical and numerical methods used.

Chapter II

Methods and Materials

2.1 Introduction

The present chapter is devoted to the presentation of the principles of each methods used along the thesis. In Section 2.2, the analytical and computational techniques used to solve the structure equations under control and plot the results are briefly presented. Section 2.3 is devoted to present the technique used to asses the performance of an isolators. In section 2.4 mathematical modelling of HSLDS-AS mechanism a presented. To end this chapter, a conclusion is given in section 2.5.

2.2 Analytical and numerical formalism

After mathematical modeling, extracting the information contained in the equations represents the very main interest of this modeling. Within the framework of this thesis, different analytical and numerical methods have been used in this objective. There are several methods presented and documented in books [6, 14, 129] and references [130–135]. In this section, we present the methods used to investigate the dynamics of structures modelled as partial differential equations (PDEs).

2.2.1 Modal Approximation

To reduce PDEs to ordinary differential equations (ODEs) [129], the Garlekin's decomposition method is used. Consider $W(x,t)$, the transverse displacement of a beam describing the dynamics of a continuous system and which verifies the associated boundary conditions. This displacement can be written in the form

$$W(x,t) = \sum_{n=1}^{N} \phi_n(x) Q_n(t) \tag{2.1}$$

where N represents the number of modes used in the approximation, $Q_n(t)$ represents the amplitude of vibrations of the structure associated with the nth mode and $\phi_n(x)$ represents the modal function solution of the nth mode of the beam linear natural equation with the associated boundary conditions. Substituting equation 2.1 into the equation governing the dynamics of the system, multiplying by $\phi_n(x)$ and integrating over the length of the beam, we obtain the modal equation (non-linear ODE).

2.2.2 Dynamic response-Analytical methods

2.2.2.1 Harmonic balance method

Among the approximation methods for the study of nonlinear dynamical systems described by ordinary non-linear differential equations. Is the Harmonic balance method is an powerfull approximate method. This analytical method is currently used to obtain periodic solution of a nonlinear differential equation [22]. Let consider the following differential equation

$$\ddot{x} + x = f(\dot{x}, x, t) \tag{2.2}$$

where (.) over the x refers to the differentiation with respect to time t, $f(\dot{x}, x, t)$ is the function contains explicitly the time t. We assume the harmonic solution of this equation expressed in the following form

$$x = x_m \cos(\omega t + \varphi) \tag{2.3}$$

where x_m is the amplitude of oscillations, ω the pulsation of the sinusoidal excitation and φ the phase at the origin. Inserting Eq.2.3 into Eq.2.2 and equating separately the coefficient of sine and cosine terms with same harmonics, one obtains after neglecting harmonics order greater than one, a system of algebraic equations which are the amplitude equations.

2.2.2.2 Method of multiple scales

The basic problem can be illustrated with a second order ordinary difierential equation (ODE). In this case, the objective is to determine the behavior of a weakly nonlinear system described by an equation of the type

$$\ddot{x} + \omega^2 x = \varepsilon f(\dot{x}, x, t) \tag{2.4}$$

where $0 < \varepsilon \leq 1$ is a dimensionless parameter. The method of multiple scales, as presented by Nayfeh (1981) [136], considers the expansion to be a function of multiple independent variables, or scales, instead of a single variable t. The independent variables are deflned as

$$T_n = \varepsilon^n t \qquad \text{for} \qquad n = 0, 1, 2, ... \tag{2.5}$$

It is assumed that the solution of interest can be represented by an expression having the form

$$x(t;\varepsilon) = x_0(T_0, T_1, T_2, ...) + \varepsilon x_1(T_0, T_1, T_2, ...) + \varepsilon^2 x_2(T_0, T_1, T_2, ...) + ... \tag{2.6}$$

where the number of independent time scales depends on the order to which the expansion is carried out. Substituting Eq.2.6 into the governing differential equation and collecting coefficients of equal powers of ε generates a system of $n+1$ differential equations.
To obtain a uniform solution, the system of ODEs needs to be solved sequentially for $k = 0, 1, ...n-1$, eliminating secular terms, those terms that will become large when t increases, in the process at each order ε^k for $k = 1, 2, ...n$. This will ensure that

$$x(t;\varepsilon) = \sum_{k=0}^{n-1} x_k(T_0, T_1, T_2, ...) + O(\varepsilon^n) \tag{2.7}$$

is a uniform $O(\varepsilon^n)$ solution. For example, consider a Duffing oscillator of the type

$$\ddot{x} + \omega^2 x - \varepsilon x^3 = 0 \tag{2.8}$$

A first-order analysis ($n = 1$) of Eq.2.8 would generate the system of equations

$$\varepsilon^0 : D_0^2 x_0 + \omega^2 x_0 = 0 \tag{2.9}$$

$$\varepsilon^1 : D_0^2 x_1 + \omega^2 x_1 = -2D_0 D_1 - \alpha x_0^3 \tag{2.10}$$

where $D_i^n = \frac{\partial^n}{\partial T_i^n}$.
The solution of Eq.2.9 can be written as

$$x_0(T_0, T_1) = A(T_1)e^{i\omega T_0} + \bar{A}(T_1)e^{-i\omega T_0} \tag{2.11}$$

Substituting Eq.2.11 into Eq.2.10, we obtain

$$D_0^2 x_1 + \omega^2 x_1 = -(2i\omega D_1 A + 2A^2\bar{A})e^{i\omega T_0} + (2i\omega D_1 \bar{A} + 2\bar{A}^2 A)e^{-i\omega T_0} - A^3 e^{3i\omega T_0} - \bar{A}^3 e^{-3i\omega T_0}. \tag{2.12}$$

To avoid the generation of secular terms in $x_1(t)$, the coefficients of $e^{i\omega T_0}$ and its complex conjugate must vanish; and then,

$$2i\omega D_1 A + 3A^2\bar{A} = 0 \tag{2.13}$$

Writing A in the polar form $A(T_1) = \frac{1}{2}ae^{i\varphi}$ and separating Eq.2.13 into its real and imaginary parts gives

$$\frac{\partial a}{\partial T_1} = 0, \tag{2.14}$$

$$a\frac{\partial \varphi}{\partial T_1} - \frac{3}{8}a^3 = 0. \tag{2.15}$$

The solution to Eq.2.4 is then given by

$$x(t) = a\cos(\omega t + \varphi) + ... \tag{2.16}$$

where a and φ are described by the so called evolution Eq.2.14 and Eq.2.15.

2.2.2.3 Stability of the non-trivial steady states solutions of the non-linear system response

Steady states solutions of any non-linear system only exist if they are stable. Hence the interest to perform a stability analysis of these solutions. To do so, we shall define first what we mean by a steady state solution and how can appreciate their stability. So, formally, we can say that

Definition [137].

The constant vector $X_0 \in C^n$ is a steady state solution of the system of differential equations

$$\frac{dX(t)}{dt} = F(X(t)) \tag{2.17}$$

if it satisfies the equation $F(t, X(t)) = 0$, where o is the null vector and $F(t, X(t))$ is a differentiable vector function. When $X_0 \neq 0$, the steady state solution is non-trivial. We can get some information about the stability of the solution of the nonlinear systems models by using Taylor's Theorem to "relate" it to a linear system. In fact, the version of Taylor's Theorem which we shall use is the following **Taylor's Theorem** [137]

If $F : C^n \to C^n$ is a continuously differentiable function and X_0 is some constant vector in C^n, then for a vector then for a vector $\delta X(t) \in C^n$

$$F(X_0 + \delta X(t)) = F(X_0) + DF(X_0) + R(\delta X(t)) \tag{2.18}$$

Note that if the function $F(X(t)) = f_1(X) + f_2(X) + ... + f_n(X)$ then DF is the Jacobian expressed as

$$DF = \begin{pmatrix} \frac{\partial f_1}{\partial X_1} & \cdots & \frac{\partial f_1}{\partial X_n} \\ \vdots & \ddots & \vdots \\ \frac{\partial f_n}{\partial X_1} & \cdots & \frac{\partial f_n}{\partial X_n} \end{pmatrix} \tag{2.19}$$

and the matrix $DF(X_0)$ is the Jacobian evaluated at X_0. Further $R(\delta X)$ has the property that: $\frac{R(\delta X)}{\|\delta X\|} \to 0$, as $\delta X \to 0$.

Loosely speaking, this means that if each entry of δX is small, then

$$F(X_0 + h) \simeq F(X_0) + DF(X_0) \tag{2.20}$$

where $\simeq$ can be interpreted as "is approximately".

Now, suppose that X_0 is a steady state solution of the previous system 2.17 , i.e.$F(X_0) = 0$

, and take $X(t)$ to be a solution of the system such that $X(0) - X_0$ is small.
If we now take system 2.17 becomes

$$\frac{d(X_0 + \delta X(t))}{dt} = F(X_0 + \delta X(t)). \tag{2.21}$$

Consequently, using Taylor's theorem, we have

$$\frac{d\delta X(t)}{dt} = \frac{d(X_0 + \delta X(t))}{dt} = DF(X_0)\delta X(t) + R(\delta X(t)) \tag{2.22}$$

And if$\delta X(t)$ is mall, we can ignore the term $R(\delta X)$. This mean that, if the quantity $\delta X(0) = X(0) - X_0$ is small, then the behaviour of the vector $\delta X(t) = X(t) - X_0$ is *qualitatively* the same as the solution to the linear system

$$\frac{d\delta X(t)}{dt} = DF(X_0)\delta X(t) \tag{2.23}$$

This analysis results in the following theorem:
Theorem [137]
Let the constant vector X_0 be a steady state solution of the system Eq.2.17 and let the matrix $DF(X_0)$ denote the Jacobian evaluated at X_0:

- If the n eigenvalues of the Jacobian matrix $DF(X_0)$ have real parts less than zero, then the steady state solution X_0 is stable;

- If at least one of the n eigenvalues of the Jacobian matrix $DF(X_0)$ has real part greater than zero, then the steady state solution X_0 is unstable. Generally, the determination of the sign of the real parts of the eigenvalues is carried out by using the Routh-Hurwitz criterion [14].

This mathematical formalism will be used in the following chapter to analyse the stability of the steady state solutions of the beam responses.

2.2.2.4 Routh-Hurwitz Stability Criterion

Routh-Hurwitz stability criterion is a method for stability analysis of linear systems. This approach is a necessary and sufficient condition for the stability of a system Eq.2.17, since it has bounded output for bounded inputs, if the roots of its characteristic equation have negative real parts only.
The characteristic equations of jacobian matrix Eq.2.18 is given by

$$f(\lambda) = a_0\lambda^n + a_1\lambda^{-1} + ... + a_{n-1}\lambda + a_n \tag{2.24}$$

where the coefficients a_i are real constants. The main diagonal of the Hurwitz's matrix are the form $\Delta_1 = a_1$, $\Delta_2 = \begin{vmatrix} a_1 & a_0 \\ a_3 & a_2 \end{vmatrix}$, $\Delta_3 = \begin{vmatrix} a_1 & a_0 & 0 \\ a_3 & a_2 & a_1 \\ a_5 & a_4 & a_3 \end{vmatrix}$,....

$$\Delta_n = \begin{vmatrix} a_1 & a_0 & 0 & \cdots & 0 \\ a_3 & a_2 & a_1 & \cdots & 0 \\ a_5 & a_4 & a_3 & \cdots & 0 \\ \cdots & \cdots & \cdots & \cdots & \cdots \\ 0 & 0 & 0 & \cdots & a_n \end{vmatrix}$$

In general, Hurwitz condition states : all of the roots of the polynomial have negative real part if the determinant of all Hurwitz matrix are positive. That is, none of them are zero or negative.

$$\Delta_1 > 0, \quad \Delta_2 > 0, \quad ....., \quad \Delta_n > 0 \tag{2.25}$$

Since $\Delta_n = a_n \Delta_{n-1}$, then the condition $\Delta_n > 0$ can be changed by a_n

$$n = 2; \quad a_1 > 0 \quad \text{and} \quad a_2 > 0 \tag{2.26}$$

$$n = 3; \quad a_1 > 0, \quad a_3 > 0 \quad \text{and} \quad a_1 a_2 > a_3 \tag{2.27}$$

$$n = 4; \quad a_1 > 0, \quad a_3 > 0, \quad a_4 > 0 \quad \text{and} \quad a_1 a_2 a_3 > a_3^2 + a_1^2 a_4 \tag{2.28}$$

Thus, conditions checked the system is considered stable. Numerical formalism can be defined as an approximate solution of problems occur for instance in physics, chemistry, biology, economics and in many field of engineering. The numerical analysis is adopted in the many case to obtain information about the response dynamics of the physical system. It is impossible to have analytical solution. The selection of integration algorithms using numerical approximation depends on of the complexity of problems and the scientific disciplines.

2.2.2.5 Taylor Expansion Serie

Taylor's theorem, [153] is taught in introductory–level calculus courses and is one of the central elementary tools in mathematical analysis. It gives simple arithmetic formulas to accurately compute values of many transcendental functions such as the exponential function and trigonometric functions. It is the starting point of the study of analytic functions, and is fundamental in various areas of mathematics, as well as in numerical

analysis and mathematical physics. Taylor's theorem also generalizes to multivariate and vector valued functions. if $f : R \rightarrow R$ infinitely differentiable at $x = x_0$ then the Taylor series for f at x is the following power series.

$$f(x) = f(x_0) + f'(x_0)\Delta x + f''(x_0)\frac{(\Delta x)^2}{2!} + ... + f^{(k)}(x_0)\frac{(\Delta x)^k}{k!} + ... \tag{2.29}$$

Truncating this power series at some power results in a polynomial that approximates f around the point x. In particular, for small,

$$f(x + \Delta x) \simeq f(x) + f'(x)\Delta x + f''(x)\frac{(\Delta x)^2}{2!} + ... + f^{(k)}(x)\frac{(\Delta x)^k}{k!} \tag{2.30}$$

Here the error of the approximation goes to zero at least as fast as $(\Delta x)^k$ as $\Delta x \rightarrow 0$. Thus, the larger the k the better is the approximation. This is called the k th–order Taylor approximation of f at x. This can be generalized to the multivariate case

2.2.3 Dynamic response-Numerical methods

Over the past decade, computational science has emerged as the most versatile tool to complement theory and experiments. Modern numerical methods, in particular those for solving nonlinear ODEs, PDEs, are at the heart of many of these advanced scientific computations. Indeed, numerical computations have not only joined experiment and theory as one of the fundamental tools of investigation, but they have also altered the kind of experiments performed and expanded the scope of theory. In this thesis, we have used the fourth-order Runge-Kutta method (RK4 method for ordinary differential equations and the Adam Baschford Method (A-B-M) predictor-corrector scheme and Newton-Leipnik method for ordinary differential equations, Newton-Raphson Method for system of equations. Those methods are described below.

2.2.3.1 Fourth-order Runge-Kutta algorithm for ordinary differential equations

Analysis of differential equation of a dynamical system are often done by numerical method. Numerical analysis is use in order to get more accurate solution or to validate the analytical solution obtained, or experimental result. There are several numerical techniques, in this thesis we used RK4 method. This method has been elaborated for the first time in 1894 by Carle Runge and has been improved by Martin W. Kutta in 1901. Their modern developments are mostly due to John Butcher in the 1960s, it is widely

used since it is most stable [138]. This method is widely used since it is most stable. Let us consider the first-order ODE as differential equation

$$\frac{dX(t)}{dt} = F(t, X(t)) \tag{2.31}$$

with the initial condition $X(t_0) = X_0$. This equation is under a vectorial form (X and F being vectors). The aim of the RK4 method is to find solutions after each time step h, the next solution as a function of the previous one. The classical RK4 flow for this problem is given by

$$\begin{aligned}
&t_i = t_0 + ih \\
&x_{0,j} = X_{0j} \\
&L_{1,j} = f_j(t_i, x_{i,j}) \\
&L_{2,j} = f_j(t_i + \tfrac{h}{2}, x_{i,j} + \tfrac{L_{1,j}}{2}) \\
&L_{3,j} = f_j(t_i + \tfrac{h}{2}, x_{i,j} + \tfrac{L_{2,j}}{2}) \\
&L_{4,j} = f_j(t_i + h, x_{i,j} + L_{3,j}) \\
&x_{i+1,j} = x_{i,j} + \tfrac{1}{6}(L_{1,j} + 2L_{2,j} + 2L_{3,j} + L_{4,j})
\end{aligned} \tag{2.32}$$

where i represents the time incrementation and j labels the variables related to $L_{1,j}$, $L_{2,j}$, $L_{3,j}$,$L_{4,j}$ are intermediate variables and h represents the time step. In the case $m-$order differential equation

$$\begin{cases} \frac{d^m X}{dt^m} = F_m\left(t, y, \frac{dX}{dt}, \frac{d^2X}{dt^2}, ..., \frac{d^{m-1}X}{dt^{m-1}}\right) \\ \frac{d^k X(t_0)}{dt^k} = X_0^{(k)} \end{cases} \tag{2.33}$$

with successive variables change, the equation can be written under the form

$$\begin{cases} \frac{d^0 X}{dt^0} = B_0 = X = F_0\left(t, B_0, B_1, ...B_{m-1}\right) \\ \frac{dX}{dt} = \frac{dB_0}{dt} = B_1 = F_1\left(t, B_0, B_1, ...B_{m-1}\right) \\ \frac{d^2 X}{dt^2} = \frac{dB_1}{dt} = B_2 = F_2\left(t, B_0, B_1, ...B_{m-1}\right) \\ . \\ . \\ . \\ . \\ . \\ \frac{d^{m-1} X}{dt^{m-1}} = \frac{dB_{m-2}}{dt} = B_{m-1} = F_{m-1}\left(t, B_0, B_1, ...B_{m-1}\right) \\ \frac{d^m X}{dt^m} = \frac{dB_{m-1}}{dt} = F_m\left(t, B_0, B_1, ...B_{m-1}\right) \\ \frac{d^k X(t_0)}{dt^k} = B_k\left(t_0\right) = X_0^{(k)} \\ k \in \{1; 2; ...; m-1\} \end{cases} \tag{2.34}$$

With this general vectorial and form, iterations can be performed to determine all the values of X and its derivative at different time separated by the time step h using:

$$B_k(t+h) = B_k(t) + \frac{1}{6}\left(L_1^k + 2L_2^k + 2L_3^k + L_4^k\right) \tag{2.35}$$

where

$L_1^k = hF_k\left(t, B_0(t), B_1(t), ...B_{m-1}(t)\right);$

$L_2^k = hF_k\left(t + \frac{h}{2}, B_0(t) + \frac{L_1^0}{2}, B_1(t) + \frac{L_1^1}{2}, ...B_{m-1}(t) + \frac{L_1^{m-1}}{2}\right);$

$L_3^k = hF_k\left(t + \frac{h}{2}, B_0(t) + \frac{L_2^0}{2}, B_1(t) + \frac{L_2^1}{2}, ...B_{m-1}(t) + \frac{L_2^{m-1}}{2}\right);$

$L_4^k = hF_k\left(t + h, B_0(t) + L_3^0, B_1(t) + L_3^1, ...B_{m-1}(t) + L_3^{m-1}\right.$

This generalized form will serve to solve numerically first-order coupled ODEs.

2.2.3.2 Numerical methods for fractional differential equations

Solving a fractional differential equation, one has to approximate the corresponding derivative operator, which means including information about previous states of the system (the so-called memory effect). For numerical solutions of the FDEs, the NewtonLeipnik and A-B-M predictor-corrector schemes [140–142] are the most used. Accordingly, particular attention will be put on NewtonLeipnik in this section. Therefore, Newton-Leipnik algorithm is suitable for Grunwald-Letnikov fractional order derivative. This approach is based on the fact that for a wide class of functions, three definitions (Grunwald-Letnikov, Riemman-Liouville and Caputo's) are equivalent. For the following fractional differential equation

$$\begin{cases} D_t^\beta X(t) = \frac{d^\alpha X(t)}{dt^\alpha} = F(t, X(t)) \\ X^{(k)}(0) = X_0^{(k)}; k = 0, 1, 2, ...m-1 \end{cases} \tag{2.36}$$

The relation to the explicit numerical approximation of q^{th} derivative at the points kh $(k = 1, 2, ...)$ has the following form [143, 144]

$${}_{k-}L_{m/h}D_{t_k}^\beta f(t_k) \approx h^{-\beta}\sum_{j=0}^{k}(-1)^j \begin{pmatrix} \beta \\ j \end{pmatrix} f(t_{k-j}) \tag{2.37}$$

Where L_m is the "memory lenth", $t_k = kh$, h is the time step of calculation and $(-1)^j \begin{pmatrix} \beta \\ j \end{pmatrix}$ are binomial coefficients $C_j^{(\beta)}$ $(j = 0, 1, ...)$.

For their calculation we can use the following expression

$$C_0^{(\beta)} = 1, C_j^{(\beta)} = \left(1 - \frac{1+\beta}{j}\right) C_{j-1}^{(\beta)} \tag{2.38}$$

According to the short memory principle [139, 142], the length of system memory can be substantially reduced in the numerical algorithm to get reliable results. Therefore, general numerical solution of the fractional differential equation can be given as

$$X^{(k)}(t_k) = F(t_k, X(t_k))h^{\beta} - \sum_{j=1}^{k} C_j^{(\beta)} X(t_{k-j}) \tag{2.39}$$

In Eq.2.39, the memory term expressed by the sum is easy to code, we will used it in the next chapter to approximate the numerical solutions of the PDEs decribing our reduced systems models.

2.2.3.3 Newton-Raphson Method for system of equations

Due to the encountered difficulties for solving the nonlinear system of equations. Many iterative methods are employed in the literature to remedy to this problem. The Newton-Raphson method is defined as an iterative procedure for finding zeros of an equation or the system of nonlinear equations. To illustrate this principle, the system of equations is defined as follows

$$\begin{cases} f(x,y) = 0 \\ g(x,t) = 0 \end{cases} \tag{2.40}$$

The functions $f(x,y)$and $g(x,y)$ are two arbitrary functions.

$$\begin{aligned} f(x,y) &= f(x_0,y_0) + \tfrac{\partial f}{\partial x}(x-x_0) + \tfrac{\partial f}{\partial y}(y-y_0) + o(x,y) \\ g(x,t) &= g(x_0,y_0) + \tfrac{\partial g}{\partial x}(x-x_0) + \tfrac{\partial g}{\partial y}(y-y_0) + o(x,y) \end{aligned} \tag{2.41}$$

The Jacobian matrix associated with above equations is found as follows

$$J(x,y) = \begin{pmatrix} \frac{\partial f}{\partial x} & \frac{\partial f}{\partial y} \\ \frac{\partial g}{\partial y} & \frac{\partial g}{\partial x} \end{pmatrix} \tag{2.42}$$

If $\det(J) \neq 0$, the iterative method is written as

$$X_{n+1} = X_n - J^{-1}(X_n)F(X_n) \tag{2.43}$$

With $X_n = (x_n, y_n)$ and $F(X_n) = (f(X_n), g(X_n))$ A convergence criterion for the solution of a system of non-linear equation could be, for example, the magnitude of the absolute values of the functions $F(X_n)$ is smaller than a certain tolerance

$$F(X_n) < \varepsilon \tag{2.44}$$

To get the algorithm started, we need to provide two initial values of X_0 . This algorithm is robust, fast and very convergent.

2.3 Performance evaluation of isolators: Transmissibility

In many engineering applications the problem is that of preventing vibrations to be transmitted: most generally, there are two categories of problems:

- The source of vibration is the payload itself, in which case the intention is to prevent the vibrations to be transmitted to its host structure : in the literature, this first case is referred as the force transmissibility problem ;
- The disturbance to the payload is caused by vibration of the host structure and the goal is to minimize the transmitted vibration : this case referred as the displacement transmissibility problem.

To quantify the effectiveness of the isolation of the system or to characterize its performance, we use the non-dimensioned parameter called transmissibility. In the case of the force transmissibility problem, this parameter (T_F) is the ratio of the force transmitted F_t by the excitation force F_e, and given by

$$T_F = \frac{|F_t(t)|}{|F_e(t)|} \tag{2.45}$$

For a displacement Transmissibility problem, the transmissibility (T_D) is defined as the ratio of the absolute motion amplitude of the isolation object (in steady state) $x(t)$ to the excitation amplitude $y(t)$ and written as

$$T_D = \frac{|x(t)|}{|y(t)|} \tag{2.46}$$

Transmissibility is usually expressed in decibel (dB) and defined as

$$\begin{array}{l} T_F(dB) = 20.\log\left(\frac{|F_t(t)|}{|F_e(t)|}\right) \\ T_D(dB) = 20.\log\left(\frac{|x(t)|}{|y(t)|}\right) \end{array} \tag{2.47}$$

For example, consider an isolator of the Kelvin-Voigt model, supporting a mass m and undergoing an excitation force $F_e(t) = asin(\omega t)$ as shown in Fig.2.1 (a); in this case the transmitted force is given by $F_t(t) = f(t) = kx + c\frac{dx}{dt}$. In another case, we consider that the isolator undergoes a displacement from below (see Fig.2.1 (b)) of expression $y(t) = Ysin(\omega t)$.
According to harmonic balance method, the responses of the structure to payload or base

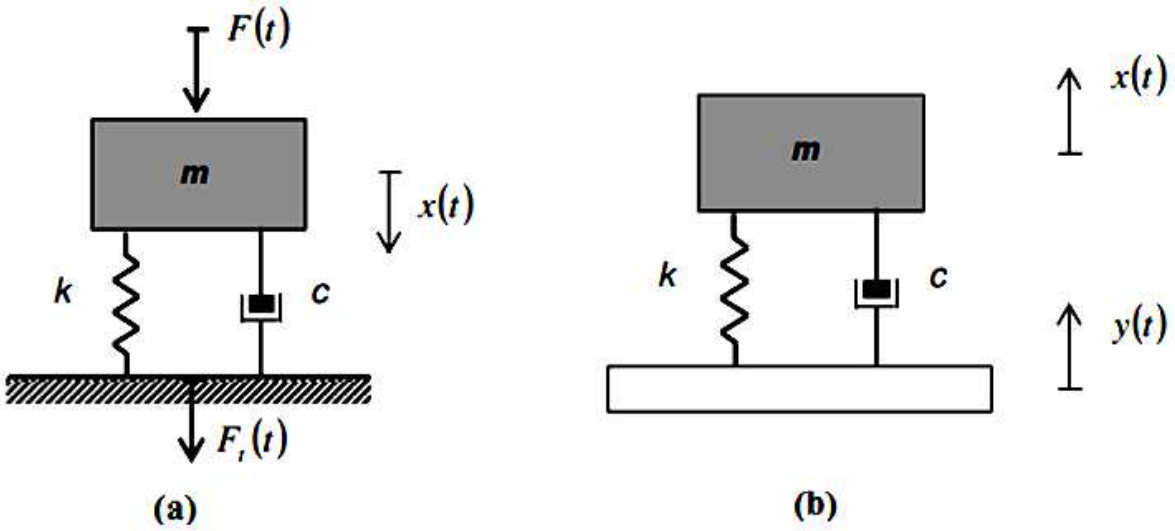

Figure 2.1: Simplest model of a linear isolator base on the Kelvin-voigt. a) Force excitation b)Base excitation

excitation in these examples are in the form $x(t) = A\sin(\omega t + \varphi)$.
Especially for this linear case, we can shows that force and displacement transmissibilities are the same, and for both the mathematical expression is [127]

$$T = T_F = T_D = \sqrt{\frac{1 + 4\xi^2 r^2}{(1 - r^2)^2 + 4\xi^2 r^2}} \tag{2.48}$$

where $\xi = \frac{c}{2}\sqrt{km}$ is the dissipation ratio and $r = \omega/\sqrt{k/m}$ is the nondimensionnal excitation frenquency or frenquency ratio.

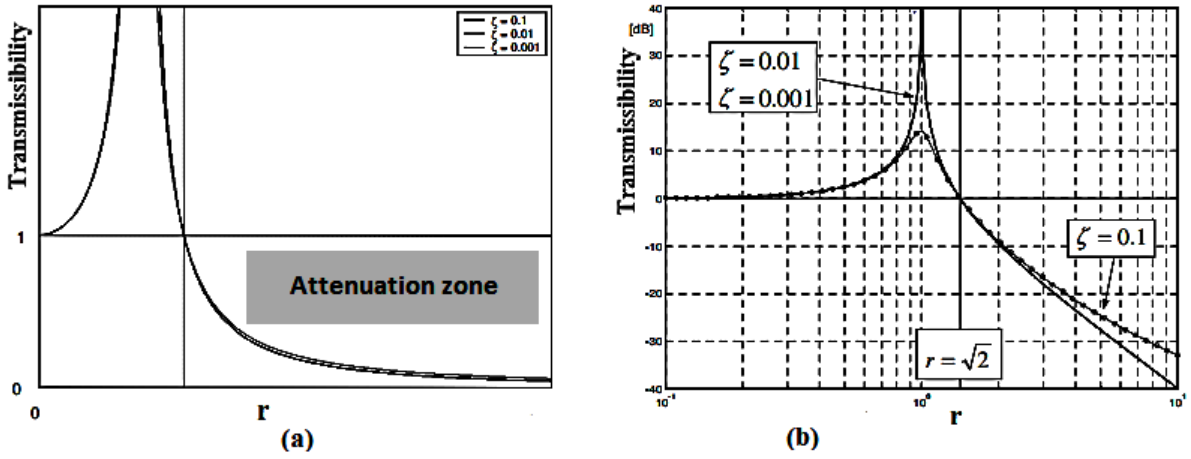

Figure 2.2: Transmissibility as a function of the frequency ratio and for diferent values of the damping ratio. a) Linear representation (left) b) representation in dB (right).

The transmissibility is represented linearly in Fig.2.2(a) and in dB with a logarithmized scale of the frequencies in Fig.2.2(b). From Eq.2.48, two observations follows:

(1) if the isolator is linear, force and displacement transmissibility are the same;

(2) in the idealised case of a mass supported on a linear isolator, transmitted vibrations are only attenuated at frequencies above the square root of two times the fundamental natural frequency of the system, i.e. $T < 1$ when $r > \sqrt{2}$.

Therefore, for a given mass, the frequency above which isolation can occur is governed by the stiffness of the isolator and there is often a practical limitation on the minimum value of this. This zone ($r > \sqrt{2}$) is called the attenuation zone. In this zone, the transmissibility is practically independent of dissipation ratio of the isolator for $\xi < 10$ [127].

2.4 Mechanism of HSLDS AS isolator : Mathematical modelling

Fig.2.3 shows the structural model of HSLDS-AS carrying an isolation object which is in the present case a beam. Fig.2.4 presents the schematic model of HSLDS characteristic when a load is applied. In fact, HSLDS is a non-linear isolator which can induces in the isolated structure non-linear phenomenon like jump [113, 114]. Thus, including the auxiliary system contribute to eliminating the jump phenomenon due to the nonlinear stiffness of the isolator [117]. The advantages of HSLDS-AS are multiple tuned parameters and the elimination of jump phenomenon due to non-linear stiffness of the isolator. A theoretical model of HSLDS-AS isolator consist of a vertical spring with stiffness k_1 and two oblique springs with same stiffness k_4 connected by two rods with the same length ℓ. The auxiliary mass m is added via two vertical springs with stiffness k_3 and k_2. The damping coefficients denoted by c_1, c_2 and c_3, are introduced regards to the energy dissipation. At the static position, springs k_4 have a compression δ_4 and the rods are horizontal; the pre-compressed horizontal spring and the rods realizes negative stiffness mechanism when a load is applied as shows Fig.2.4.

The corresponding force displacement relation of HSLDS is given by [117, 120]

$$F_{HSLDS}(W) = 2k_4 \left(\frac{\ell - \delta_4}{\sqrt{\ell^2 - W^2}} - 1 \right) W + k_1 W \ . \tag{2.49}$$

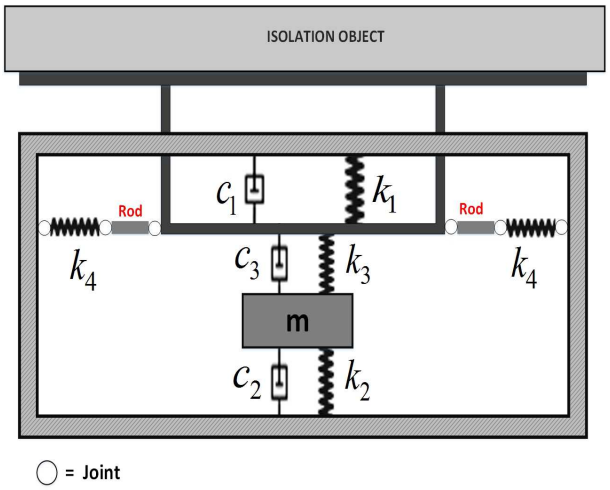

Figure 2.3: Structural model of HSLDS-AS

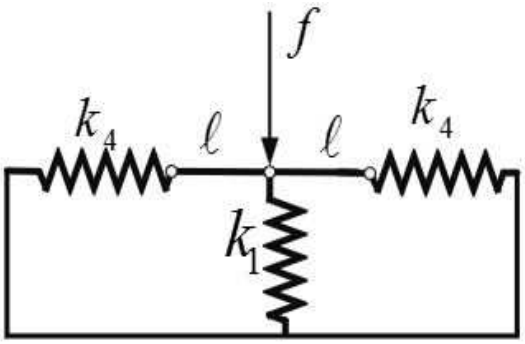

Figure 2.4: Schematic model of HSLDS characteristic.

W is the transversal displacement of the beam.

Setting $W^* = \frac{W}{\ell}$, the non-dimensional form of Eq.2.49 is:

$$F^* = \frac{F_{HSLDS}}{k_1 \ell} = 2\lambda_4 \left(\frac{1-e}{\sqrt{1-W^{*2}}} - 1 \right) W^* + W^*, \tag{2.50}$$

differentiating Eq.2.50 with respect of W^*, we obtains the non dimensional stiffness

$$K^* = 2\lambda_4 \left(\frac{1-e}{(1-W^{*2})^{\frac{3}{2}}} - 1 \right) + 1. \tag{2.51}$$

Considering that the system exhibits small displacement, Eq.2.50 and Eq.2.51 can be approximated by using Taylor series expansion at third order and we one obtain

$$F^* \simeq \alpha^2 W^* + \beta W^{*3}, \tag{2.52}$$

$$K^* \simeq \alpha^2 + 3\beta W^{*2}. \tag{2.53}$$

where

$$\begin{aligned} \alpha^2 &= 1 - 2\lambda_4 e; \\ \beta &= \lambda_4(1-e); \\ \lambda_4 &= k_4/k_1; \\ e &= \delta_4/\ell. \end{aligned} \quad . \tag{2.54}$$

Fig.2.5a and Fig.2.5b shows the comparative curves of F^* and K^*, for exact and approx-

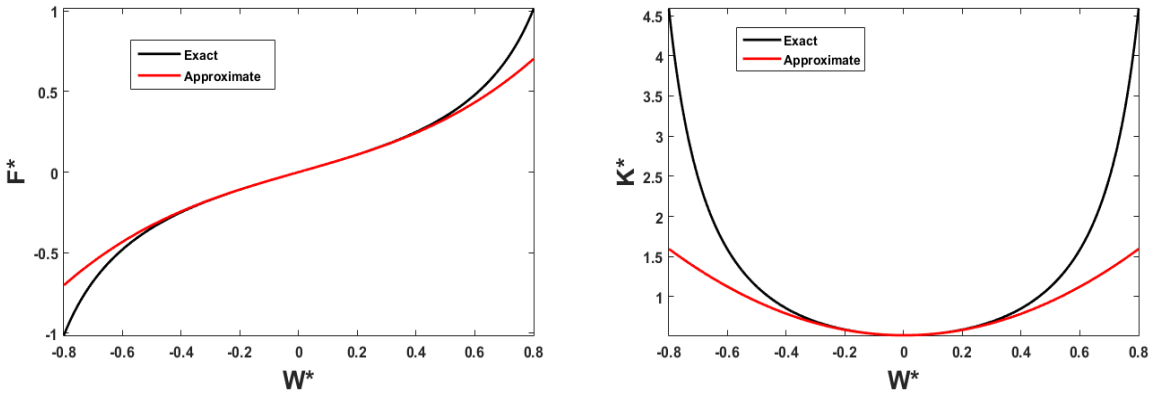

Figure 2.5: Comaprison between the exact and approximate non-dimensional expressions: a) force-displacement relationships and b) stiffness of HSLDS system for $\lambda_4 = 1.0$ and $e = 0.5$.

imate expressions. In case of small displacement, one can conclude a good correlation. Because of the satisfactory precision, the following approximate expression of force displacement are used for our study:

$$F_{HSLDS} \simeq k_1 \ell (\alpha^2 \frac{W}{\ell} + \beta \frac{W^3}{\ell^3}) \tag{2.55}$$

2.5 Hardware and software

As machine support during this thesis work, we used a Laptop computer running Ubuntu and Windows 10 Pro operating system and five major software's: Microsoft visio for desgin the structure, Python and Fortran for differential equations, Matlab for data analysis and Maple for integral calculus.

2.6 Conclusion

The present chapter has been devoted to the presentation of mathematical and numerical used for the analysis of the problem of this thesis. Also, tool for evaluated performance and established mathematical mode of an isolator have been presented. Using all these methods, techniques and materials, we are now able to follow this study and obtain different results that give us informations about the different states of the studied systems. The results are presented in Chapter 3.

Chapter III

Results and discussion

3.1 Introduction

Thermal effect on structure is of great theoretical and practical significance in structural engineering. This third chapter is devoted to the results and discussions on the work carried out in this thesis. The work done by others researchers is extend by proposing the solutions to some of the limits encountered in this field of research which are identified and listed in chapter I. Due to the complexity of thermal loads on structure, various assumptions are taking into account, including the constitutive material of structure. Thus, in the second and the third sections, the effect of thermal variations on two types of structure (isolated by a non-linear isolator or constituted by a material containing fractional derivative order) is well established. Modelled as an Euler Bernoulli beam, the considered structures are subjected to the combined action of wind load flow and platoon moving loads in the first and, to a simple moving load results and for in the second results. The last section summarises our results and concludes the chapter.

3.2 On the non-linear thermomechanical analysis of a stayed-beam having fractional viscoelastic properties in complex environment.

In this section, non-linear thermomechanical analysis of a stayed-beam having fractional viscoelastic properties taking into account a complex environment; thus thermal loads, wind loads and platoon moving load condition, is investigated. Using Newton's second law on the movement, the equation of dynamics is derived and reduced to generalized modal forms using Garlerkin's technique. At the first mode of vibration, the Analytical solution is established via multiple scales methods. Also the appearance condition of divers type of bifurcation is obtained using linear analysis ; and then, numerical methods are employed for analysis the effect of the fractional viscoelastic, thermal variation and loads spacemen on structural dynamics.

3.2.1 Mathematical modelling

3.2.1.1 Dynamical analysis

In the present study, the structure described in Fig.3.1 is a beam suspended by a massless inextensible cable. Cosidering the physical model (see Fig. 3.2)we see that,the system is subjected to the combined action of a platoon moving loads and turbulent wind. The Euler Bernoulli beam is modeled here by a fractional hereditary material involving the Kelvin-Voigt model with real order fractional derivatives [147, 148]. The homogeneous beam is simply supported and placed in an environment subjected to a change in temperature variation. Since the temperature induces axial tension in the beam [158], additional stresses and strains are created in the structure.

Figure 3.1: Real model of the structure (Pont Mohammed VI à Rabat).

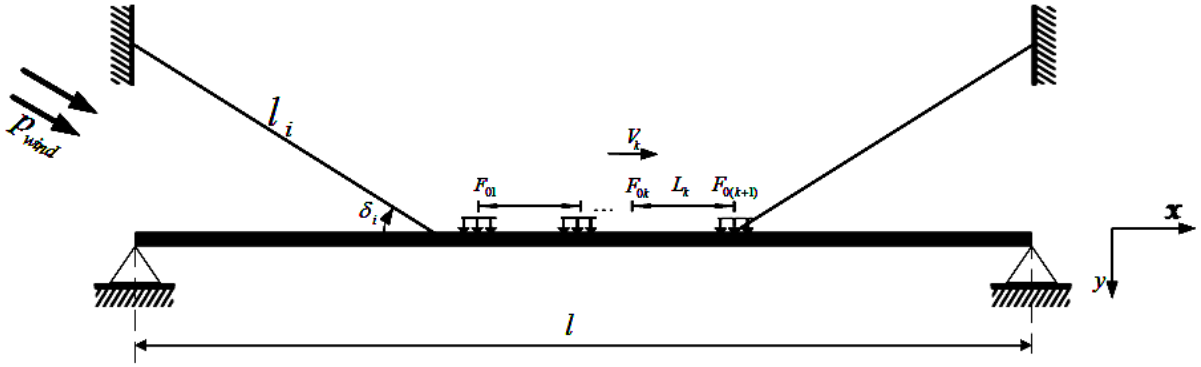

Figure 3.2: Physical model.

Taking into account the external loads on the structure and the action of the cables, the application of Newton's second law of motin on the movement leads to the equation

of dynamics shown in Eq.3.1 [126, 134, 153]

$$\rho S\frac{\partial^2 W(x,t)}{\partial t^2}+EI\left(\frac{\partial^4 W(x,t)}{\partial x^4}-\frac{3}{2}\frac{\partial^2}{\partial x^2}\left(\frac{\partial^2 W(x,t)}{\partial x^2}\left(\frac{\partial W(x,t)}{\partial x}\right)^2\right)\right)+\xi\frac{\partial W(x,t)}{\partial t}+(\theta_{NL}+H^c)\frac{\partial^2 W}{\partial x^2}$$
$$-\frac{ES}{2l}\frac{\partial^2 W}{\partial x^2}\int_0^l\left(\frac{\partial W(x,t)}{\partial x}\right)^2 dx+\sum_{i=1}^{N_c}K_i^c\delta(x-\tfrac{il}{N_c})W(x,t)=p_{wind}+p_{mov} \tag{3.1}$$

$W(x,t)$ denotes the transversal displacement of the beam, l the length of the beam, S the cross-section area, I the moment of inertia, ρ is the density of the material, and ξ the dissipation coefficient of the beam. As that external force can induce large deformations and bring the geometrical non-linearity effect on the response of the structure, the terms $\frac{3}{2}EI\frac{\partial^2}{\partial x^2}\left(\frac{\partial^2 W(x,t)}{\partial x^2}\left(\frac{\partial W(x,t)}{\partial x}\right)^2\right)$ refer to large deformations in the structure and $\frac{ES}{2l}\frac{\partial^2 W}{\partial x^2}\int_0^l\left(\frac{\partial W(x,t)}{\partial x}\right)^2 dx$ to geometrical non-linearity.

The action of the cables on the structure is taken into account by the introducing H^c (the horizontal component of the total tension due to the cables) in the beam and K_i^c the linear stiffness of each cable, defined by Eq.3.2 [122]

$$K_i^c=\frac{E_iS_i}{l_i}\sin^2\delta_i \tag{3.2}$$

with N_c ,E_i ,S_i ,l_i and δ_i respectively, the number of cables, the Young's modulus, the section, the length and the angle of inclination of the ith cable. Each pair of cables is located on the beam by $\delta(x-x_i)$, where $\delta(.)$ is the Dirac function and $x_i(i=1,2)$ denotes the position of the ith cable on the beam. To model the viscoelastic behavior with the fractional order model, the Young's modulus is written as in Eq.(3.3) [146]

$$E=E_0+\mu D_t^\beta; \tag{3.3}$$

where E_0 represents the Young's modulus of the beam and μ the coefficient of viscoplasticity. D_t^β is the fractional derivative of real order β with $\beta\in]0;1]$. There are several definitions of fractional order, the fractional order use in this paper is defined by [150,151,160] Eq.3.4

$$D_t^\beta q(t)=\frac{d^\beta q(t)}{dt^\beta}=\frac{d}{dt}\int_{-\infty}^{t}\frac{q(u)du}{\Gamma(1-\beta)(t-u)^\beta}, \tag{3.4}$$

The part $\theta_{NL}\frac{\partial^2 W}{\partial x^2}$ reflects the thermal effect on the structure which is an axial force per unit length due to a thermal variation ΔT. In the present case, the nonlinear thermal stress distribution [46, 126] is considered and given by Eq.3.5

$$\theta_{NL}=EA(\kappa\Delta T+\frac{\hbar}{E}(\kappa\Delta T)^2), \tag{3.5}$$

where $\hbar = \hbar_1(1-2\nu) - 2\hbar_2(\nu^2-1) + \hbar_3\nu^2$ in which,$\hbar_1$,$\hbar_2$ and $\hbar_3$ are Murnaghan's constants; ν the Poisson's ratio of the material. The contribution of the non-linear term which depends on $\frac{\hbar}{E}$ defines negative and that depends on the nature of the material. As we focus on uniform thermal variation, Eq.3.5 can be rewrite as Eq.3.6

$$\theta_{NL} = E_0 A(\kappa\Delta T + \frac{\hbar}{E_0}(\kappa\Delta T)^2). \tag{3.6}$$

The wind load is taking into acount by the term p_{wind} which is the aerodynamic force due to the wind determined according to the quasi-steady theory [68, 69, 125] and given by Eq.3.7

$$p_{wind} = \frac{1}{2}\rho_a U^2 b \left[A_1\left(\frac{\dot{W}}{U}\right) + A_3\left(\frac{\dot{W}}{U}\right)^3\right], \tag{3.7}$$

Where, $U = \bar{u} + u(t)$ is the wind speed devised into the turbulent part $u(t)$ and stationary part $\bar{u}$ (average wind speed in the region); b is the thickness of the beam, A_1 and A_3 are the aerodynamic coefficients given in [70]. Considering $\bar{u}$ very large than turbulence, a Taylor expansion allows us to obtain Eq.3.8

$$p_{wind} = \frac{1}{2}\rho_a \bar{u}^2 b \left[A_1(1+\frac{u(t)}{\bar{u}})\frac{\dot{W}}{\bar{u}} + A_3\left(1-\frac{u(t)}{\bar{u}}\right)\left(\frac{\dot{W}}{\bar{u}}\right)^3\right] \tag{3.8}$$

The moving load problem modelled here by p_{mov} , is the force due to a platoon moving loads made up of K moving loads. The mathematical expression of the loads due to this type of traffic, which takes into account the roughness of the deck is given by Eq.3.9 [86]

$$p_{mov} = \sum_{k=1}^{K} F_{0k}\cos(\Omega_k t)\delta\left(x - Vt - \sum_{k'=1}^{k} L_{k'}\right) \tag{3.9}$$

$L_k > 0$ is the distance between the charges ($k = 1, 2, 3....K; L_1 = 0$), F_{0k} represents the amplitude, and Ω_k the frequency due to the roughness of the road and V_k the travel speed of the k^{th} load.

For a simply supported beam, the boundary conditions can be defined as Eq.**??**

$$\begin{aligned} &W(0,t) = W(l,t) = 0 \\ &\tfrac{\partial^2 W}{\partial x^2}\,|_{x=0} = \tfrac{\partial^2 W}{\partial x^2}\,|_{x=l} = 0 \end{aligned} \tag{3.10}$$

In the next section, modal equation is derived taking into account boundary conditions.

3.2.1.2 Modal governing equation

The Galerkin's approximation is often used to transform the partial derivative equation into an ordinary differential equation [125]; according to this method, the solution of the

partial differential Eq.3.1 is given by Eq.3.11

$$W(x,t) = \sum_{n=1}^{\infty} \phi_n(x) q_n(t), \tag{3.11}$$

where n is the mode index, $q_n(t)$ is the time function of each mode and $\phi_n(x)$ is the solution of the eigenvalue problem depending on the boundary conditions of the cable stayed-beam. For a simply supported beam the spacial function is given by Eq.3.12

$$\phi_n(x) = \sin(\frac{n\pi x}{l}). \tag{3.12}$$

Setting ${q_n}^* = \frac{q_n}{l}$; $u^* = \frac{u}{\bar{u}_0}$; $t^* = \omega_{0n} t$ and considering Eq.3.1, the modal equation is obtained. Omitting the asterisk, this modal equation is writing as Eq.3.13

$$\begin{aligned}
&\ddot{q}_n(t) + \omega_n^2 q_n(t) + (\xi - \chi_1(\bar{u} + u(t)))\dot{q}_n(t) + \eta_n^\beta D_t^\beta q_n(t) - D_t^\beta \sum_{i=1}^{\infty}\sum_{j=1}^{\infty}\sum_{k=1}^{\infty} \gamma_{1nijk}^\beta q_i(t) q_j(t) q_k(t) \\
&- \sum_{i=1}^{\infty}\sum_{j=1}^{\infty}\sum_{k=1}^{\infty} \gamma_{2nijk} q_i(t) q_j(t) q_k(t) - \left(\tfrac{1}{\bar{u}} - \tfrac{u(t)}{\bar{u}^2}\right) \sum_{i=1}^{\infty}\sum_{j=1}^{\infty}\sum_{k=1}^{\infty} \chi_{3nijk} \dot{q}_i(t)\dot{q}_j(t)\dot{q}_k(t) \\
&= \sum_{k=1}^{K} f_{0k} \left[\sin(\Omega_{2k} t + \varphi_k) + \sin(\Omega_{1k} t + \varphi_k)\right]
\end{aligned} \tag{3.13}$$

where,

$$\begin{aligned}
&\omega_n^2(\theta_{nl}) = \tfrac{2E_0 I}{\rho S l \omega_0^2} \int_0^l \phi_n(x) {\phi''''}_n(x) dx + 2(l\theta_{nl} + \tfrac{2H^c}{\rho S l \omega_0^2}) \int_0^l {\phi''}_n(x) \phi_n(x) dx + \sum_{i=1}^{N_c} \tfrac{2K_i^c}{\rho S l \omega_0^2} \phi_n^2(x_i) \\
&\gamma_{1nijk}^\beta = \tfrac{\mu \omega_0^{\beta-2}}{\rho} \left(\tfrac{3Il}{S} \int_0^l \phi_n(x) \left({\phi''}_i(x) {\phi'}_j(x) {\phi'}_k(x)\right)'' dx + \int_0^l \phi_n(x) {\phi''}_i(x) \int_0^l {\phi'}_j(x) {\phi'}_k(x) dx dx \right) \\
&\gamma_{2nijk} = \tfrac{E_0}{\rho \omega_0^2} \left(\tfrac{3Il}{S} \int_0^l \phi_n(x) \left({\phi''}_i(x) {\phi'}_j(x) {\phi'}_k(x)\right)'' dx + \int_0^l \phi_n(x) {\phi''}_i(x) \int_0^l {\phi'}_j(x) {\phi'}_k(x) dx dx \right) \\
&\eta_n^\beta = \tfrac{2\mu I \omega_0^{\beta-2}}{\rho S l} \int_0^l \phi_n(x) {\phi''''}_n(x) dx; \chi_{3nijk} = \tfrac{\rho_a b A_3 l \omega_0}{\rho S u_0} \int_0^l \phi_n(x) \phi_i(x) \phi_j(x) \phi_k(x) dx \\
&\xi = \tfrac{c}{\rho S \omega_0}; \chi_1 = \tfrac{\rho_a b A_1 u_0}{2\rho S \omega_0}; \omega_0^2 = \tfrac{E_0 I \pi^4}{\rho S l^4}; f_{0k} = \tfrac{F_{0k}}{\rho S l^2 \omega_0^2}; v_k = \tfrac{V_k}{l\omega_0}; \omega_k = \tfrac{\Omega_k}{\omega_0} \\
&l_k = \tfrac{L_k}{l}; u_0 = 1.0 m.s^{-1}; \varphi_k = \pi \sum_{k'=1}^{k} l_{k'}; \Omega_{2k} = \pi v_k + \omega_k; \Omega_{1k} = \pi v_k - \omega_k.
\end{aligned} \tag{3.14}$$

The non-dimensional non-linear thermal stress is written as $\theta_{nl} = \frac{\theta_{NL}}{\rho S l^2 \omega_0^2}$. For the sake of simplicity let us consider negligible the roughness of the road and the mechanical vibrations of loads i.e. $\omega_k = 0$ thus $\Omega_{2k} = \Omega_{1k}$. For this model, a set of loads of the same speed is considered, thus $v_k = v$ and then $\Omega_{2k} = \Omega_{1k} = \Omega_1$. Following this, the equation of the dynamics at the first order of vibrations is written [155, 156] as Eq.3.15

$$\begin{aligned}
\ddot{q} + \omega_n^2(\theta_{nl}) q + (\xi - \chi_1(\bar{u} + u(t)))\dot{q} + \eta^\beta D_t^\beta q - \gamma_1^\beta D_t^\beta q^3 - \gamma_2 q^3 \\
-\chi_3 \left(\tfrac{1}{\bar{u}} - \tfrac{u(t)}{\bar{u}^2}\right) \dot{q}^3 = \sum_{k=1}^{K} 2 f_{0k} \sin(\Omega_1 t + \varphi_k)
\end{aligned} \tag{3.15}$$

The Multi-scale method is an alternative to solve this last equation containing the fractional real order [154]. The steps of the resolution according to the multiple scale method are given in the following sections.

3.2.2 Analytical exploration using perturbation method

To solve non-linear differential equation, methods of perturbation are most often used in the case of parametric systems. The multi-step scale method is used to analytically investigate the dynamics of the system. In this article, the wind turbulence is setting as a harmonic function $u(t) = u_1 \sin(\Omega t)$.

Assuming that ξ , χ_1 ,η^β ,γ_1^β ,γ_2 ,χ_3 and f_{0k} are small perturbed and considering the case of primary resonance which is the most important [68], Ω defined as Eq.3.16

$$\Omega = 2\omega(\theta_{nl}) + \varepsilon\sigma_0 \tag{3.16}$$

In the case of moving load, we consider the first primary resonance as Eq.3.17

$$\Omega_1 = \omega(\theta_{nl}) + \varepsilon\sigma_1 \tag{3.17}$$

Eq.**??** can be rewritten as Eq.3.18

$$\ddot{q} + \omega_n^2(\theta_{nl})q = \varepsilon\tilde{H}(q, \dot{q}) \tag{3.18}$$

with $\tilde{H}(q, \dot{q})$ given by Eq.3.19

$$\begin{aligned}\tilde{H}(q, \dot{q}) = &-(\xi - \chi_1(\bar{u} + u(t)))\dot{q} - \eta^\beta D_t^\beta q + \gamma_1^\beta D_t^\beta q^3 + \gamma_2 q^3 \\ &+ \chi_3\left(\tfrac{1}{\bar{u}} - \tfrac{u(t)}{\bar{u}^2}\right)\dot{q}^3 + \sum_{k=1}^{K} 2f_{0k}\sin(\Omega_1 t + \varphi_k)\end{aligned} \tag{3.19}$$

In the above relations, ε is the bookkeeping parameters; σ_0 and σ_1 are deturning parameters.

The first order uniform expansion using this procedure is in the form

$$q(t) = q_0(T_0, T_1) + \varepsilon q_1(T_0, T_1) + ... \tag{3.20}$$

with $T_0 = t$ and $T_1 = \varepsilon t$. T_0 is the fast time and T_1 slow time. Combining Eq.3.18 and Eq.3.20 and equaling the coefficients of the same order as ε , Eq.3.21 and Eq.3.22 are derived.

Order ε^0

$$\left(D_0^2 + \omega^2(\theta_{nl})\right) q_0 = 0 \tag{3.21}$$

Order ε^1

$$\begin{aligned}&(D_0^2+\omega^2(\theta_{nl}))\,q_1=-2D_0D_1q_0-(\xi-\chi_1(\bar{u}+u(t)))D_0q_0-\eta^\beta D_0^\beta q_0\\&+\gamma_2q_0^3+\gamma_1^\beta D_0^\beta q_0^3+\chi_3(\tfrac{1}{\bar{u}}-\tfrac{u(t)}{\bar{u}^2})(D_0q_0)^3+\sum_{k=1}^{K}2f_{0k}\sin(\Omega_1t+\varphi_k)\end{aligned}\tag{3.22}$$

where $\frac{\partial^m}{\partial t^n}=D_n^m,\quad m=1;\quad n=0,1$ and $D^\beta=\left(\frac{d}{dt}\right)^\beta=(D_0+\varepsilon D_1+\varepsilon^2D_2+.....)^\beta$ $=D_0^\beta+\varepsilon D_0^{\beta-1}D_1+\varepsilon^2\beta(\beta-1)D_0^{\beta-2}D_2$ D_0^β is calculated from relation Eq.3.4 by replacing t by T_0. So, the fractional derivative is defined as the fractional power of the differentiation operator. For the sack of simplicity, $\omega=\omega(\theta_{nl})$. Then, the general solutions of Eq.3.21 is sought as Eq.3.23

$$q_0=A(T_1)\exp(j\omega T_0)+cc\tag{3.23}$$

By combining relations Eq.3.18, Eq.3.22 and Eq.3.23 and the eliminating the secular term Eq.3.24is obtained:

$$\begin{aligned}&j\omega(2A'+\xi A-\chi_1\bar{u}A)+\tfrac{1}{2}\omega\chi_1u_1\bar{A}\mathrm{e}^{j\sigma_1T_0}-(j\omega)^\beta(3\gamma_1^\beta A^2\bar{A}-\eta^\beta A)-3\gamma_2A^2\bar{A}\\&-3\tfrac{j\chi_3\omega^3}{\bar{u}}A^2\bar{A}-\tfrac{\chi_3\omega^3}{2\bar{u}^2}u_1(A^3\mathrm{e}^{-j\sigma_1T_1}-3\bar{A}^2\mathrm{A}\mathrm{e}^{j\sigma_1T_0})+jF_0e^{j\sigma_0T_0}=0,\end{aligned}\tag{3.24}$$

where $F_0=\sum_{k=1}^{K}f_{0k}e^{j\varphi_k}$ is the amplitude of the force due to moving load which is a function of load and the distance between the charges. In the next section on linear and non-linear analysis of the structure are investigated.

3.2.2.1 Analysis of linear stability

For this issues, the solution of Eq.3.24 is setting in cartesian forms as shown in Eq.3.25

$$A=Z(t)e^{j\frac{\sigma}{2}t}=(X(t)+iY(t))e^{j\frac{\sigma}{2}t}\tag{3.25}$$

Inserting Eq.3.25 in Eq.3.24 and separating the real part to the imaginary part, Eq.3.26 is derived

$$\begin{pmatrix}X'\\Y'\end{pmatrix}=J\begin{pmatrix}X\\Y\end{pmatrix}+n(n_X,n_Y)\tag{3.26}$$

J is the Jacobian matrix evaluated at the trivial solution given by Eq.3.27

$$J=\begin{bmatrix}-\frac{1}{2}(\xi-\chi_1\bar{u}+\eta^\beta\omega^{\beta-1}\sin(\frac{\beta\pi}{2}))&\frac{1}{2}(\sigma+\frac{\chi_1u_1}{2}-\eta^\beta\omega^{\beta-1}\cos(\frac{\beta\pi}{2}))\\\frac{1}{2}(-\sigma+\frac{\chi_1u_1}{2}+\eta^\beta\omega^{\beta-1}\cos(\frac{\beta\pi}{2}))&-\frac{1}{2}((\xi-\chi_1\bar{u})+\eta^\beta\omega^{\beta-1}\sin(\frac{\beta\pi}{2}))\end{bmatrix}\tag{3.27}$$

The non-linear terms are given by Eq.3.28

$$\begin{aligned} n_X &= \tfrac{3}{2}(\gamma_2\omega^{-1} + \gamma_1^{\beta}\omega^{\beta-1}\cos(\tfrac{\beta\pi}{2}))(YX^2+Y^3) + \tfrac{3}{2}(\tfrac{\chi_3\omega^2}{\bar{u}} + \gamma_1^{\beta}\omega^{\beta-1}\sin(\tfrac{\beta\pi}{2}))(X^3+XY^2) \\ &+ \tfrac{\chi_3\omega^2}{4\bar{u}^2}u_1\left((-Y^3-3YX^2) - 3Y(X^2+Y^2)\right) - \tfrac{1}{2}F_0\omega^{-1}\cos\tfrac{\sigma}{2}t \\ n_Y &= -\tfrac{3}{2}(\gamma_2\omega^{-1} + \gamma_1^{\beta}\omega^{\beta-1}\cos(\tfrac{\beta\pi}{2}))(X^3+XY^2) + \tfrac{3}{2}(\tfrac{\chi_3\omega^2}{\bar{u}} + \gamma_1^{\beta}\omega^{\beta-1}\sin(\tfrac{\beta\pi}{2}))(YX^2+Y^3) \\ &- \tfrac{\chi_3\omega^2}{4\bar{u}^2}u_1\left((X^3-3XY^2) - 3X(X^2+Y^2)\right) - \tfrac{1}{2}F_0\omega^{-1}\sin\tfrac{\sigma}{2}t \end{aligned} \tag{3.28}$$

The stability of the system is established when the real parts of eigenvalues of Jacobian matrix are negative. The defined bifurcation parameters is $(\bar{u}, u_1, \sigma)$. The eigenvalues of Jacobian matrix are given by Eq.3.29

$$\mu_{\pm} = (\xi - \chi_1\bar{u} + \eta^{\beta}\omega^{\beta-1}\sin(\frac{\beta\pi}{2})) \pm \sqrt{\Delta_{\beta,\theta_{nl}}(\sigma,u_1)} \tag{3.29}$$

with $\Delta_{\beta,\theta_{nl}}(\sigma,u_1) = -(\sigma - \eta^{\beta}\omega^{\beta-1}\cos(\frac{\beta\pi}{2}))^2 + (\chi_1 u_1)^2$

It is important to observe that, fractional order and thermal effect, modifies the appearance condition of bifurcation. This observation is discussed in this thesis. Depending on the sign of $\Delta_{\beta,\theta_{nl}}(\sigma,u_1)$, we can distinguished flip bifurcation obtained when the eigenvalue values are all real and Neimark-Sacker bifurcation obtained when the eigenvalues are complex; the appearance of these types of bifurcation is largely discussed in [68]. Following this last issue, we will focus on the effects of fractional derivative order and thermal load on the linear stability domain.

When $\Delta_{\beta,\theta_{nl}}(\sigma,u_1) = 0$; μ_- and μ_+ are real and equal. Then, critical speed is reached if $\mu_- = \mu_+ = 0$, and Hopf bifurcation (a type of flip bifurcation) is observed. In many studies the critical speed is called as the galloping speed of the structure. If the condition of appearance of Hopf bifurcation is satisfied [68], critical speed is written as Eq.3.30.

$$\bar{u}_c = \bar{u}_c(\theta_{nl},\beta) = \frac{\xi + (\omega(\theta_{nl}))^{\beta-1}\eta^{\beta}\sin(\frac{1}{2}\beta\pi)}{\chi_1} \tag{3.30}$$

It is clear that, fractional derivative order and thermal variation affects the critical speed. So, to clarify the effect of thermal variation and fractional derivative order on critical speed, the following ratios are defined as Eq.3.31

$$R_{\bar{u}_c}(\theta_{nl},\beta) = \frac{\bar{u}_c(\theta_{nl},\beta) - \bar{u}_{c0}}{\bar{u}_{c0}} \times 100 \tag{3.31}$$

where $\bar{u}_{c0} = \frac{\xi}{\chi_1}$ is the critical speed in the absence of fractional derivative order. Also, thermal loads and fractional order interacts together on the structure; in order to clarify this interaction Eq.3.32 is defined as

$$R_0(\theta_{nl},\beta)=\frac{\bar{u}_c(\theta_{nl},\beta)-\bar{u}_c(\theta_{nl}=0,\beta)}{\bar{u}_c(\theta_{nl}=0,\beta)}\times 100 \tag{3.32}$$

$\bar{u}_c(\theta_{nl}=0,\beta)$is the critical speed in the absence of thermal variation for a given fraction derivative order.

3.2.2.2 Non-linear problem analysis

To derive real equations, the amplitude of Eq.3.24 is set in polar form as Eq.3.33

$$A=\frac{1}{2}a(T_1)e^{j\psi(T_0)} \tag{3.33}$$

In this later relation, a and ψ are the amplitude and the phase successively. By integrating Eq.3.33 into Eq.3.31, Eq.3.34 is derived.

$$\begin{aligned}&j\omega a'-\omega\psi' a+\tfrac{1}{2}j\omega\xi a-\tfrac{1}{2}j\omega\chi_1\bar{u}a+\tfrac{1}{4}\omega\chi_1 u_1 a\mathrm{e}^{j(\sigma_0T_1-2\psi)}-\tfrac{3}{8}\gamma_2a^3-\tfrac{3}{8}\frac{j\chi_3\omega_b^3}{\bar{u}}a^3\\&-\tfrac{\chi_3\omega^3u_1}{16\bar{u}^2}a^3\mathrm{e}^{-j(\sigma_0T_1-2\psi)}+\tfrac{3\chi_3\omega^3u_1}{16\bar{u}^2}a^3\mathrm{e}^{j(\sigma_0T_1-2\psi)}-(j\omega)^\beta(\tfrac{3\gamma_4^\beta}{8}a^3-\tfrac{\eta^\beta}{2}a)+jF_0\mathrm{e}^{j(\sigma_1T_1-\psi)}=0\end{aligned} \tag{3.34}$$

Setting $\phi_0=\sigma_0T_0-2\psi$ and $\phi_1=\sigma_1T_0-\psi$ the trivial periodic solution of Eq.3.24 is obtained for $\phi_0'=\phi_1'=0$, that means $2\sigma_1=\sigma_0=\sigma$; thus $2\sigma_1=\omega$

For the sake of simplicity choosing $\phi=\sigma t-2\psi(t)$ and taking Eq.3.34 into account, we establish the autonomous modulation equations by separating the real part from the imaginary part are given by Eq.3.35

$$\begin{aligned}&a\phi'=a\sigma+\tfrac{3}{8}\gamma_3\omega^{-1}a^3+\omega^{\beta-1}(\tfrac{3\gamma_1^\beta}{8}a^2-\tfrac{1}{2}\eta^\beta)acos(\tfrac{1}{2}\beta\pi)\\&-(\tfrac{\chi_3\omega^2}{8\bar{u}^2}a^2+\tfrac{\chi_1}{4})au_1cos(\phi)+\sum_{k=1}^{K}f_{0k}\omega^{-1}\sin(\tfrac{1}{2}\phi+\varphi_k)\\&a'=-\tfrac{1}{2}\xi a+\tfrac{1}{2}\chi_1\bar{u}a+\tfrac{3}{8}\tfrac{\chi_3\omega^2}{\bar{u}}a^3+\omega^{\beta-1}(\tfrac{3\gamma_1^\beta}{8}a^2-\tfrac{1}{2}\eta^\beta)a\sin(\tfrac{1}{2}\pi\beta)\\&-(\tfrac{\chi_3\omega^2}{4\bar{u}^2}a^2+\tfrac{1}{4}\chi_1)au_1\sin(\phi)-\sum_{k=1}^{K}f_{0k}\omega^{-1}\cos(\tfrac{1}{2}\phi+\varphi_k)\end{aligned}. \tag{3.35}$$

The expression of the time dependent equation derived from Eq.3.23 is given by Eq.3.36

$$q(t)=a(t)\sin(\frac{\Omega}{2}t-\frac{\phi(t)}{2}) \tag{3.36}$$

The non-trivial periodic solutions of the cable stayed beam are obtained by setting $a'=\phi'=0$. For investigating the stability of non-trivial periodic solution, the nature of fixed points of Eq.3.35 is interesting. Introducing small perturbation such as Eq.3.37

$$\begin{aligned}a&=a_0+a_1\\\phi&=\phi_0+\phi_1\end{aligned} \tag{3.37}$$

where a_0 and ϕ_0 are non-trivial periodic solutions, a_1 and ϕ_1 are small perturbations. Inserting Eq.3.37 in the modulations equations and keeping the linear terms of these two variables we obtains Eq.3.38

$$\begin{aligned} 4\omega a'_1 &= a_1\Gamma_1 + \phi_1\Gamma_2 \\ 4\omega \phi'_1 &= a_1\Gamma_3 + \phi_1\Gamma_4 \end{aligned} , \tag{3.38}$$

where

$$\begin{aligned} \Gamma_1 &= -2\omega_b\xi + 2\omega_b\chi_1\bar{u} + \tfrac{9}{2}\tfrac{\chi_3\omega_b^3}{\bar{u}}a_0^2 - \tfrac{3\chi_3\omega_b^3u_1}{\bar{u}^2}a_0^2\sin(\phi_0) - 2\chi_1u_1\omega_b\sin(\phi_0) \\ &\quad + \tfrac{9(\omega_b)^\alpha\gamma_4^\alpha}{2}a_0^2\sin(\tfrac{1}{2}\pi\alpha) - 2(\omega_b)^\alpha\eta^\alpha\sin(\tfrac{1}{2}\pi\alpha) \\ \Gamma_2 &= -\tfrac{\chi_3\omega_b^3u_1}{\bar{u}^2}a_0^3\cos(\phi_0) - 2\chi_1u_1\omega_ba_0\cos(\phi_0) + 8F_0\sin(\tfrac{1}{2}\phi_0) \\ \Gamma_3 &= 3\gamma_3a_0 - \tfrac{2F_0}{a_0}\cos(\tfrac{1}{2}\phi_0) + 3(\omega_b)^\alpha\gamma_4^\alpha a_0 cos(\tfrac{1}{2}\alpha\pi) - \tfrac{\chi_3\omega_b^2}{\bar{u}^2}a_0u_1\omega_b cos(\phi_0) \\ \Gamma_4 &= \tfrac{\chi_3\omega_b^2}{2\bar{u}^2}a_0^2u_1\omega_b\sin(\phi_0) - 2\chi_1u_1\omega_b\sin(\phi_0) + \tfrac{4F_0}{a_0}\cos(\tfrac{1}{2}\phi_0) \end{aligned} , \tag{3.39}$$

Then we derive Eq.3.40

$$\begin{bmatrix} a'_1 \\ \phi_1{}' \end{bmatrix} = \frac{1}{4\omega}\begin{bmatrix} \Gamma_1 & \Gamma_2 \\ \Gamma_3 & \Gamma_4 \end{bmatrix}\begin{bmatrix} a_1 \\ \phi_1 \end{bmatrix}. \tag{3.40}$$

Setting Eq.3.41

$$A = \begin{bmatrix} \Gamma_1 & \Gamma_2 \\ \Gamma_3 & \Gamma_4 \end{bmatrix}, \tag{3.41}$$

the stability of the non-trivial periodic solution depends on the eigenvalues of the Jacobian matrix A. Then, the non-trivial periodic solution are stable if and only if the real parts of the eigenvalues of A are negative.

For numerical analysis, wind loads and moving loads are separately investigated, since the case of combined action these types of loads is well clarified in the literature [11, 69].

3.2.2.3 Analytical solution for the cable stayed-beam subject to wind load only

Consider the existing structure only under the action of wind loads, the modulation equations are given by cancelling the terms related to platoon of moving loads in the modulation equation (Eq.3.35). Taking ϕ as a slave variable and considering the trivial solution $a = 0$, the parametric excitation due to wind load is responsible for the galloping phenomenon appearance which cause a classic bifurcation when turbulence components is absence ($u_1 = 0$) [67]. In this case only the second modulation equation is concerned, so Eq.3.35 becomes Eq.3.42

$$a = \sqrt{\frac{4\bar{u}}{3\omega(\theta_{NL})^2}\frac{\xi - \chi_1\bar{u} + (\omega(\theta_{nl}))^{\beta-1}\eta^\beta\sin(\frac{1}{2}\beta\pi)}{(\chi_3 + \bar{u}(\omega(\theta_{nl}))^{\beta-3}\gamma_1^\beta\sin(\frac{1}{2}\beta\pi))}} \tag{3.42}$$

setting $a = 0.0$ Eq.3.30 is obtained, and the critical speed is reached. When $\sigma \neq 0$ and $u_1 \neq 0$ using the combination $\cos^2(\phi) + \sin^2(\phi) = 1$ we obtains the quadratic equation at the amplitudes Eq.3.43

$$\frac{\eta_1^2}{u_1^2\left(\frac{\chi_3\omega^2}{2\bar{u}^2}a^2 + \chi_1\right)^2} + \frac{\eta_2^2}{u_1^2\left(\frac{\chi_3\omega^2}{\bar{u}^2}a^2 + \chi_1\right)^2} = 1, \tag{3.43}$$

where $\eta_1 = \sigma + \frac{3}{2}\gamma_3\omega^{-1}a^2 + \omega^{\beta-1}(\frac{3\gamma_1^\beta}{2}a^2 - 2\eta^\beta)cos(\frac{1}{2}\beta\pi)$ and

$\eta_2 = -2\xi + 2\chi_1\bar{u} + \frac{3}{2}\frac{\chi_3\omega^2}{\bar{u}}a^2 + \omega^{\beta-1}(\frac{3\gamma_1^\beta}{2}a^2 - 2\eta^\beta)\sin(\frac{1}{2}\pi\beta)$.

The stability of the trivial solution is explored as indicated in the previous section.

3.2.2.4 Analytical solution for the cable stayed-beam subject to platoon moving load only

In this case the terms resulting of wind load is setting equal to zero in the modulation equation (Eq.3.35) and following the same scheme for finding the trivial solution in the wind load case, the resulting quadratic equation is given by Eq.3.44

$$a^2\omega^2(\eta_1^2 + \eta_2^2) = \left(\sum_{k=1}^{K} f_{0k}\cos\varphi_k\right)^2 + \left(\sum_{k=1}^{K} f_{0k}\sin\varphi_k\right)^2 \tag{3.44}$$

The stability of the trivial solution depend on the sign of the real part of the eigenvalues of matrix A eliminating the terms.

For all above case the fractional and thermal loads affect the dynamics of the structure. Following parts of this studies is devotes to numerical analysis.

3.2.3 Numerical analysis

To validate the analytical investigation, a good quantitative and qualitative agreement between analytical and numerical solutions must be guaranteed. Therefore, a numerical method based on the Grünwald-Letnikov definition of the fractional derivative order [141, 151] and the Newton–Leipnik algorithm is used to solve Eq.3.15 [150,160] The relation to the explicit numerical approximation of q^{th} derivative at the points kh $(k = 1, 2, ...)$ has the form Eq.3.45

$$D_t^\beta q(t_k) \approx h^{-\beta}\sum_{j=0}^{k}(-1)^j \begin{pmatrix} \beta \\ j \end{pmatrix} q(t_{k-j}), \tag{3.45}$$

Table 3.1: Physical parameters and material properties.

Parameters	Symbols	Values	Units
Length of the beam	l	628.1	m
Density of the beam	ρ	7850.0	kg.m^{-3}
Elastic modulus of the beam	E	210	GPa
Area moment of inertia of the beam	I	12.0	m^4
Cross-section area of the beam	S	4.80	m^2
Thickness of the beam	b	10.0	m
Materials heat dissipation coefficient	K	10^{-5}	^{o}C^{-1}
Elastic modulus of stay cables	E_i	210	GPa
Coefficient of viscosity	μ	$6.1.10^{10}$	N.S$^\alpha$.m^{-1}
Area of cross-sectional of stay cables	S_i	0.05	m^2
Total horizontal tension	H_c	10.0	MN
Inclination angle of the cables	α_i	30.0	^{o}

where $t_k = kh$, h is the time step of calculation and $(-1)^j \begin{pmatrix} \beta \\ j \end{pmatrix}$ are binomial coefficients noted $C_j^{(\beta)}$ $(j = 0, 1, ...)$. For their calculations, we can use Eq.(3.46)

$$C_0^{(\beta)} = 1, \quad C_j^{(\beta)} = \left(1 - \frac{1+\beta}{j}\right) C_{j-1}^{(\beta)} \tag{3.46}$$

In the present study, we consider that cables have the same geometric and physical parameters. The parameters of cables and the beam listed in Table3.1 are inspired by models already studied in the literaturer [122, 155, 159].

As in the literature, the air density is set as $\rho_a = 1.25kg.m^{-3}$, the aerodynamic coefficients confirmed via wind test tunnel [71, 161, 162] are given by $A_1 = 0.9298$ and $A_3 = -7.677$. The non-dimensional damping coefficient of the beam is 0.05. In this study, the analysis is extended to the case of extreme wind results to tornado, with velocity up to $570km/h$ which corresponds to $\bar{u} = 160.0$. As in the previous study [163], the temperature change domain is set $[-40; +40]$ ^{o}C and corresponds to the non-dimensional non-linear thermal stress in the interval $[-0.68; +0.61]$. Investigations in the case of platoon moving load are conducted for default dimensionless force $f_{0k} = 0.00025$ and the number of loads $K = 10$.

3.2.3.1 Stability analysis

The results of previous studies can be confirmed on Fig.3.3 and Fig.3.4; indeed, turbulence significantly affects the critical speed of the structure because it induces a dangerous instability phenomenon in the structure. When the Hopf bifurcation is reached, the limit cycle appears and the amplitude increases exponentially.

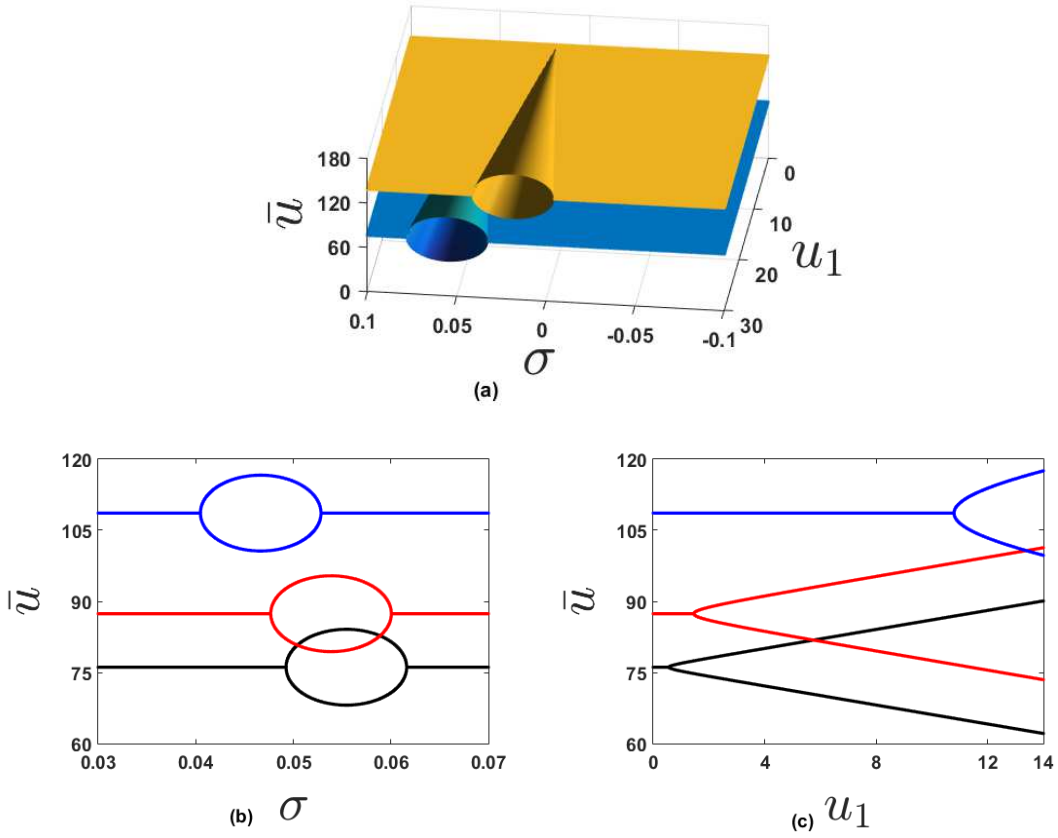

Figure 3.3: Stability domain of the trivial solutions for $\theta_{nl} = 0.0$. **(a)** 3D plot for $\beta = 0.1$ (blue) and $\beta = 0.8$ (yellow) **(b)** $(\bar{u}, \sigma)$ plane for $u_1 = 8.0$ and **(c)** $(\bar{u}, u_1)$ plane for $\sigma = 0.055$. $\beta = 0.1$ (black); $\beta = 0.2$ (red); $\beta = 0.4$ (blue)

The 3D plot of the stability domains is shown in Fig.3.3 for different values of β, and the stability domains in two planes, as a function of β, are clearly represented. It is observed that, when β increases, the stability domains are shifted upwards for both plane and $(\bar{u}, \sigma)$, $(\bar{u}, u_1)$ which means an increase of the critical speed. But, the first one shifted to the left and the second to the right. This means an decrease in the values of σ (Fig.3.3b) and an increase in turbulence values u_1 (Fig.3.3c); for which Hopf bifurcation phenomenon appears. Thus, it can be seen that great values of β are beneficial for stability; but, make the structure more sensitive to small wind turbulence frequencies (Fig.3.3b), while the

high values of β leads to good structural stability for high wind turbulences.

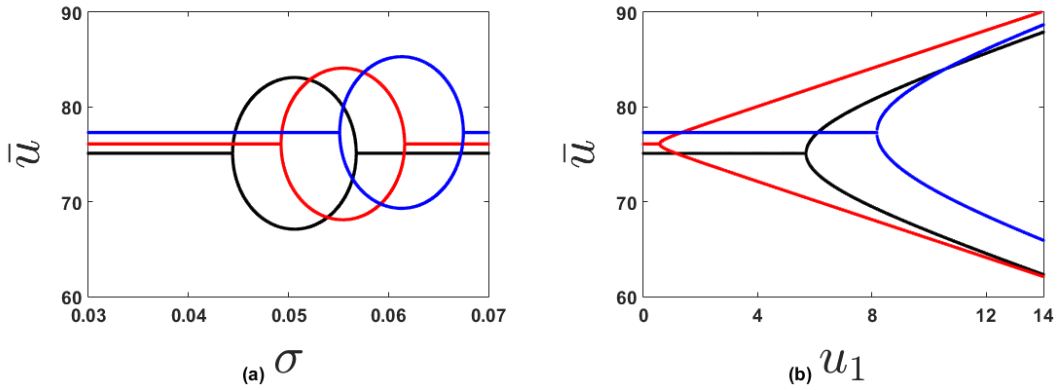

Figure 3.4: Stability domain of the trivial solution for $\theta_{nl} = -0.68$ (black); $\theta_{nl} = 0.0$ (red); $\theta_{nl} = +0.61$ (blue)**(a)** $(\bar{u}, \sigma)$ plane for $u_1 = 8.0$ and **(b)** $(\bar{u}, u_1)$ plane for $\sigma = 0.055$. $\beta = 0.1$

Fig.3.4 clarifies the effect of thermal fluctuations on the stability domains in the planes $(\bar{u}, \sigma)$ and $(\bar{u}, u_1)$. In the plane $(\bar{u}, \sigma)$ (Fig.3.4a), one can observe that the increase of the temperature causes an upward and to the right translation of the stability domain; it therefore comes from the fact that, an increase in temperature causes the increase in critical velocity as in the case of fractional order, the temperature is beneficial for the structural stability at low frequencies. In the plan $(\bar{u}, u_1)$ (Fig.3.4b) , the effect of temperature variations on the stability domain is depicted; from Eq.(3.30), we clearly notice that the influence of the temperature on the stability diagrams is transported by the fractional order, this justifies the non-linearity noticed in the impact of the temperature on this domain which will be well elucidated in the following paragraph. Besides the observed discontinuity for $\theta_{nl} = 0.0$, one can notice that, an increase in temperature increases the chance of the structure to avoid instability in the presence of small turbulence.

Fig.3.5 and Fig.3.6 present the variation of the critical velocity (obtained from Eq.(3.31) and Eq.(3.32)). In figures Fig.(3.5b) and Fig.(3.5c), it is clear that the large values of the fractional order are beneficial because it increases the galloping speed and the thermal effect is small on speed variation due to β. But the critical speed increases with temperature and more obvious for high values of fractional order (Fig.(3.5c)).

Also from Fig.3.6, it is important to notice that thermal effect in presence of β is very complex (Fig.3.6a); but, it is clear in Fig.3.6b that, when the fractional order increases, the critical speed increases for positive variations in temperature, which is the opposite for negative variations. Especially the critical speed remains unchanged when the fractional

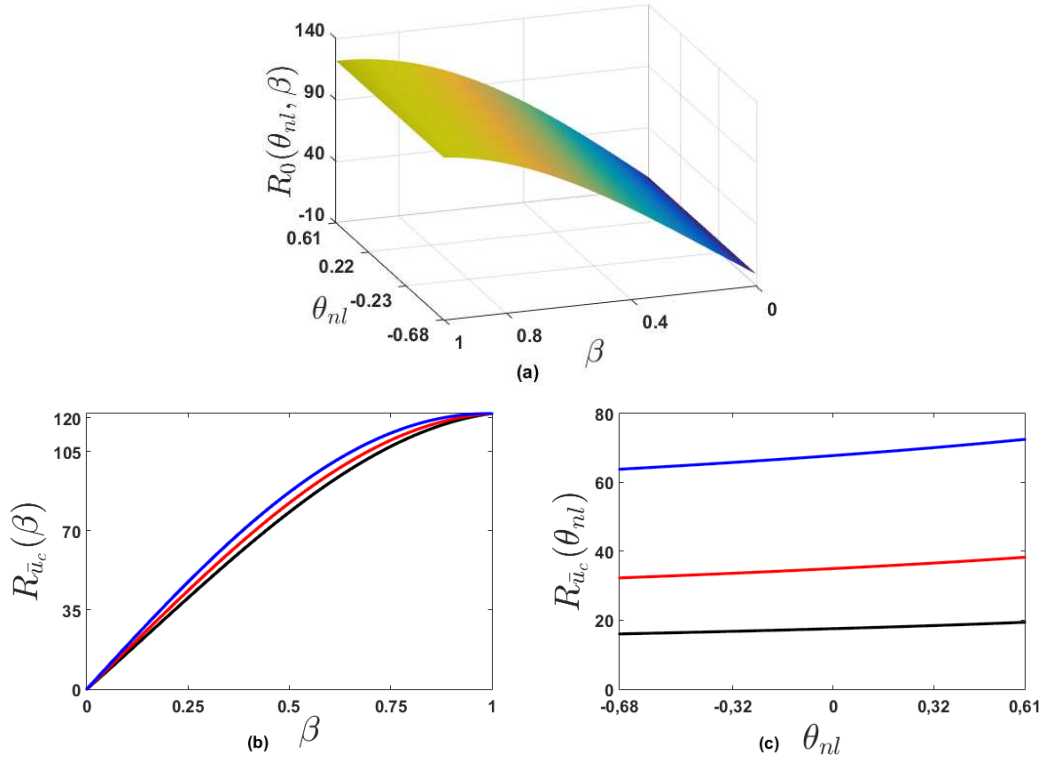

Figure 3.5: Critical speed variation **(a)** 3D plot; **(b)** versus β for $\theta_{nl} = -0.68$ (black); $\theta_{nl} = 0.0$ (red); $\theta_{nl} = +0.61$ (blue)and **(c)** versus θ_{nl} for $\beta = 0.1$ (black); $\beta = 0.2$ (red); $\beta = 0.4$ (blue)

order increases in the absence of temperature variations ($\theta_{nl} = 0.0$), which justifies the results obtained from Fig.3.4c.

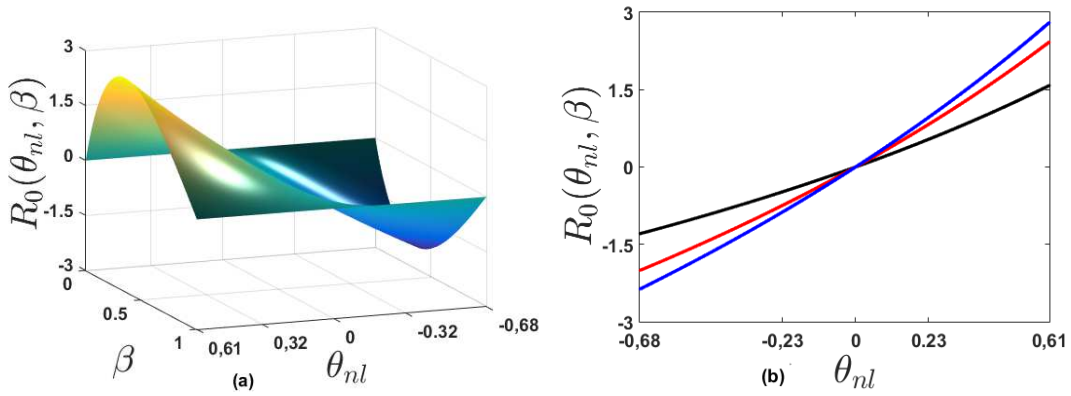

Figure 3.6: Critical speed variation versus **(a)** 3D plot **(b)** θ_{nl} for $\beta = 0.1$ (black); $\beta = 0.2$ (red); $\beta = 0.4$ (blue)

3.2.3.2 Non-linear analysis

Periodic solutions of the non-linear system in the two types of loads are analysed separately. In this part of the work dedicated to the numerical resolution, solid line denotes the stable solutions and pointed line denotes the unstable solutions. So, from Fig.3.7 to Fig.3.8 the case of the structure under the wind flow is depicted.

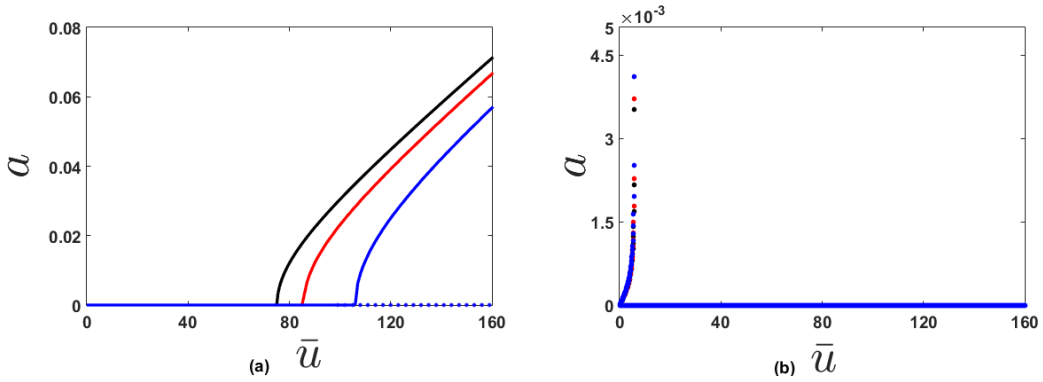

Figure 3.7: Response of the structure for $\theta_{nl} = -0.68$ **(a)** In the absence of the turbulent wind ($u_1 = 0.0$) **(b)** In the presence turbulent wind ($u_1 = 8.0; \sigma = 0.055$): $\beta = 0.1$ (black); $\beta = 0.2$ (red); $\beta = 0.4$ (blue)

Regarding the effect of the fractional derivative order θ on the appearance condition of classical Hopf bifurcation Eq.(3.42), Fig.3.7 is plotted. Thus, large values of θ lead to small vibration of the amplitude after the appearance of Hopf bifurcation (Fig.3.7a). The existence of a trivial solution is assumed and there are two branches: stable and unstable. In the stable branch, the cable stayed beam exhibits periodic oscillations in the wind direction, while it is stationary for subcritical wind speed values. Fig.3.7b shows the amplitude response as a function of mean velocity in the presence of turbulence; for the quasi-resonant case, the influence of the fractional order is highlighted; the peak amplitude increases slightly with the order of the fractional derivative.

Fig.3.8 shows the effect of thermal loads on the bifurcation diagram. From Fig.3.8a, the increase of the thermal effect causes the amplitude curves to bend to the right. After the Hopf bifurcation occurs, the amplitude increases with temperature. Thus, temperature is beneficial in mitigating the galloping phenomenon by increasing the galloping speed; but in the event of the onset of galloping, temperature increases the amplitude of the vibration, which is not suitable for the safety of the structure. One can confirm the result obtained in Fig.3.5a; thus, for a value of fractional order, the influence of temperature on the critical speed is less. But, it is consequent on the amplitude because it increases the

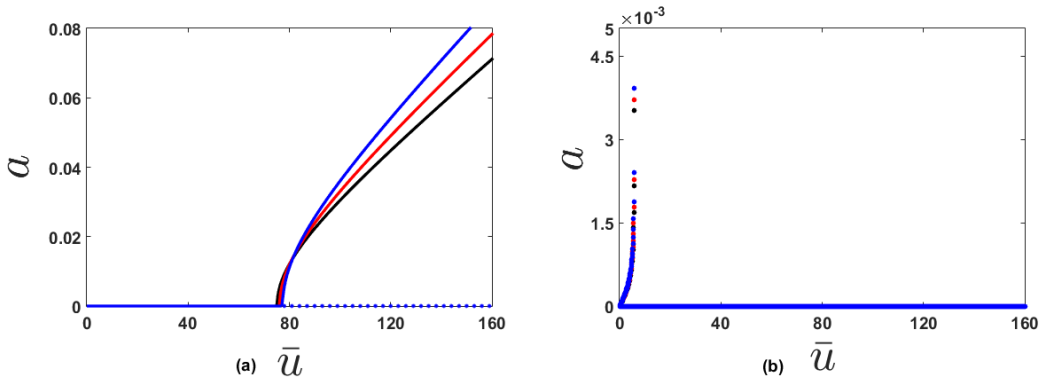

Figure 3.8: Response of the structure for $\beta = 0.1$ **(a)** In the absence of the turbulent wind ($u_1 = 0.0$) **(b)** In the presence of turbulent wind wind ($u_1 = 8.0; \sigma = 0.0055$): $\theta_{nl} = -0.68$ (black); $\theta_{nl} = 0.0$ (red); $\theta_{nl} = +0.61$ (blue)

amplitude of the vibration after the appearance of the galloping phenomenon, which is dangerous for the stability of the structure. In the presence of turbulence, as shown in Fig.3.8b, the amplitude of vibration increases with temperature. The dangerous effect of the thermal variation is thus highlighted, which is consistent with the classical case of Hopf bifurcation.

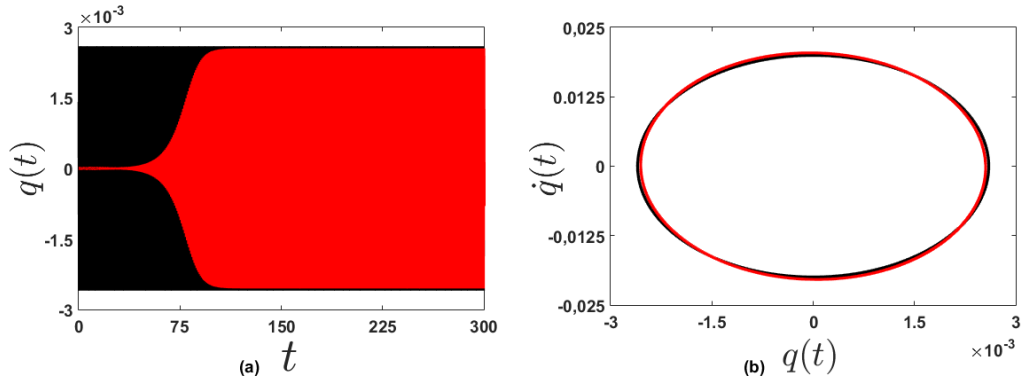

Figure 3.9: Approximate analytic solutions and the numerical solution for the case of wind loads **(a)** time history curves **(b)** phase diagrams

Fig.3.9 shows time history curves (Fig.3.9a) and phase diagrams (Fig.3.9b), obtained via analytical (black line) and numerical (red line) procedures. These curves are plotted for $\bar{u} = 77.3$; $u_1 = 0.0$; $\theta_{nl} = 0.0$ and $\beta = 0.1$. The numerical phase diagram is obtained after transient regime exhausted. One observes that the motion stabilizes on a limit cycle of amplitude $q(t)$. A comparison of these curves shows a good quantitative and qualitative agreement between analytical and numerical solutions.

Structural dynamic is investigated in the case of platoon moving loads. Only effect

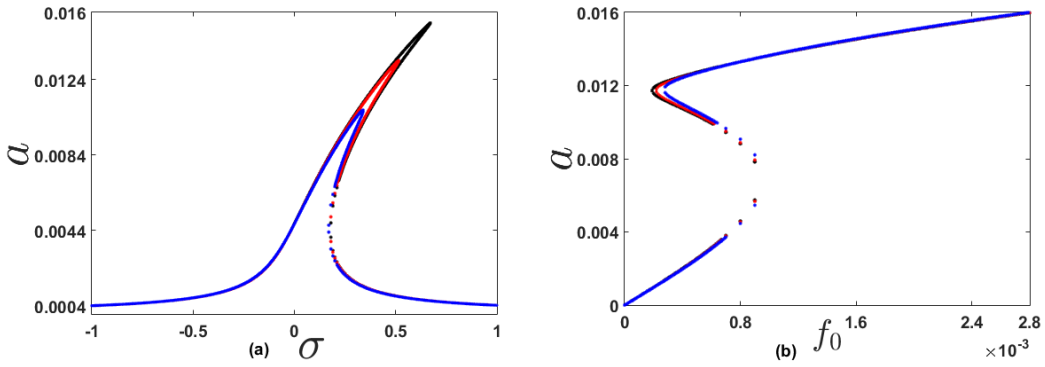

Figure 3.10: Response of the structure on the platoon moving load for $\theta_{nl} = 0.0$ **(a)** Amplitude response **(b)** Force amplitude responses. $\beta = 0.1$ (black); $\beta = 0.2$ (red); $\beta = 0.4$ (blue)

of thermal loads; fractional order and loads spacing are studied conveniently. Fig.3.10 presents the effect of fractional order on amplitude response of the cable-stayed beam. From Fig.3.10a, it is observed that, material with great values of fractional order is beneficial to reduce the peak amplitude. It is also clearly shown that the system is more stable for the highest order of the derivative. Looking at the effects of the fractional order on the force amplitude response of the beam, Fig.3.10b is plotted. From this last figure, it is necessary to conclude that, fractional derivative order does not have a significant effect on the amplitude force response. Multi-value solutions and up to three coexisting solutions are observed. Note that the bi-stability region (region with three periodic solutions) gives the range of dangerous weights of moving charges, this region is slightly modified by increasing the fractional order. Thus, by increasing the order of the fractional derivative, the three simultaneous solutions gradually disappear.

Thermal effects on amplitude frequency response is illustrated in Fig.3.11a. The cubic non-linearity is at the origin of the hardening behavior of the cable stayed beam as well as an increase of the temperature. Then, with the increase in the thermal load, the amplitude curve bends more to the right and the structure exhibits stronger hardening-spring behaviour. It should be mentioned that, as the temperature increases the peak amplitude increases, which is not in a good agreement with those reported in [152] for linear thermal variation. As observed in Fig.3.11b, the jump phenomenon in the excitation response curves results from the multi-value frequency response curves due to the non-linearity. Thermal changes cause significant quantitative changes of this curve. We can also say that, thermal effects are different, in the range of the large and small response

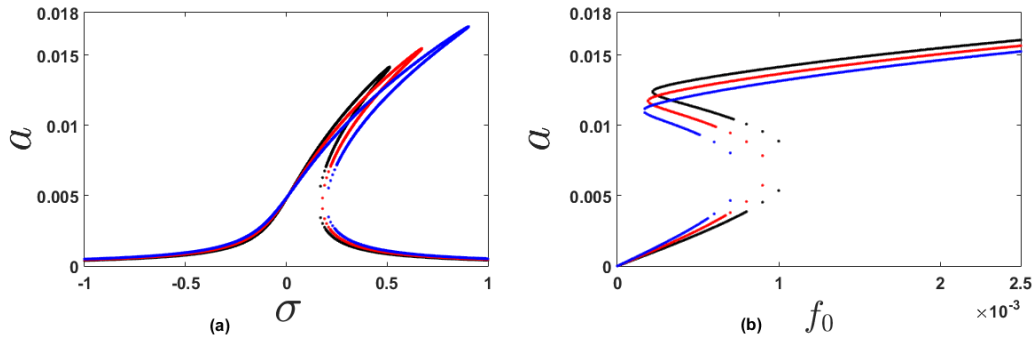

Figure 3.11: Response of the structure on the platoon moving load for $\beta = 0.1$ **(a)** Amplitude response **(b)** Force amplitude responses. $\theta_{nl} = -0.68$ (black); $\theta_{nl} = 0.0$ (red); $\theta_{nl} = +0.61$ (blue)

amplitudes. Specifically, for small value of the amplitude, as the temperature increases, the response amplitude increases slightly. Whereas, for large one, the amplitude response decreases significantly in the same condition. Moreover, the bi-stability is significantly changed with temperature variation.

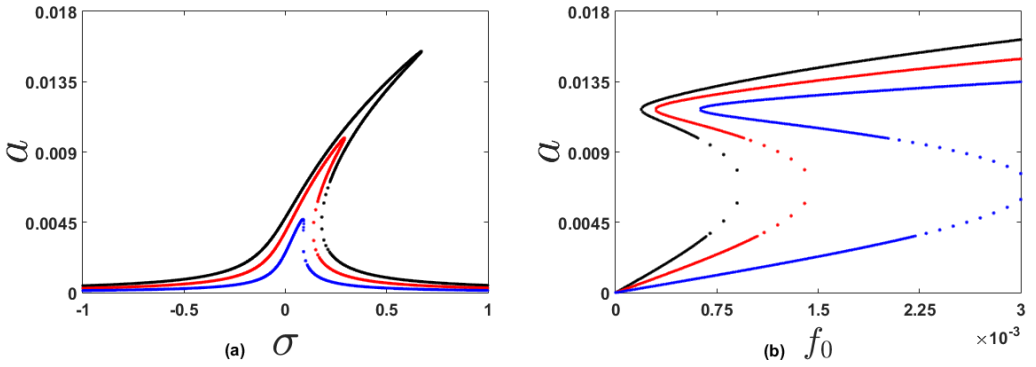

Figure 3.12: Response of the structure on the platoon moving load for $\theta_{nl} = 0.0$ and $\beta = 0.1$ **(a)** Amplitude response **(b)** Force amplitude responses. $l_0 = 0.01$ (black); $l_0 = 0.1$ (red); $l_0 = 0.15$ (blue)

Looking at the loads spacing on the dynamic response, Fig.3.12 is plotted. From Fig.3.12a, one can notice that great values of loads spacing decrease the amplitude response. Investigating amplitude force response, Fig.3.12b is plotted. According to that, it can be observed that, large values of loads spacing lead to enlarge the bi-stability region. Although large values lead to a low amplitude response, the possibility of bifurcation is increased. Thus, many loads with small load spacing can lead to a dangerous dynamic phenomenon.

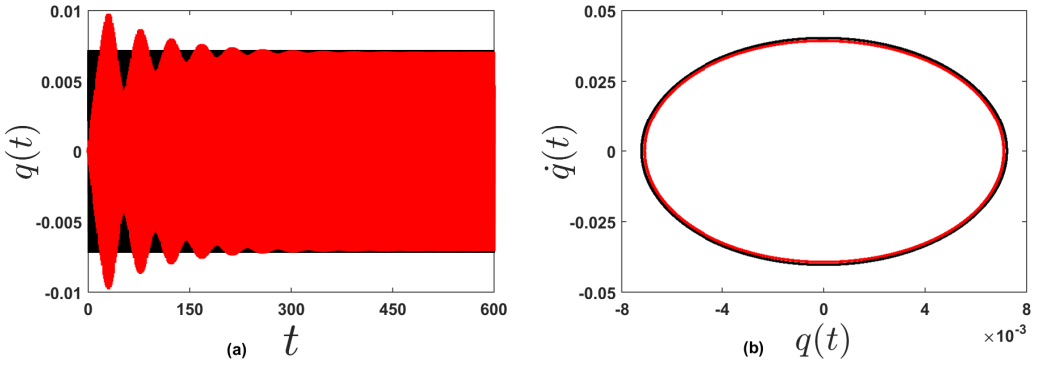

Figure 3.13: Approximate analytic solutions and the numerical solution for the case of platoon moving loads **(a)** time history curves **(b)** phase diagrams

As in the case of wind loads, Fig.3.13 shows time history curves (Fig.3.13a) and phase diagrams (Fig.3.13b) obtained via analytical (black line) and numerical (red line) procedures. These curves are plotted for $f_0 = 0.00025$; $l_0 = 0.01$; $\sigma = 0.1$; $\theta_{nl} = 0.0$ and $\beta = 0.1$. The numerical phase diagram is obtained after transient regime exhausted. A comparison of these curves shows a good quantitative and qualitative agreement between analytical and numerical solutions.

3.3 Effect of thermal and high static low dynamics stiffness isolator with the auxiliary system on a beam subjected to traffic loads

This section is devoted to study a high static low dynamic stiffness isolator with the auxiliary system (HSLDS-AS) used to control the vibrations characteristics of a hinged-hinged beam subjected to an axial and a constant moving load, taking into account the effect of the temperature on the structure. After he mathematical model via the newton second law of motion is obtained, the Galerkin's discretization technique is used to derive the modal's equation, which are solved by the harmonic balance method (HBM) coupled to averaging method for stability analysis. Following this the numerical analysis are conducted.

3.3.1 Description of the system and mathematical modelling

Fig.3.14 presents the real struture studied; thus, Fig.3.15 shows the physical system as hinged-hinged Euler Bernoulli beam isolated by a HSLDS-AS isolator. The simplified mechanical model of the studied system derived from Fig.2.5 is shown in Fig.3.16. The constituted system is placed in an environment where the temperature varies uniformly considering an axial compression load P [145]. The moving load expression used in this paper is given by Eq.3.47. δ is the Dirac delta function and V the velocity of moving load.

$$F(x,t) = F\delta(x - Vt). \tag{3.47}$$

The thermal stress due to the thermal change is given by Eq.3.48 [30].

Figure 3.14: Real model of the structure

$$\theta = \mathrm{E}K\Delta T, \tag{3.48}$$

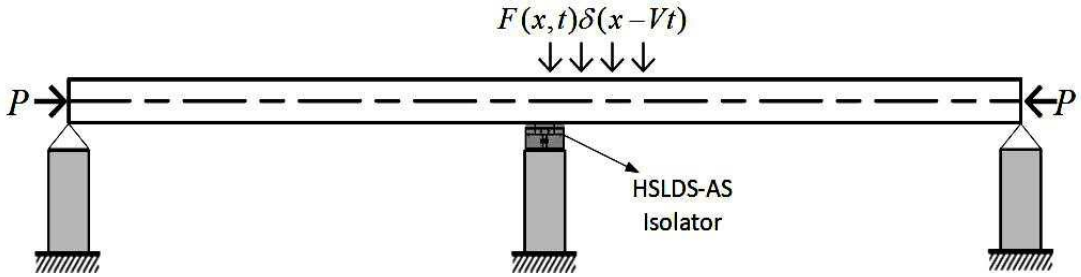

Figure 3.15: Physical model of a the structure controlled by a HSLDS-AS isolator

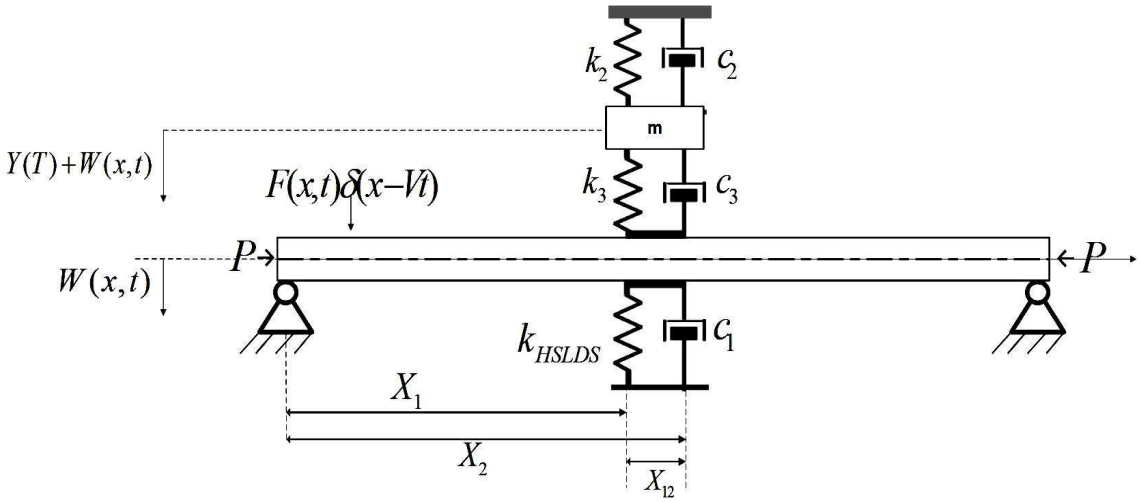

Figure 3.16: Simplified mechanical model of the system

where ΔT is the uniform temperature variation and K the thermal expansion coefficient of the material. Thus, the total stress in the structure is [126]

$$\sigma = \mathrm{E}\varepsilon = \mathrm{E}\left(\frac{\partial U}{\partial x} + \frac{1}{2}\left(\frac{\partial W}{\partial x}\right)^2 - \frac{\theta}{E}\right), \tag{3.49}$$

where E denotes the Young's modulus of the material. Considering Eq.3.47, Eq.3.47, Eq.3.49 and applying the Newton second law of motion [13, 126, 134], the equations of motion are

$$\begin{cases} \rho A\frac{\partial^2 W}{\partial t^2} + EI\frac{\partial^4 W}{\partial x^4} + \mathrm{c}\frac{\partial W}{\partial t} + (\mathrm{P}+\theta\mathrm{A})\frac{\partial^2 W}{\partial x^2} - \frac{EA}{2L}\frac{\partial^2 W}{\partial x^2}\int_0^L \left(\frac{\partial W}{\partial x}\right)^2 dx \\ + \frac{1}{x_{12}}\left(\mathrm{k}_1\ell(\alpha^2\frac{\mathrm{W(x,t)}}{\ell} + \beta\frac{\mathrm{W}^3}{\ell^3}) + c_1\frac{dW}{dt} - k_3 Y - c_3\frac{dY}{dt}\right) G(x) = F\delta(x - Vt) \\ m\frac{d^2 Y}{dt^2} + c_2\frac{dY}{dt} + m\frac{\partial^2 W}{\partial t^2} + c_2\frac{\partial W}{\partial t} + k_2 W + k_2 \mathrm{Y} + c_3\frac{dY}{dt} + k_3 Y = 0 \end{cases}, \tag{3.50}$$

where $G(x)$ is defined by

$$G(x) = H(x-x_1) - H(x-X_2) = \begin{cases} 0 & if \quad x \leq X_1 \\ 1 & if \quad X_1 < x < X_2 \\ 0 & if \quad x \geq X_2 \end{cases}, \tag{3.51}$$

where $H(.)$ is a Heaviside function. $Y = Y(t)$ is the relative displacement of the auxiliary mass to the beam and t the time in second. In order to obtains the nondimensional equation, the dimensionless constants are setting as

$$\begin{array}{l} t^*{=}t\sqrt{\frac{P}{\rho AL^2}}; \quad v_f^2{=}\frac{EI}{PL^2}; \quad v_1^2{=}\frac{EA}{P}; \quad \theta_1{=}\frac{A\theta}{P}; \quad k{=}\frac{k_1 L\alpha^2}{P} \quad ; \beta_0{=}\frac{k_1 L^3\beta}{P\ell^2}; \quad \varepsilon{=}\frac{1}{2}c\sqrt{\frac{L^2}{\rho AP}} \\ \varepsilon_1{=}\frac{c_1}{2}\sqrt{\frac{1}{\rho AP}}; \quad \varepsilon_2{=}\frac{c_2}{2}\sqrt{\frac{1}{\rho AP}}; \quad \varepsilon_3{=}\frac{c_3}{2}\sqrt{\frac{1}{\rho AP}}; \quad \lambda_2{=}\frac{k_2 L}{P}; \quad \lambda_3{=}\frac{k_3 L}{P}; \quad \mu{=}\frac{m}{\rho AL} \\ f_0{=}\frac{F}{P}; \quad V^* = V\sqrt{\frac{P}{\rho A}}; \quad x^* = \frac{x}{L}; \quad y = \frac{Y}{L}; \quad w = \frac{W}{L} \\ x_1 = \frac{X_1}{L}; \quad x_2 = \frac{X_2}{L} \text{and} \quad x_{12} = \frac{X_{12}}{L} \end{array} \tag{3.52}$$

Omitting asterisk son t, x and V, the non-dimensional equations are derived as

$$\begin{cases} \frac{\partial^2 w}{\partial t^2} + 2\varepsilon\frac{\partial w}{\partial t} + v_f^2\frac{\partial^4 w}{\partial x^4} + (1+\theta_1)\frac{\partial^2 w}{\partial x^2} - \frac{v_1^2}{2}\frac{\partial^2 w}{\partial x^2}\int_0^1\left(\frac{\partial w}{\partial x}\right)^2 dx \\ \quad + \frac{1}{x_{12}}\left(kw + \beta_0 w^3 + 2\varepsilon_1\frac{dw}{dt} - \lambda_3 y - 2\varepsilon_3\frac{dy}{dt}\right)g(x) = f_0\delta(x-Vt) \\ \mu\frac{d^2 y}{dt^2} + \mu\frac{\partial^2 w}{\partial t^2} + 2\varepsilon_2\frac{\partial w}{\partial t} + \lambda_2 w + 2(\varepsilon_2+\varepsilon_3)\frac{dy}{dt} + (\lambda_2+\lambda_3)y = 0 \end{cases}, \tag{3.53}$$

where:

$$g(x) = H(x-x_1) - H(x-x_2) = \begin{cases} 0 & If \quad x \leq x_2 \\ 1 & If \quad x_1 < x < x_2 \\ 0 & If \quad x \geq x_2 \end{cases} \tag{3.54}$$

3.3.2 Modal equation

As indicated Wahrhaftig *et al.* [123, 124] the are many analytical procedures to solve this mathematical problem. To obtain the modal equations, Galerkin's technique is used. According to this method, the solution of the partial differential Eq.3.53 for the hinged-hinged beam, is assumed to be in the form [125]

$$w(x,t) = \sum_{n=1}^{\infty} q_n(t)\sin(n\pi x). \tag{3.55}$$

With this, the modal equations are given by

$$\begin{cases} \ddot{q}_n(t) + 2\varepsilon_{cn}\dot{q}_n(t) + \omega_n^2 q_n(t) + \Gamma_n q_n^3(t) - \alpha_{1n}y - \alpha_{2n}\dot{y} = 2f_0\sin(n\pi Vt) \\ \mu\ddot{y} + \beta_{2n}\dot{y} + \beta_{3n}y + \mu\ddot{q}_n(t) + 2\varepsilon_2\dot{q}_n(t) + \lambda_2 q_n(t) = 0 \end{cases}, \tag{3.56}$$

where

$$\begin{array}{l}\alpha_{1n}=\frac{2}{n\pi x_{12}}(\cos n\pi x_1-\cos n\pi x_2)\lambda_3 \quad ; \quad \alpha_{2n}=\frac{4}{n\pi x_{12}}(\cos n\pi x_1-\cos n\pi x_2)\varepsilon_3 \\ \beta_{1n}=\frac{2(1-(-1)^n)}{n\pi}\mu \quad ; \quad \beta_{2n}=4(\varepsilon_2+\varepsilon_3)\frac{(1-(-1)^n)}{n\pi} \quad ; \quad \beta_{3n}=\frac{2(1-(-1)^n)}{n\pi}(\lambda_2+\lambda_3) \\ \omega_{bn}^2=(n\pi)^4v_f^2-(1+\theta_1)(n\pi)^2+\frac{k}{x_{12}}(x_2-x_1-\frac{1}{2\pi n}(\sin 2n\pi x_2-\sin 2n\pi x_1)) \\ \Gamma_n=\frac{1}{4}\left(2(n\pi)^4v_1^2+\frac{\beta_0}{x_{12}}(3(x_2-x_1) \ +\frac{\sin(4n\pi x_2)-\sin(4n\pi x_1)}{4n\pi}-2\frac{\sin(2n\pi x_2)-\sin(2n\pi x_1)}{n\pi}\right) \\ \varepsilon_{cn}=\varepsilon+\frac{\varepsilon_1}{x_{12}}(x_2-x_1-\frac{1}{2\pi n}(\sin 2\pi nx_2-\sin 2\pi nx_1))\end{array} . \tag{3.57}$$

3.3.3 Dynamical responses and stability analysis

3.3.3.1 Resonance responses

The harmonic balance method offers an alternative for analysis of cases where steady state periodic solutions to the non-linear equation of motion are sought. Furthemore, due to the fact that simple HBM don't give the stability of the solution, the averaging method and the harmonic balance method [13, 134] are combined to analyse the stability of periodic solutions for the system at the first mode of vibration. According to this method we set

$$\begin{cases} q(t)=a_1(t)\cos\omega t+a_2(t)\sin\omega t \\ y(t)=b_1(t)\cos\omega t+b_2(t)\sin\omega t \end{cases} , \tag{3.58}$$

where $\omega=\pi v$ is the excitation frequency due to the moving load. Substituting Eq.3.58 into Eq.3.56 for $n=1$, and equating the coefficients proportional to, $\cos\omega t$ and $\sin\omega t$, we obtains with the conditions $\ddot{a}_1=\ddot{a}_2=\ddot{b}_1=\ddot{b}_2=0$,

$$\begin{array}{l} 2\varepsilon_c\dot{a}_1+2\omega\dot{a}_2-\alpha_2\dot{b}_1+a_1(\omega_b^2-\omega^2+\frac{3}{4}\Gamma A^2) \\ +2\varepsilon_c\omega a_2-\alpha_1b_1-\alpha_2\omega b_2=0 \\ -2\omega\dot{a}_1+2\varepsilon_c\dot{a}_2-\alpha_2\dot{b}_2+a_2(\omega_b^2-\omega^2+\frac{3}{4}\Gamma A^2) \\ -2\varepsilon_c\omega a_1+\alpha_2\omega b_1-\alpha_1b_2=2f_0 \end{array} . \tag{3.59}$$

$$\begin{array}{l} 2\varepsilon_2\dot{a}_1+2\mu\omega\dot{a}_2+\beta_2\dot{b}_1+2\beta_1\omega\dot{b}_2+(\lambda_1-\mu\omega^2)a_1 \\ +2\varepsilon_2\omega a_2+(\beta_3-\beta_1\omega^2)b_1+\beta_2\omega b_2=0 \\ -2\mu\omega\dot{a}_1+2\varepsilon_2\dot{a}_2-2\beta_1\omega\dot{b}_1+\beta_2\dot{b}_2-2\varepsilon_2\omega a_1 \\ +(\lambda_1-\mu\omega^2)a_2-\beta_2\omega b_1+(\beta_3-\beta_1\omega^2)b_2=0 \end{array} . \tag{3.60}$$

To derive the amplitude responses equations let us set $a_1=a\sin\varphi_1$; $a_2=a\cos\varphi_1$; $b_1=b\sin\varphi_2$ and $b_2=b\cos\varphi_2$. Where a and φ_1 are amplitude and phase angle of $q(t)$. In

the same way, b and φ_2 are amplitude and phase angle of $y(t)$. At the stationary state, we have $\dot{a}_1 = \dot{a}_2 = \dot{b}_1 = \dot{b}_2 = 0$, the amplitudes a and b satisfies the following non-linear equations:

$$\begin{cases} 4f_0^2 P_0(\omega) - a^2(P_1(\omega,a) + P_2(\omega,a) + P_3(\omega) + P_4(\omega) + P_5(\omega,a)) = 0 \\ a^2 P_6(\omega) = b^2 P_0(\omega) \end{cases} \tag{3.61}$$

$$tg(\varphi_1) = -\frac{(2\varepsilon_c(\beta_3 - \beta_1\omega^2) + \tau_{11}) + \chi_1(4\omega^2\varepsilon_c\beta_2 - \tau_{12})}{\frac{1}{\omega}(\tau_{22} + \tau_{12}) + \chi_1\omega(2\beta_2(\omega_b^2 - \omega^2 - \frac{3}{4}\Gamma a^2) + \tau_{11})} \tag{3.62}$$

$$tg(\varphi_2) = \frac{-(2\tau_{21} + \alpha_2(\lambda_2 - \mu\omega^2)) + \chi_2(\tau_{22} - 4\omega^2\varepsilon_c\beta_2 - 2\omega^2\alpha_2\varepsilon_2)}{\frac{1}{\omega}(\tau_{22} - 4\omega^2\varepsilon_c\beta_2 + \alpha_1(\lambda_2 - \mu\omega^2)) + 2\omega\chi_2(\tau_{21} + \varepsilon_2\alpha_1)}, \tag{3.63}$$

where:

$$\begin{aligned} &P_0(\omega) = ((\beta_3 - \beta_1\omega^2)^2 + 4\omega^2\beta_2^2) P_1(\omega,a) = ((\omega_b^2 - \omega^2 + \tfrac{3}{4}\Gamma a^2)(\beta_3 - \beta_1\omega^2) + \alpha_1(\lambda_2 - \mu\omega^2))^2 \\ &P_2(\omega,a) = 4\omega^2(\beta_2(\omega_b^2 - \omega^2 + \tfrac{3}{4}\Gamma a^2) + \alpha_1\varepsilon_2)^2 \\ &P_3(\omega) = \omega^2(2\varepsilon_c(\beta_3 - \beta_1\omega^2) + \alpha_2(\lambda_2 - \mu\omega^2))^2 \\ &P_4(\omega) = 4\omega^4(2\varepsilon_c\beta_2 + \alpha_2\varepsilon_2)^2 \\ &P_5(\omega,a) = 4\omega^2(\alpha_2(\omega_b^2 - \omega^2 + \tfrac{3}{4}\Gamma a^2) - 2\varepsilon_c\alpha_1) \times (\beta_2(\lambda_2 - \mu\omega^2) - \varepsilon_2(\beta_3 - \beta_1\omega^2)) \\ &P_6(\omega) = (\lambda_2 - \mu\omega^2)^2 + 4\omega^2\varepsilon_2^2 \\ &\chi_1 = \tfrac{2\beta_2}{(\beta_3 - \beta_1\omega^2)} \quad ; \quad \tau_{11} = 2\alpha_1\varepsilon_2 + \alpha_2(\lambda_2 - \mu\omega^2) \end{aligned} \tag{3.64}$$

$$\begin{aligned} &\tau_{12} = -2\omega^2\alpha_2\varepsilon_2 + \alpha_1(\lambda_2 - \mu\omega^2) \quad ; \quad \chi_2 = \tfrac{2\varepsilon_2}{(\lambda_2 - \mu\omega^2)} \\ &\tau_{21} = \beta_2(\omega_b^2 - \omega^2 + \tfrac{3}{4}\Gamma a^2) + \varepsilon_c(\beta_3 - \beta_1\omega^2) \quad ; \quad \tau_{22} = (\omega_b^2 - \omega^2 + \tfrac{3}{4}\Gamma a^2)(\beta_3 - \beta_1\omega^2) \end{aligned} \tag{3.65}$$

3.3.3.2 Stability analysis

For the stability analysis, we set $a_i = a_{i0} + \delta a_i$ and $b_i = b_{i0} + \delta b_i$ $(i = 1, 2)$; where δa_i and δb_i are small perturbations. Expanding for this small perturbations and keeping linear terms, one obtains the following equations around the stationary harmonic oscillatory state amplitudes a_{i0} and b_{i0}

$$\delta\dot{r} = A\delta r, \tag{3.66}$$

where

$$\delta r = (\delta a_1; \delta a_2; \delta b_1; \delta b_2), \tag{3.67}$$

$$A = M.D, \tag{3.68}$$

$$M = \begin{bmatrix} 2\varepsilon_c & 2\omega & -\alpha_2 & 0 \\ -2\omega & 2\varepsilon_c & 0 & -\alpha_2 \\ 2\varepsilon_2 & 2\mu\omega & \beta_2 & 2\beta_1\omega \\ -2\mu\omega & 2\varepsilon_2 & -2\beta_1\omega & \beta_2 \end{bmatrix}^{-1}, \tag{3.69}$$

$$\begin{array}{l} D_{11} = D_{22} = -(\omega_b^2 - \omega^2 + \frac{3}{2}\Gamma(2a_{20}^2 + A^2) \quad ; \quad D_{21} = -(\frac{3}{2}\Gamma a_{10}a_{20} - 2\varepsilon_c\omega) \\ D_{12} = -(\frac{3}{2}\Gamma a_{10}a_{20} + 2\varepsilon_c\omega) \quad ; \quad D_{13} = D_{24} = \alpha_1; \quad D_{14} = -D_{23} = \alpha_2\omega \\ D_{31} = D_{42} = -(\lambda_1 - \mu\omega^2); \quad D_{41} = -D_{32} = 2\varepsilon_2\omega \\ D_{33} = D_{44} = -(\beta_3 - \beta_1\omega^2); \quad D_{43} = -D_{34} = \beta_2\omega \end{array} . \tag{3.70}$$

The eigenvalues (s) is given by solving

$$Det(A - s * I) = 0. \tag{3.71}$$

The stability of the stationary oscillatory state solutions depends on the eigenvalues of the Jacobian matrix A. Then, the solution is stable if a eigenvalues have a negative real parts.

3.3.4 Force transmissibillty

At the first mode vibration, the expression of the force transmitted to the isolator support is

$$f_t(t) = 2\varepsilon_c\dot{q}(t) + \omega^2 q(t) + \Gamma q^3(t) - \alpha_1 y - \alpha_2\dot{y} \ . \tag{3.72}$$

The force transmissibillity when the dimensionless excitation force is $f_e(t) = 2f_0\sin(\pi v t)$ is given by [113]

$$T_f = |\tfrac{f_t(t)}{f_e(t)}|. \tag{3.73}$$

By inserting the analytical solution at first mode in Eq.3.73, T_f is given as follows

$$T_f = \frac{1}{2f_0}\sqrt{a^2\kappa_1 + b^2\kappa_2 + 2ab\sqrt{\kappa_1\kappa_2}\cos(\phi_2 - \phi_1)}, \tag{3.74}$$

with

$$\begin{array}{l} tg(\phi_1) = \frac{-(\omega^2 + \frac{3}{4}\Gamma a^2) + 2\varepsilon_c\omega tg(\varphi_1)}{(\omega^2 + \frac{3}{4}\Gamma a^2)tg(\varphi_1) + 2\varepsilon_c\omega} \\ tg(\phi_2) = \frac{-\alpha_1 + \alpha_2\omega tg(\varphi_2)}{\alpha_1 tg(\varphi_2) + \alpha_2\omega} \end{array} , \tag{3.75}$$

Table 3.2: Simulation parameters.

Parameters	Symbols	Values	Units
Density	ρ	7781.0	kg/m^3
Length	L	24.072	m
young's modulus	E	210.0	GPa
Area of cross section	A	0.03	m^2
Thermal expansion coefficient	K	10^{-5}	^{o}C^{-1}
Axial load	P	130.0	KN
Area moment of inertia	I	$3.0 * 10^{-4}$	m^4
HSLDS Rod length	l	0.35	m

$$\kappa_1 = ((\omega^2 + \tfrac{3}{4}\Gamma a^2)^2 + 4\varepsilon_c^2\omega^2), \qquad (3.76)$$
$$\kappa_2 = (\alpha_1^2 + \omega^2\alpha_2^2).$$

The absolute force transmissibillity of HSLDS-AS is defined as follow

$$T_{f_m} = 20log(T_f). \qquad (3.77)$$

3.3.5 Study parameters selection

For numerical investigation, the dimensionless material properties of the beam and fixed parameters of HSLDS-AS are chosen from Table3.2. The current beam can be considered as a idealist modified deck beam [122] a cable stayed bridge. In the following analysis the non-dimensional transversal moving load magnitude is $f_0 = 0.05$ and the damping coefficient of the beam $\varepsilon = 0.05$. By using Eq.3.52, we have the dimensionless values $v_f^2 = 0.8866$ and $v_1^2 = 50319.2308$. Taking into account Eq.3.48 we have:

$$\beta_0 = \frac{L^2}{\ell^2}\frac{\lambda_4(1-e)}{1-2\lambda_4 e}k, \qquad (3.78)$$

where k is the linear spring coefficient and β_0 the non-linear spring coefficient of the HSLDS isolator. For a fixed values of L, ℓ, λ_4 and e, Eq.3.78 shows that β_0 and k are directly proportional and have the same influences on the system; therefore, the analysis of one of these parameters will be sufficient. Furthermore, for a performant control [117], $\lambda_4 e$ must be less than 0.5 so that the term α^2 is close to zero. In the present analysis,

the default values of isolator parameters are $\varepsilon_1 = 2.5$; $\lambda_2 = 100.0$; $\lambda_3 = 10.0$; $\lambda_4 = 1.0$; $\varepsilon_2 = \varepsilon_3 = 1.0$; $e = 0.4$; $\mu = 0.003$; $k = 0.2$. For the localization of HSLDS-AS isolator the default values are $x_1 = 0.475$ and $x_2 = 0.525$. To study the performance of the isolator, we focused on the effect of ε_1, ε_2, ε_3, λ_2, λ_3, k, x_1, x_2 and x_{12} (thickness over which the isolator is in contact with the beam). In order to study the effect of temperature on the beam, with and without control, we set the variation of the non-dimensional thermal stress θ_1 in the interval [-20.03; +20.03], which corresponds to dimensional temperature change domain
$[-39.80^oC; +39.80^oC]$.

3.3.6 Dynamical explanation

We describe the effect of location, parameters of the HSLDS-AS and thermal variation on natural frequencies, amplitude curve and force transmissibility of the system.

3.3.6.1 Natural frequency study

In order to clarify the effect of the temperature rise on the dimensionless frequency, we consider a frequency variation factor as [126]

$$R_\omega = \frac{\omega_n(\theta_1 \neq 0) - \omega_n(\theta_1 = 0)}{\omega_n(\theta_1 = 0)}. \tag{3.79}$$

$\omega_n(\theta_1 \neq 0)$ and $\omega_n(\theta_1 = 0)$ are the natural frequencies when θ_1 is different from zero and equal to zero respectively.

In Fig.(3.17), we note that for the controlled beam, increase in the temperature causes the natural frequency to decrease and decreasing the temperature increasing the natural frequency. Moreover, the thermal effect is more obvious at the first mode and the effect of thermal change on natural frequency becomes less with the increase of the order's mode. With the uncontrolled beam, the same result was founded and the same conclusion is drawn. The same effects on natural frequencies was observed in other studies [35,96]. The influence of the linear spring coefficient, thickness of control's force action x_{12} and the position of the HASLDS-AS Isolator on natural frequencies was investigated. By analysing the results in Table 3.3 with $\theta_1 = 0$, we conclude that:

(1) Changing the HSLDS-AS positions from the left-end to the mid-span of the beam results in an increase of the values of natural frequency of the system.

(2) Increasing the value of the thickness of action of the control, result in a decrease of

Table 3.3: First natural frequencies for different values of location and linear spring coefficient of the HSLDS-AS Isolator.

	ω_1					
	$x_1 = 0.275$	$x_1 = 0.475$	$x_1 = 0.675$	$x_1 = 0.24$	$x_1 = 0.44$	$x_1 = 0.64$
k	$x_2 = 0.325$	$x_2 = 0.525$	$x_2 = 0.725$	$x_2 = 0.36$	$x_2 = 0.56$	$x_2 = 0.76$
	$x_2 - x_1 = 0.05$	$x_2 - x_1 = 0.05$	$x_2 - x_1 = 0.05$	$x_2 - x_1 = 0.12$	$x_2 - x_1 = 0.12$	$x_2 - x_1 = 0.12$
0.02	8.746	8.746	8.746	8.746	8.7467	8.746
0.20	8.747	8.747	8.747	8.748	8.749	8.748
10.00	8.783	8.803	8.783	8.835	8,881	8,835
20.00	8.821	8.860	8.821	8.923	9.013	8.923
100.00	9.112	9.299	9.112	9.598	10.011	9.598

the natural frequencies.

(3) Increasing of the linear spring coefficient increase the natural frequencies.

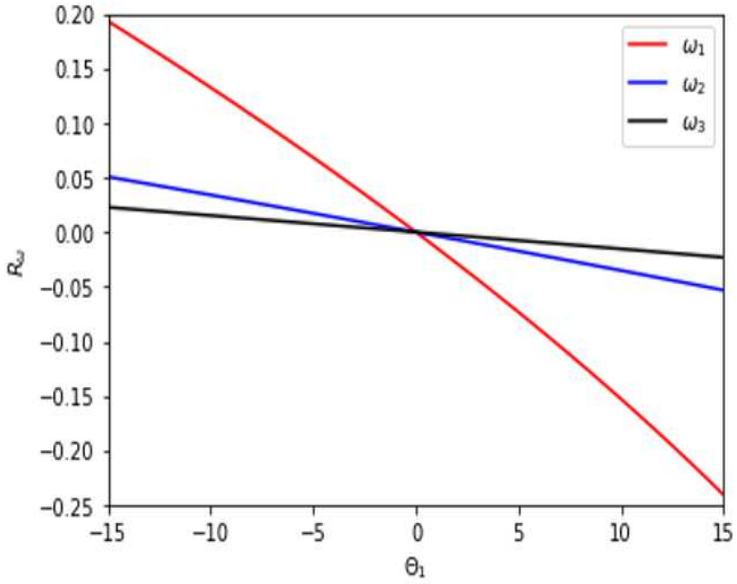

Figure 3.17: Temperature effect on the first three natural frequencies of controlled and uncontrolled beam.

3.3.6.2 Amplitude curves and force transmissibility

Numerical solutions are obtained by solving the equation Eq.3.56 using the fourth order Runge-Kutta algorithm. Fig.3.18 show the amplitude and force transmissibility curves for two types of solutions. by comparing these curves, we therefore end up with a validation

of the results obtained with HBM.

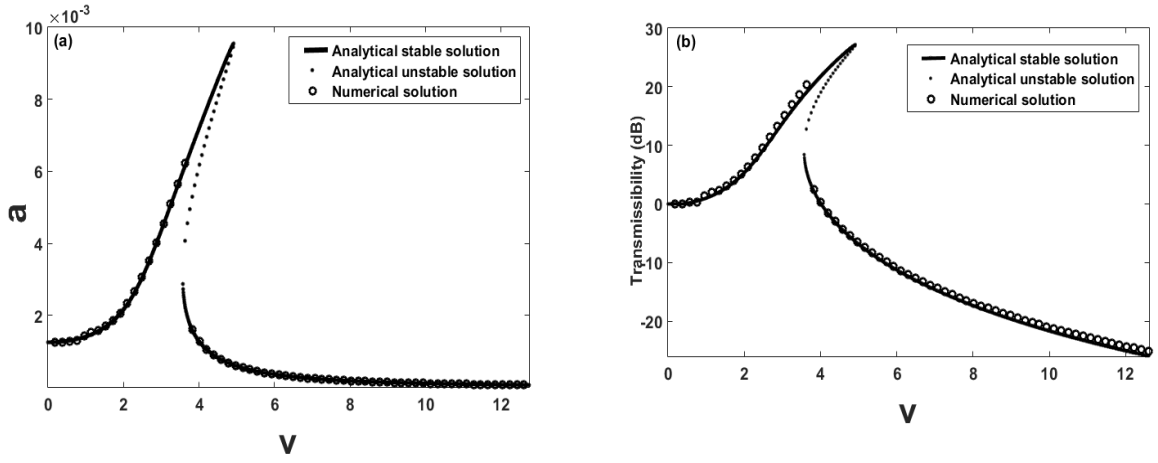

Figure 3.18: **a)**Analytical and numerical Amplitude responses of the structure with HSLDS-AS.**b)**Analytical and numerical Absolute force transmissibility of the system with HSLDS-AS. Solid line denotes the stable responses and pointed line denotes the unstable responses for defaults parameters.

Fig.3.19 illustrates the amplitude responses and force transmissibility curves for default parameters. The peak amplitude is reduced close to 33 percent and the peak transmissibility reduced close to 50 percent. Then, the isolator is very performant for amplitude control and absolute force transmissibility reduction.

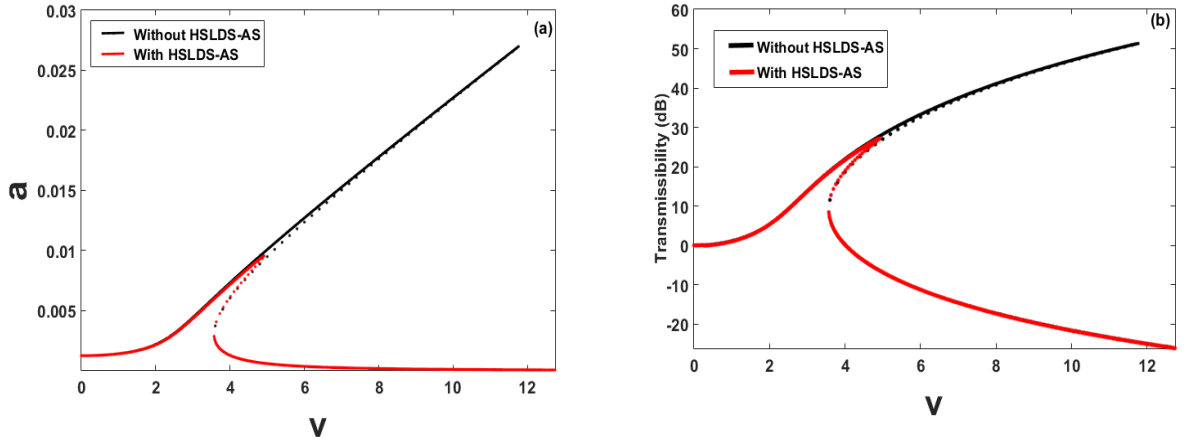

Figure 3.19: **a)**Amplitude responses of the beam without and with HSLDS-AS. **b)**Absolute force ransmissibility. Solid line denotes the stable responses and pointed line denotes the unstable responses for defaults parameters.

Fig. 3.20 describes the amplitude responses and force transmissibility curves with linear spring stiffness k. Theses two curves depend strongly on the values of k. Increasing of k causes the hardening behaviour and peak transmissibility to increase. This is justified By Eq.3.78. The least values of this parameter are beneficial for a performant control or isolation. Especially the isolator can be ideal when the linear spring stiffness is set to zero and we have a quasi zero stiffness isolator with auxiliary system (QZS-AS).

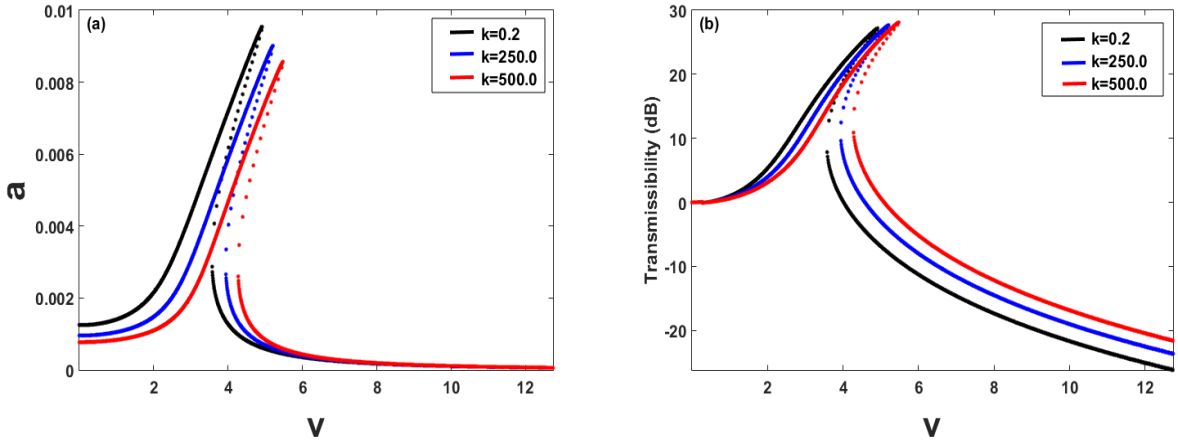

Figure 3.20: Effet of k on: **a)**Amplitude responses of the isolated beam. **b)** Absolute force ransmissibility. Solid line denotes the stable responses and pointed line denotes the unstable responses for defaults parameters.

Fig. 3.21 shows the dynamics behaviors, by using non-linear amplitude response and absolute force transmissibility curves with damping coefficient ε_1. It is pointed out that, at the low velocity, increasing the value of damping ratio causes the peak amplitude and transmissibility to decrease. But, this result is opposite at the high velocity. Then, the greatest values of this parameters is beneficial for a best isolation or control in case of low velocity.

Fig. 3.22 explains the amplitude response and absolute force transmissibility curves with damping ratios ε_2 and ε_3. Increasing of these two paramaters reduce the peak amplitude of the system. At the low velocity, increasing these parameters cause the force transmissibility to decrease, their effects are opposite at high velocity. It is convenient to use a pratical value of these parameters. This result is opposite to the case of displacement transmissibility as studied by [117]; in the present case, effect of ε_3 is similar to that of ε_1 and is more notable than ε_2.

The amplitude and absolute force transmissibility curves with different values of stiff-

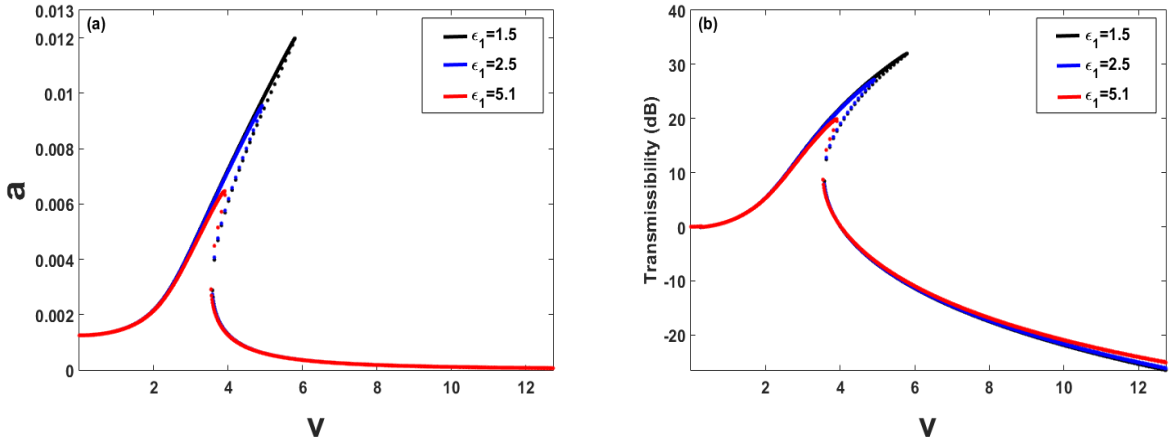

Figure 3.21: Effet of ε_1 on: **a)**Amplitude responses of the isolated beam. **b)** Absolute force transmissibility. Solid line denotes the stable responses and pointed line denotes the unstable responses for defaults parameters.

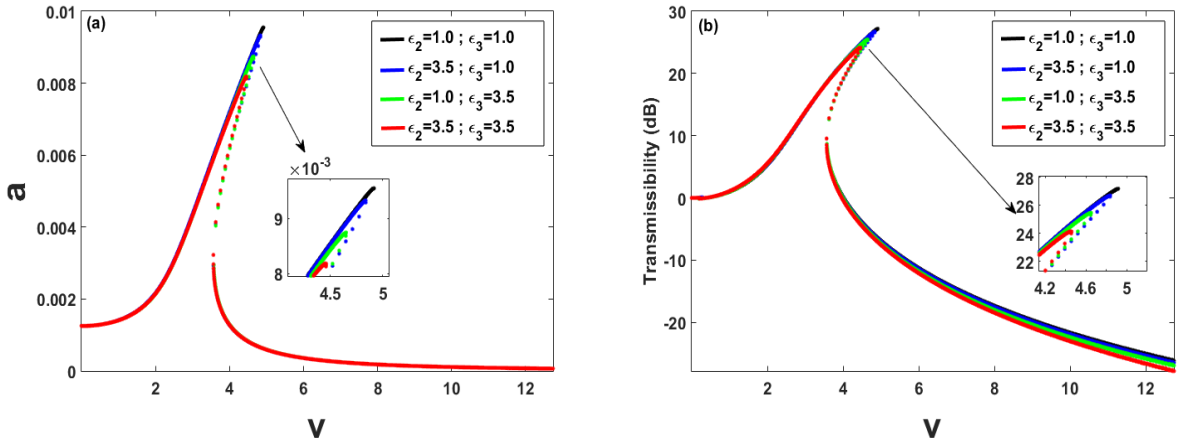

Figure 3.22: Effet of ε_2 and ε_3 on: **a)**Amplitude responses of the isolated beam. **b)** Absolute force ransmissibility. Solid line denotes the stable responses and pointed line denotes the unstable responses for defaults parameters.

ness ratios λ_2 and λ_3 are presented in Fig.3.23. For a smallest value of λ_3, increasing λ_2 reduce the peak amplitude and absolute force transmissibility. Also we remarks that, peak amplitude and transmissibility increase as λ_3 increase. Especially, when λ_2 is too great, increasing λ_3 may change the peak frequency and create a discontinuity in absolute force transmissibility as shown in Fig. 3.23 (b). This discontinuity is due to instability in dynamics of auxiliary mass. One can conclude that these last two stiffness must be moderate, great λ_2 and small λ_3 is recommended for a perfomant isolator. In another

these effect are the same for low and high frequency. Effect of x_{12} is depicted on Fig. 3.24.

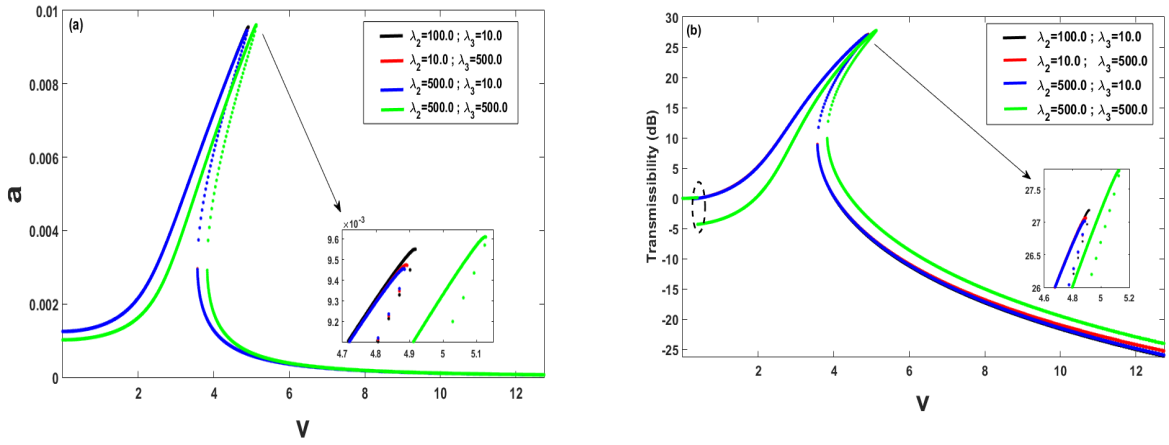

Figure 3.23: Effet of λ_2 and λ_3 on: **a)**Amplitude responses of the isolated beam. **b)** Absolute force ransmissibility. Solid line denotes the stable responses and pointed line denotes the unstable responses for defaults parameters.

Since, at low velocity, increasing this value contribute to decrease the peak amplitude and absolute force transmissibility. Furthermore, at high velocity, the effect is opposite to the case of low amplitude. To be realistic for a practical application, a smallest value of x_{12} must be chosen.

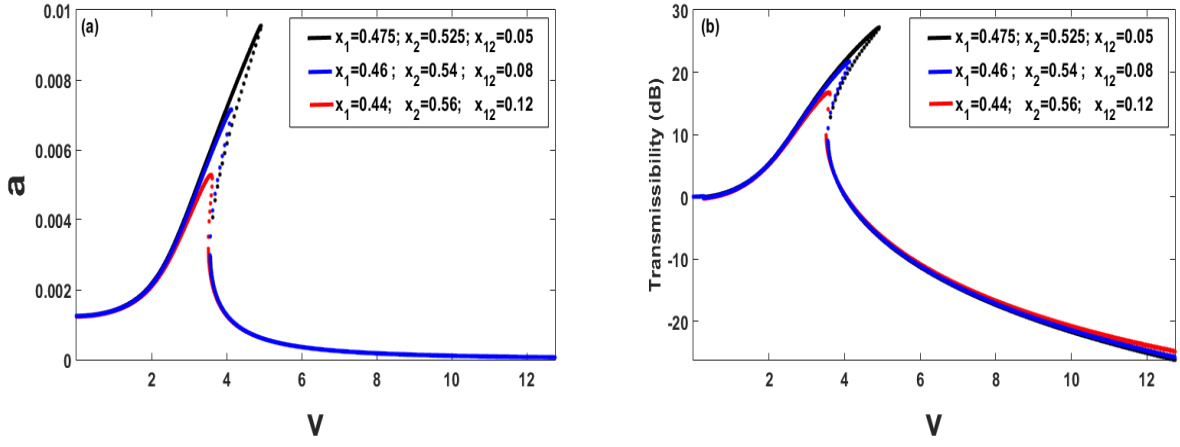

Figure 3.24: Effect of x_{12} on: **a)**Amplitude responses of the isolated beam. **b)** Absolute force ransmissibility. Solid line denotes the stable responses and pointed line denotes the unstable responses for defaults parameters.

Figs. 3.25 and 3.26 displays the effect of thermal change in amplitude responses and

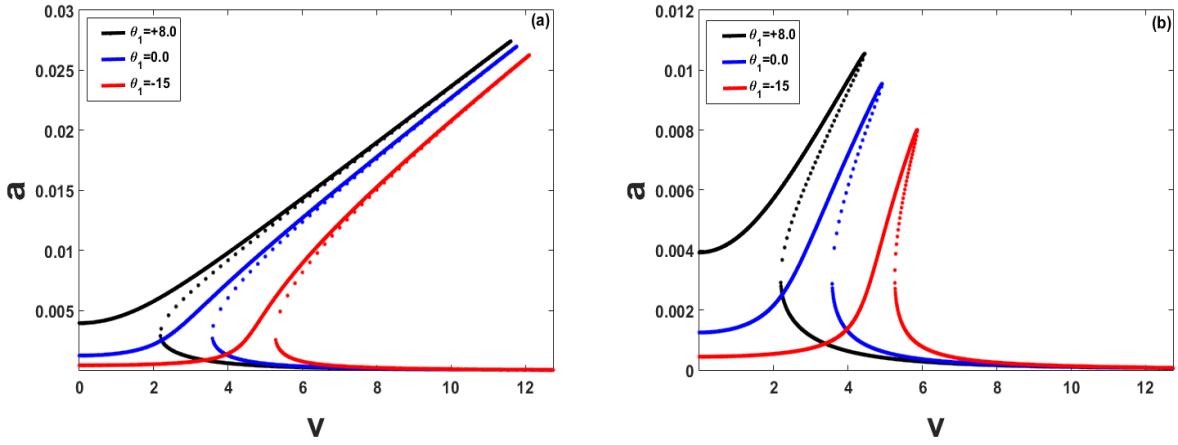

Figure 3.25: Amplitude responses of the beam for different values of θ_1: a) Without HSLDS-AS b) and With HSLDS-AS for default parameters. Solid line denotes the stable responses and pointed line denotes the unstable responses.

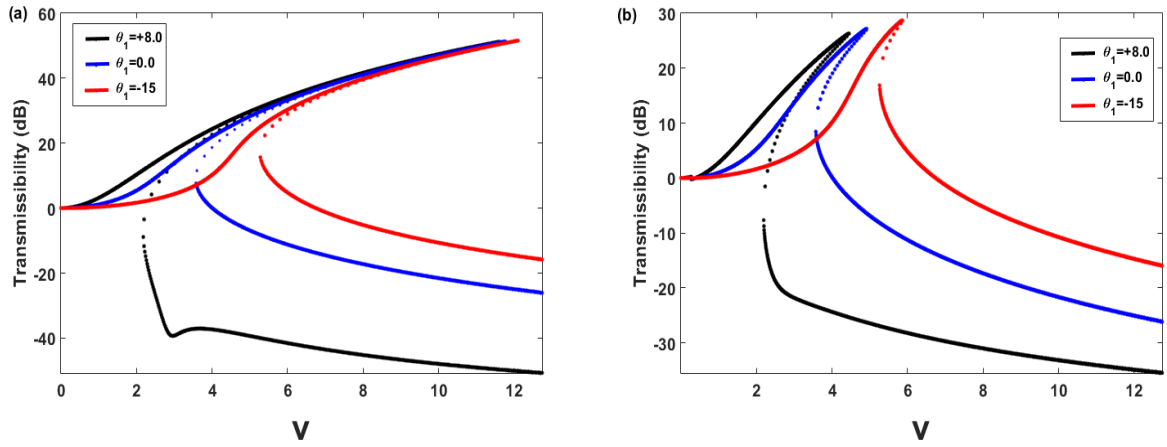

Figure 3.26: Absolute force transmissibility for different values of θ_1: a) Without HSLDS-AS b) and With HSLDS-AS for default parameters. Solid line denotes the stable responses and pointed line denotes the unstable responses.

absolute force transmissibility. It can be observed that, for the uncontrolled and controlled beam, decrease temperature increase the hardening behaviour and causes the amplitude curves to bend right. In another, the reduction of peak amplitude with temperature rise is more obvious for controlled beam (Fig. 3.25(b)). Besides, when the temperature increases, the tranmissibility increase at low velocity and decrease at high velocity. This means that the force transmitted to substructure increase with decreasing in temperature (Fig. 3.26). We concluded that, the temperature do not only reduce or increase the natural frequency

or amplitude of a structure but, this variation affect consequently the transmissibility of the structure and can cause damage on the supports due to the redundant force transmitted due to temperature variation. This results must be taking on to account when designing isolator or supports.

3.4 Conclusion

The present chapter has presented the results obtained in this thesis work. Firstly, thermomechanical analysis of a cable stayed beam subjected to wind load and platoon moving load is investigated. A partial differential equation governing the vibration is proposed and deduced from a Bernoulli-Euler beam where the geometrical non-linearity is taken into account. The analysis shows that, effect of thermal load on the structure depend on the constituted material, types of loads and geometrical parameters of the structure. Secondly, a beam isolated by a HSLDS-AS on the thermal condition is evaluated. It is shown that thermal variation affect significantly the performance of the control system. Comparing these results, it is obvious that effects of temperature variation on an structure are more complex and depend on the geometrical parameters, materials constitution of the structure. Thus, taking into account thermal loads due to temperature change in environment, materials properties and loads conditions, many complex phenomenon or loss stability depending on the type of external loads can be avoided. Also, ignoring thermal effect, the damaged detection based on the vibration characteristics and control of structure will be no more efficient.

General conclusion

This dissertation has dealt with dynamics analysis of controlled and uncontrolled structure subjected to thermal environmental change, under the action of traffic loads and wind loads. The studied structures include simply support beam controlled by an non-linear isolator, and a cable-stayed beam. The traffic loads has been modelled firstly as a simple moving load and secondly as a platoon moving load which is an idealised multiple moving vehicles with regular uniform intervals.

In the first chapter, the state of art on the structural modelling using dynamics of Euler-Bernoulli, Rayleigh and Timoshenko beam via dynamics fundamental relationship approach have been made. The mathematical models of used mechanical action and thermal load due to environmental change in temperature have been done. Then the generalities on vibration control systems are presented, by a review on some structural control methods before the problematic of the thesis.

In the second chapter,analytical and numerical tools used for development and analysis were presented. More precisely, four analytical techniques including the classical harmonic balance method, multiples scales method to aproach the non-linear SDEs, Routh-Hurwitz criterion to give the decision on the stability of the non-trivial steady-states solutions of the non-linear ODEs. Numerical methods RK4 for the ODEs, the Newton-Leipnik and the A-B-M predictor-corrector schemes to integrate the non-linear FDEs and the Newton-Raphson method to solve complex or non-trivial polynomial equations, have been presented. Furthermore the methods to assess performance of an isolator, and HSLDS-AS mechanism are clearly explained.

The third chapter has been devoted to the dynamical behaviour of some models of structure in thermal condition and subject to moving loads and/or wind flows. Two models have been studied and the main results obtained have been presented and discussed. In the first set of results, a cable-stayed beam having fractional derivative order subjected to non-linear thermal load and loaded by a platoon moving loads and wind flow has been investigated. On the basis of the multiple scales method, using linear analysis we have demonstrated that wind flow leads to two types of bifurcation whose appearance conditions are modified by thermal loads and fractional derivative order. Furthermore, considering the two types of loads differently, and conducting a non-linear analysis, there have been found that, thermal effect on structure is modified by the presence of fractional derivative order and many dangerous effect can be observed and mitigated by choosing a convenient structural parameter. In the second set of results, the problem of the non-linear response of an axial compressing Euler Bernoulli beam, subjected to a moving single

force and thermal loads and isolated by a non-linear isolator (HSLDS-AS isolator) has been considered. Using the theory of Harmonic balance method, we have demonstrated the effect of thermal loads on the performance of the isolator and the response of the structure under traffic loads. The analytic approach has been also checked with numerical simulations and we have observed a fairly good agreement. In this thesis, some of the results have opened interesting perspectives for future investigations. For example, It might also be interesting to extend this work to include the higher coupled modes which have been neglected. Also developing novel active device for mitigated the thermal effect on structure is a promised subject. So thermal effect can induce false damage detection, it could be interesting to find suitable algorithm which taking into account the thermal change in sensing; in this ways, Artificial Neural Network and Deep learning can be a powerful tool for this issue.

Bibliography

Bibliography

[1] P. Lenkei ,(2007), Climate change and structural engineering, *Periodica polytechnica, Civil Engineering 51/2, 47–50.*

[2] A. Dlugoseci et al. ,(2009), Coping with Climate Change: Risks and opportunities for Insurers,*Charted Insurance Institute, London /CII-3112, 31p.*

[3] UNECE (2013), Climate Change Impacts and Adaptation for International Transport Networks,United Nations, *New York and Geneva, 248p.*

[4] E. Simiu and R. H. Scanlan, (1996), Wind effects on structures: Fundamentals and Applications to Design,*John Wiley and Sons Publication.*

[5] C. G. Bucher and Y. K. Lin, (1988), Stochastic stability of bridges considering coupled modes, *Journal of Engineering Mechanics. ASCE 114: 2055-2071.*

[6] B.R. Nana Nbendjo, (2004), Dynamics and active control with delay of the dynamics of unbounded monostable mechanical structures with ϕ^6 potential, *PhD Thesis in Non-linear Mechanics, University of Yaoundé 1, Yaoundé, Cameroon.*

[7] Shafic Sami Oueini,(1999),Techniques for Controlling Structural Vibrations, *Virginia Polytechnic Institute and State University,177.*

[8] [Ashour Osama Naim, Nonlinear control of plate vibrations,(2001), *PhD Thesis, Virginia Polytechnic Institute and State University.*

[9] A.A. Nanha Djanan ,(2010), Dynamic and Control of a hinged-hinged beam supporting a DC motor , *Master's Degree Thesis, University of Yaounde I.*

[10] A.A. Nanha Djanan , B.R. Nana Nbendjo, P. Woafo,(2013), Electromechanical control of vibration on a plate submitted to a non-ideal excitation, *Mechanics Research Communications, 54: 72-82.*

[11] Anague Tabejieu Lionel Merveil, (2017), on the dynamics of bridges subjected to service loads: roads traffic, train traffic and wind actions, *PhD dissertation, Universit Younde I, Cameroon.*

[12] S.M. Han, H.B. and T. Wan, (1999), Dynamics of transversely vibrating beams using four engineering theories, *Journal of Sound and Vibration 225(5) 935-988.*

[13] A.H. Nayfeh, D.T. Mook, (1979), Nonlinear oscillations, *John Wiley, New York, 704.*

[14] Hayashi C., (1964), Nonlinear oscillations in physical systems. *Mc Graw-Hill Inc, New York.*

[15] M. T. Song D. Q. Cao W. D. Zhu Q. S. Bi, (2013), Dynamic response of a cable-stayed bridge subjected to a moving vehicle load, *Acta of Mechanical 227 : 2825-2945.*

[16] Singiresu S. Rao, (2007), Vibration of Continuous Systems, *John Wiley and Sons, Inc., Hoboken, New Jersey.*

[17] Mosaad AF., (1999), Influence of shear deformation and rotary inertia on nonlinear free vibration of a beam with pinned ends, *Computers and Structures 1 : 663-670.*

[18] S.Timoshenko, Vibration Problems In Engineering, *New York, D. Van Nostrand Company, inc.*

[19] Chen Z., Xu Y., Wang X., (2011), SHMS-based fatigue reliability analysis of multi loading suspension bridges. *Journal of Structural Engineerging 138 : 299–307*

[20] Chen Z., Xu Y-L., Li Q., Wu D-J., (2011), Dynamic stress analysis of longue suspension bridge under wind, railway, and highway loadings, *Bridge Engigneering 16 : 383–391.*

[21] Yi TH., Li HN., Gu M., (2013), Wavelet based multi-step filtering method for bridge health monitoring using GPS and accelerometer, *SSS 11 : 331–348.*

[22] Maleki S., Maghsoudi-Barmi A., (2016), Effects of concurrent earthquake and temperature loadings on cable stayed bridges, *International Journal of Structural Stabability Dynamics 16 : 1550020.*

[23] Anague Tabejieu L.M., Nana Nbendjo B.R., Filatrella G., Woafo P., (2017), Amplitude stochastic response of Rayleigh beams to randomly moving loads, *Nonlinear Dynamics 89 : 925–937.*

[24] Sahoo PR., Barik M., (2021), Dynamic response of stiffened bridge decks subjected to moving loads, *Journal of Vibration Engigneering and Technologie, https://doi.org/10.1007/s42417-021-00344-4.*

[25] Salawu OS., (1997), Detection of structural damage through changes in frequency : a review, *Engigneering Structures 19 : 718–723.*

[26] Xu YL., Chen B., Ng CL., Wong KY, Chan WY., (2010), Monitoring temperature effect on a long suspension bridge, *Structural Control Health Monitoring 17 : 632–653.*

[27] Boley, B.A., Weiner, J.H., (1960), Theory of Thermal Stress. , *Wiley, New York.*

[28] Nowacki, W., (1975), Dynamic Problems of Thermoelasticity, *Noordhoff, Leyden.*

[29] Thorton, E.A., (1996), Thermal Structures for Aerospace Applications, *AIAA Education Series, Reston.*

[30] Wu GY., (2005), The analysis of dynamic instability and vibration motions of a pinned beam with transverse magnetic fields and thermal loads, *Journal of Sound and Vibbration 284:343–36.*

[31] Wu GY., (2007), The analysis of dynamic instability on the large amplitude vibrations of a beam with transverse magnetic fields and thermal loads, *Journal of Sound and Vibbration 302 : 167–177.*

[32] Manoach E., Ribeiro P., (2004), Coupled thermoelastic, large amplitude vibrations of Timoshenko beams, *International Journal of Mechanical science Sci 46 :1589–1606.*

[33] Ribeiro P, Manoach E, (2005), The effect of temperature on the large amplitude vibrations of curved beams, *Journal of Sound and Vibbration 285 :1093–1107.*

[34] Guo XX., Wang ZM., Wang Y., Zhou YF., (2009), Analysis of the coupled thermoelastic vibration for axially moving beam, *Journal of Sound and Vibbration 325 : 597–608.*

[35] Ghayesh MH., Kazemirad S., Darabi MA., Woo P., (2020), Thermomechanical nonlinear vibration analysis of a spring mass-beam system, *Archieve of Applied Mechanics 82 : 317–331.*

[36] Warminska A., Manoach E., Warminski J., (2014), Nonlinear dynamics of a reduced multimodal Timoshenko beam subjected to thermal and mechanical loadings, *Meccanica 49 : 1775–1793.*

[37] Warminska A., Manoach E., Warminski J., Samborski S., (2015) ; Regular and chaotic oscillations of a Timoshenko beam subjected to mechanical and thermal loadings, *Continuum Mechanics and Thermodynamics 27 : 719–737.*

[38] L. Gu, Z. Qin, F. Chu, (2015), Analytical analysis of the thermal effect on vibrations of a damped Timoshenko beam, *Mechanical Systems and Signal Processing, http://dx.doi.org/10.1016/j.ymssp.2014.11.014.*

[39] Ndoukouo, A. N., Metsebo, J., and Njankouo, J. M., (2021), Vibrational analysis of a metallic column submitted to mechanical axial load and fire exposure, *Chaos Theory and Applications, 3(2) :77-86.*

[40] Yong Xia, Bo Chen, Shun Weng, Yi-Qing Ni, You-Lin Xu, (2012), Temperature effect on vibration properties of civil structures : a literature review and case studies, *Journal of Civil Structural Health Monitoring 2 : 29-46, DOI 10.1007/s13349-011-0015-7.*

[41] Guang-Dong Zhou and Ting-Hua Yi, (2013), Thermal Load in Large-Scale Bridges : A State-of-the Art Review, *International Journal of Distributed Sensor Networks, http://dx.doi.org/10.1155/2013/217983.*

[42] Guang-Dong Zhou and Ting-Hua Yi, (2014), A Summary Review of Correlations between Temperatures and Vibration Properties of Long-Span Bridges, *Mathematical Problems in Engineering, http://dx.doi.org/10.1155/2014/638209.*

[43] Li XY., Zhao X., Li YH., (2014), Green's functions of the forced vibration of Timoshenko beams with damping effect, *Journal of Sound and Vibration 333 : 1781-95.*

[44] A. G.,SEIBERT, J. S. RiCE, (1973), Coupled ThermallyInduced Vibrations of Beams, *AIAA JOURNAL 11 :1033-1035.*

[45] Jadwiga Kidawa-Kukla, (2013), Thermally induced vibration of a cantilever beam with periodically varying intensityof a heat source, *Journal of Applied Mathematics and Computational Mechanics, 12 (4) : 59-65.*

[46] T. Jekot, (1996), Nonlinear problems of thermal postbuckling of a beam, *Journal of Thermal Stresses 19 : 359–367.*

[47] Novak, M., (1972), Galloping oscillations of prismatic structures. *Journal of Engineering Mechanics, 98 (1) :27–46 .*

[48] Piccardo, G., Pagnini, L.C., Tubino, F., (2015), Some research perspectives in galloping phenomena: critical conditions and post-critical behavior, *Continuum Mechanics and Thermodynamics 27(1–2) : 261–285.*

[49] Iannelli, A., Marcos, A., Lowenberg, M., (2018), Aeroelastic modeling and stability analysis: a robust approach to the flutter problem, *International Journal of Robust Nonlinear Control 28(1) : 342–364.*

[50] Kim, Taehyoun, (2019), Flutter prediction methodology based on dynamic eigen decomposition and frequency-domain stability, *Journal of Fluids Structural. 86 : 354-367.*

[51] Williamson, C.H.K., Govardhan, R., (2004), Vortex-induced vibrations, *Annual Revue of Fluids Mechanics 36 : 413–455.*

[52] Brika, D., Laneville, A., (1993), Vortex-induced vibrations of a long flexible circular cylinder, *Journal of Fluids Mechanics 250 : 481–508.*

[53] Parkinson, G.V., Wawzonek, M.A., (1981), Some considerations of combined effects of galloping and vortex resonance, *Journal of Wind Engineering Industrial Aerodynamics 8 (1–2) : 135–143.*

[54] Luongo, A., Zulli, D., (2012), Dynamic instability of inclined cables under combined wind flow and support motion. *Nonlinear Dynamics. 67 (1) :71–87.*

[55] Mannini, C., Marra, A.M., Bartoli, G., (2014), Viv-galloping instability of rectangular cylinders: Review and new experiments *Journal of Wind Engineering Industrial Aerodynamics 132 :109–124.*

[56] Sourav, K., Sen, S., (2019), Transition of viv-only motion of a square cylinder to combined viv and galloping at low reynolds numbers, *Ocean Engineering 187.*

[57] Warminski, Jerzy, (2020), Nonlinear dynamics of self-, parametric, and externally excited oscillator with time delay : van der pol versus rayleigh models, *Nonlinear Dynamics 99(1) : 35–56.*

[58] Lu, O.S., To, C.W.S., (1991), Principal resonance of a nonlinear system with two-frequency parametric and self-excitations, *Nonlinear Dynamics. 2(6) : 419–444.*

[59] Szabelski, K., Warminski, J., (1995), Parametric self-excited nonlinear system vibrations analysis with inertial excitation, *International Journal of Nonlinear Mechanics 30(2) : 179–189.*

[60] El-Bassiouny, A.F., (2005), Principal parametric resonances of nonlinear mechanical system with two-frequency and selfexcitations, *Mechanics Research Communication 32(3) : 337–350.*

[61] Di Nino, S., Luongo, A., (2020), Nonlinear interaction between selfand parametrically excited wind-induced vibrations, *Nonlinear Dynamics 1–23.*

[62] Luongo, A., Zulli, D., (2011), Parametric, external and selfexcitation of a tower under turbulent wind flow, *Journal of Sound and Vibration 330 (13) : 3057–3069.*

[63] Zulli, Daniele, Luongo, Angelo, (2012), Bifurcation and stability of a two-tower system under wind-induced parametric, external and self-excitation, *Journal of Sound and Vibration 331 (2) : 365–383.*

[64] Kirrou, Ilham, (2013), Mokni, Lahcen, Belhaq, Mohamed : On the quasiperiodic galloping of a wind-excited tower, *Journal of Sound and Vibration 332 (18) : 4059–4066.*

[65] Belhaq, Mohamed, (2013), Kirrou, Ilham, Mokni, Lahcen : Periodic and quasiperiodic galloping of a wind-excited tower under external excitation, *Nonlinear Dynamics. 74 (3) : 849–867.*

[66] Zulli, D., Di Egidio, A., (2015), Galloping of internally resonant towers subjected to turbulent wind, *Continuum Mechanics Thermodynalic27 (4–5) : 835–849.*

[67] Angelo Luongo, Daniele Zulli, (2011), Parametric, external and self-excitation of a tower under turbulent wind flow, *Journal of Sound and Vibration 330 : 3057–3069.*

[68] Simona Di Nino, Angelo Luongo, (2020), Nonlinear dynamics of a base-isolated beam under turbulent wind flow, *Nonlinear Dynamics https://doi.org/10.1007/s11071-021-06412-4.*

[69] Mohamed Abdel-Rohman, (2011), The influence of the higher order modes on the dynamic response of suspension bridges, *Journal of Vibration and Control (9) : 1380-1405.*

[70] L.M. Anague Tabejieu, B.R. Nana Nbendjo, G. Filatrella, (2019), *Effect of the fractional foundation on the response of beam structure submitted to moving and wind loads, Chaos, Solitons and Fractals (127) : 178–188.*

[71] M. Abdel-Rohman, (2001), *Effect of unsteady wind flow on galloping of tall prismatic structures, Nonlinear Dynamics 26 (3) : 233-254.*

[72] Frýba, L., (1972), Vibration of Solids and Structures Under Moving Loads, *Thomas Telford, London.*

[73] Au, F.T.K., Cheng, Y.S. and Cheung, Y.K., (2001), Vibration analysis of bridges under moving vehicles and trains : An overview, *Progress in Structural Engineering and Materials, 3 (3) : 299-304.*

[74] A.N. Krylov, (A.N. Kriloff) ,(1905), Über die erzwungenen Schwingungen von gleichformigen elastichen Stäben, *Mathematische Annalen, 61 : 211-234 (in German)* .

[75] S.P. Timoshenko, Forced vibration of prismatic bars, (1908), *Izvestiya Kievskogo politekhnicheskogo instituta (in Russian)* ; (1911), *Erzwungene Schwingungen prismatischer Stabe, Zeitschrift für Mathematik und Physik 59 (2) : 163–203 (in German)* .

[76] C.E. Inglis, (1934), A Mathematical Treatise on Vibration in Railway Bridges, *The Cambridge University Press, Cambridge.*

[77] A.N. Lowan, (1935), "On transverse oscillations of beams under the action of moving variable loads", *Philosophical Magazine, Series 7, 19 (127) :708–715.*

[78] V. Koloušek, Dynamics of Civil Engineering Structures, (1967, 1956, 1961), *Part I : General problems, 2nd ed. — Part II : Continuous Beams and Frame Systems,*

2nd ed— Part III : Selected Topics, SNTL, Prague (in Czech.). (1973), *Dynamics in engineering structures, Academia, Prague, Butterworth, London.*

[79] S.P. Timoshenko, (1926), Statical and dynamical stresses in rails, *Proceedings of the 2nd International Congress for Applied Mechanics, Zürich (Switzerland), 407-418.*

[80] Xia, H., Zhang, N. and Guo, W. W., (2006), Analysis of resonance mechanism and conditions of train-bridge system, *Journal of Sound and Vibration, 297 (3) : 810-822.*

[81] Bruno, D., F. Greco and P. Lonetti., (2008), Dynamic impact analysis of long span cable-stayed bridges under moving loads, *Engineering Structures, 30 (4)* .

[82] Mao, L. and Lu, Y., (2011), Critical speed and resonance criteria of railway bridge response to moving trains, *Journal of Bridge Engineering, 18 (2) : 131-141.*

[83] Cheng, Y. S., Au, F. T. K. and Cheung, Y. K., (2001), Vibration of railway bridges under a moving train by using bridge-track-vehicle element, *Engineering Structures, 23(12) : 1597-1606.*

[84] Yau, J. D. and Yang, Y. B., (2004), Vibration reduction for cable-stayed bridges traveled by high-speed trains, *Finite Elements in Analysis and Design, 40(3) : 341-359.*

[85] SONFACK BOUNA Hervé, (2020), Dynamics and vibration isolation of two multi-span continuous beam bridges coupled by their close environment, *Ph.D. Dissertation, University of Yaound » I, Cameroon.*

[86] Lu Sun, Feiquan Luo, (2008), Steady-State Dynamic Response of a Bernoulli–Euler Beam on a Viscoelastic Foundation Subject to a Platoon of Moving Dynamic Loads, *Journal of Vibration and Acoustics, (130) : 051002-19.*

[87] Y. B. Yang, J. D. Yau and L. C. Hsu, (1997), *Vibration of simple beams due to trains moving at high speeds. Engineering Structures 19 : 936-944.*

[88] Y. S. Wu, Y. B. Yang and J. D. Yau, (2001), *Three-dimensional analysis of train-railbridge interaction problems. Vehicle System Dynamics 36 : 1-35.*

[89] Tarek Edrees Saaed, George Nikolakopoulos, (2013), Jan-Erik Jonasson and Hans Hedlund, A state of-the-art review of structural control systems, *Journal of Vibration and Control 0(0) : 1–19.*

[90] M. A. Lackner and M. A. Rotea, (2011), Passive structural control of offshore wind turbines, *Wind Energy 14(3) : 373–388.*

[91] G. W. Housner, L. A. Bergman, T. K. Caughey, A. G. Chassiakos, R. O. Claus, S. F. Masri, R. E. Skelton, T. T. Soong, B. F. Spencer and J. T. P. Yao, (1997), Structural control : Past, present, and future, *Journal of Engineering Mechanics 123(9) : 897–971.*

[92] A. R. Pandit and K. C. Biswal, (2019), Seismic control of structures using sloped bottom tuned liquid damper, *International Journal of Structural Stability Dynamics 19(8) : 1950096.*

[93] T.T. Soong and M.C. Costantinou, (1994), passive and active structural vibration control in civil engineering, *Wien-New York.*

[94] B. R. Nana Nbendjo, (2013), "Cours de PHY 440 : Contrôle des structures", *Master 1 de Physique, Option : Modélisation et Simulation en Ingénierie et Bioingénierie, Département de Physique, Université de Yaoundé I.*

[95] Mallik, A., Kher, V., Puri, M., Hatwal, H., (1999), On the modelling of non-linear elastomeric vibration isolators *Journal of Sound Vibration, 219 : 239–253.*

[96] Ibrahim, R., (2008), Recent advances in nonlinear passive vibration isolators, *Journal of Sound Vibration, 31 : 371–452.*

[97] Kabori T., (1999), Mission and Perspective towards Future Structural Control Research, *Proceedings of the Second World Conference on Structural Control, Vol. I, Kyoto, Japan, ISBN 0471 9831011999.*

[98] Marazzi F., (2002), Semi-active Control of Civil Structures : Implementation Aspects, *Phd thesis, University of Pavia, Structural Mechanics Department.*

[99] Sen M. Kuo and Dennis R. Morgan, (1999), Active Noise Control : A Tutorial Review, *Proceedings of the IEEE, 87 (6).*

[100] Christensen, R.M., (2003), Theory of Viscoelasticity, *Second ed. Dover Publications, Mineola, NY, USA.*

[101] E.I. Rivin, (2003), Passive vibration isolation, *New York, ASME Press.*

[102] Sudhir Kaul, (2021), Modeling and analysis of passive vibration isolation systems, *Cullowhee, NC, USA*.

[103] De Espindola, J.J., Bavastri, C.A., Lopes, E.M.D, (2008), Design of optimum systems of viscoelastic vibration absorbers for a given material based on the fractional calculus model, *Journal of Sound Vibration, 14 (9–10) : 1607–1630*.

[104] Wollscheid, D., Lion, A., (2014), The benefit of fractional derivatives in modelling the dynamics of filler-reinforced rubber under large strains : a comparison with the Maxwell-element approach, *Computer Mechanics 53 : 1015–1031*.

[105] S. Krenk and J. Hogsberg, (2014), Tuned mass absorber on a flexible structure, *Journal of Sound and Vibration, 333 : 1577-1595*.

[106] Morris, K.A., (2011), What is Hysteresis ? , *Applied Mechanics Revue 64 (5) : 050801–050814*.

[107] Ye, M., Wang, X., (2007), Parameter estimation of the Bouc-Wen hysteresis model using particle swarm optimization, *Smart Materials Structures 16 : 2341–2349*.

[108] F. Bourquin, G. Caruso, M. Peigney and D. Siegert, (2014), Magnetically tuned mass dampers for optimal vibration damping of larges structures, *Smart Materials and Structures 23(8) : 085009*.

[109] H. Yu, F. Gillot and M. Ichchou, (2013), Reliability based robust design optimization for tuned mass damper in passive vibration control of deterministic/uncertain structures, *Journal of Sound and Vibration 332(9) : 2222-2238*.

[110] Shaw AD., Neild SA., Wagg DJ., Weaver PM., Carrella A., (2013), A nonlinear spring mechanism incorporating a bistable composite plate for vibration isolation, *Journal of Sound and Vibration 332 : 6265–6275*.

[111] Huang XC., Liu XT., Hua HX., (2014), On the characteristics of an ultra-low frequency nonlinear isolator using sliding beam as negative stiffness, *Journal of Mechanical Science and Technologie 28 : 813–822*.

[112] Huang XC., Liu XT., Sun JY., Zhang ZY., Hua HX., (2014), Effect of the system imperfections on the dynamic response of a highstatic-low-dynamic stiffness vibration isolator, *Nonlinear Dynamics 76 : 1157–1167*.

[113] Carrella A., Brennan MJ., Kovacic I., Waters TP., (2009), On the force transmissibility of a vibration isolator with quasi-zero stiffness, *Journal of Sound and Vibration 322 : 707–717.*

[114] Carrella A., Friswell MI, Zotov A., Ewins DJ., Tichonov A. , (2009), Using nonlinear springs to reduce the whirling of a rotating shaft, *Mechanical System Signal Processing 23 : 2228–2235.*

[115] Kovacic I., Brennan MJ., Waters TP. , (2008), A study of a nonlinear vibration isolator with a quasi-zero stiffness characteristic, *Journal of Sound and Vibration 315 : 700–711.*

[116] Lan CC., Yang SA., Wu YS., (2014), Design and experiment of a compact quasi-zero-stiffness isolator capable of a wide range of loads, *Journal of Sound and Vibration 333 : 4843–4858.*

[117] Liu C., Yu K., (2018), A high-static-low-dynamic-stiffness vibration isolator with the auxiliary system, *Nonlinear Dynamics 94 : 1549–1567.*

[118] Thakadu K., Li KA., (2021), Passive vibration isolator integrated a dynamic vibration absorber with negative stiffness spring, *Journal of Vibration Engineering and Technologie. https://doi.org/10.1007/s42417-021-00364-0.*

[119] Bhowmik K., Debnath N., (2021), On stochastic design of negative stiffness integrated tuned mass damper (NS-TMD), *Journal of Vibration Engineering and Technologie. https://doi.org/10.1007/s42417-021-00356-0.*

[120] Abbasi A., Khadem SE., Bab Saeed, (2016), Vibration control of a continuous rotating shaft employing high-static low-dynamic stiffness isolators, *Journal of Vibration And Control 24 : 760–783.*

[121] Sonfack Bouna H., Nana Nbendjo BR., Woafo P., (2020), Isolation performance of a quasi-zero stiffness isolator in vibration isolation of a multi-span continuous beam bridge under pier base vibrating excitation, *Nonlinear Dynamics 100 : 1125–1141.*

[122] Raid Karoumi, (1998), Response of Cable-Stayed and Suspension Bridges to Moving Vehicles: Analysis methods and practical modeling techniques, *PhD dissertation, Royal institute of technology, SE 10044 Stockholm, Sweden.*

[123] Wahrhaftig ADM., Magalhães KMM., Brasil RMLRF., Murawski Krzysztof, (2021), Evaluation of Mathematical Solutions for the Determination of Buckling of Columns Under Self-weight, *Journal of Vibration Engineering and Technologie 9, 733-749.*

[124] Wahrhaftig ADM., Brasil RMLRF., (2017), Vibration analysis of mobile phone mast system by Rayleigh method,*Applied Mathematics Modelling 42:330-45.*

[125] Wahrhaftig ADM, Silva MAD, Brasil RMLRF, (2019), Analytical determination of the vibration frequencies and buckling loads of slender reinforced concrete towers, *Latine America Journal of Solids Structures 16 (05) .*

[126] Zhao Y. and Huang C., (2018), Temperature Effects on Nonlinear Vibration Behaviors of Euler-Bernoulli Beams with Different Boundary Conditions, *SHOCK and VIBRATION 6:1-11.*

[127] A. Carrella, M.J. Brennan T.P. Waters , V. Lopes Jr., (2012), Force and displacement transmissibility of a nonlinear isolator with high-static-low-dynamic-stiffness, *International Journal of Mechanical Sciences 55 :22-29.*

[128] Jean-Claude Pascal, (2008), Vibrations et Acoustiques 1, *Ecole Nationale d'ingenieurs du Mans, Université Du Maine, France.*

[129] A.H. Nayfeh, (1973), Perturbation Methods, *John Wiley and Sons.*

[130] D.W. Jordan and P. Smith, (1999), Nonlinear Ordinary Differential Equations, *Oxford,3th Edn.*

[131] J.J. Thomsen, (1997), Vibration and Stability - Order and Chaos, *McGraw Hill.*

[132] L. Meirovitch, (1986), Elements of Vibration Analysis, *McGraw Hill, International Edn.*

[133] A. Rand, (2005), Lecture Notes on Nonlinear Vibration, *Wiley.*

[134] C. Hayashi, (1964), Nonlinear Oscillations in Physical Systems, *McGraw Hill.*

[135] B.G. Galerkin, (1915), Series solution of some problems of elastic equilibrium of rods and plates, *Vestn. Inzh. Tekh 19 : 897-908.*

[136] Nayfeh, A.H, (1981), Introduction to Perturbation Techniques, *New York: Wiley.*

[137] C. P. Simon and L. Blume, (1994), *Mathematics for economists. W.W. Norton and company New York.*

[138] W.H. Press, S.A. Teukolsky, W.T. Vetterling and B.P. Flannery, (2007), Numerical Recipes: The Art of Scientific Computing, *Cambridge University Press ISBN 0521880688, August.*

[139] I.Petráš, (2011), Fractional-order Nonlinear Systems: Modeling, Analysis and Simulation, *Higher Education Press Beijing.*

[140] W. Deng, (2007) , Short memory principle and a predictor-corrector approach for fractional differential equations, *Journal of Computer Applied Mathematics 206 : 174-188.*

[141] K. Diethelm, N.J. Ford, D.Freed, (2002), A predictor-corrector approach for the numerical solution of fractional differential equations, *Nonlinear Dynamics. 29:3-22* .

[142] G. S. Ngueteu Mbouna and P. Woafo, (2012) , Dynamics and synchronization analysis of coupled fractional-order nonlinear electromechanical systems, *Mechanichs Resarch Communications46 : 20-25.*

[143] I. Podlubny, (1999), Fractional Differential Equations, *Academic Press San Diego.*

[144] L. M. Anague Tabejieu, B. R. Nana Nbendjo, P. Waofo, (2016) , On the dynamics of Rayleigh beams resting on fractional-order viscoelastic Pasternak foundations, *Chaos Solitons and Fractals 93 : 39-47.*

[145] Wahrhaftig, A. D. M., Brasil, R. M. L. R. D. F., Groba, T. B., Rocha, L. M. L., Balthazar, J. M., Nascimento, L. S. M. S. C. ,(2020), *Resonance of a rotary machine support beam considering geometric stiffness. Journal of Theoritical Applied Mechanics 58(4), 1023-1035.*

[146] Y.A. Rossikhin, M. V. Shitikova, A.I. Krusser,(2016), To the question on the correctness of fractional derivative models in dynamic problems of viscoelastic bodies, *Mechanics Research Communication 77: 44-49* .

[147] G. T. Oumbé Tékam, C. A. Kitio Kwuimy, and P. Woafo,(2015), Analysis of tristable energy harvesting system having fractional order viscoelastic material, *Chaos: An Interdisciplinary Journal of Nonlinear Science 25, 013112* .

[148] P.R. Nwagoum tuwa , C.H. Miwadinou , A.V. Monwanou , J.B. Chabi orou , P. Woafo ,(2019), Chaotic vibrations of nonlinear viscoelastic plate with fractional derivative model and subjected to parametric and external excitations, *Mechanics Research Communications, doi: https://doi.org/10.1016/j.mechrescom.2019.04.001* .

[149] M. D. Ortigueira and J. 0A. T. Machado, "What is a fractional derivative?",*Journal of Computational Physics, (published online).*

[150] M. D. Ortigueira,(2011), Fractional Calculus for Scientists and Engineers, *Lecture Notes in Electrical Engineering,Springer, Berlin, Heidelberg.*

[151] S. Samko, A. Kilbas, and O. Marichev,(1993), Fractional Integrals and Derivatives: Theory and Applications, *Gordon and Breach Science Publishers, Amsterdam.*

[152] T. B. Djuitchou Yaleu, J. Metsebo, B. R. Nana Nbendjo, P. Woafo, (2021), Effect of Thermal and High Static Low Dynamics Stiffness Isolator with the Auxiliary System on a Beam Subjected to Traffic Loads, *Journal of Vibration Engineering and Technologies, https://doi.org/10.1007/s42417-021-00399-3.*

[153] AH. Nayfeh , DT. Mook,(1979), *Nonlinear oscillations. Wiley, New York.*

[154] A. L. Katembo and M. V. Shitikova, (2019), Influence of fractional calculus model parameters on nonlinear forced vibrations of suspension bridges, *IOP Conference Series: Materials Science and Engineering 489: 012037.*

[155] CA. Kitio Kwuimy , BR. Nana Nbendjo , P. Woafo, (2006), Optimization of electromechanical control of beam dynamics: Analytical method and finite differences simulation, *Journal of Sound and Vibration 298:180–93* .

[156] D. Liu, W. Xu, Y. Xu,(2013), Stochastic response of an axially moving viscoelastic beam with fractional order constitutive relation and random excitations, *Acta Mechanica Sinica 29(3):443–51.*

[157] MD. Paola, FP. Pinnola, M. Zingales, (2013), A discrete mechanical model of fractional hereditary materials, *Meccanica 48(7):1573–86* .

[158] LB. Eldred , WP. Baker ,AN. Palazotto, (1995), Kelvin-voigt vs fractional derivative model as constitutive relations for viscoelastic materials, *American Institute of Aeronautics and Astronautics Journal 33:547–50* .

[159] Houjun Kang, Yunyue Cong, Guirong Yan, (2020), Theoretical analysis of dynamic behaviors of cable-stayed bridges excited by two harmonic forces, *Nonlinear Dynamics, https://doi.org/10.1007/s11071-020-05763-8* .

[160] L. Debnath (2003), Recent applications of fractional calculus to science and engineering. *International Journal of Mathematics and Mathematical Sciences 54: 3413–42* .

[161] I. Robertson, L. Li, S.J. Sherwin, P.W. Bearman,(2003) A numerical study of rotational and transverse galloping rectangular bodies. *Journal of Fluids Structures 17(5): 681–699.*

[162] M. Novak, (1972), Galloping oscillations of prismatic structures. *Journal of engineering Mechanics* 98(1):27–46

[163] Yaobing Zhao, Chaohui Huang, Lincong Chen, Jian Peng,(2018), Nonlinear vibration behaviors of suspended cables under two-frequency excitation with temperature effects, *Journal of Sound and Vibration 416: 279-294.*

List of publications

1- **T.B. Djuitchou Yaleu**, J. Metsebo, B.R. Nana Nbendjo, P. Woafo, (2022), Effect of Thermal and High Static Low Dynamics Stiffness Isolator with the Auxiliary System on a Beam Subjected to Traffic Loads, *Journal of Vibration Engineering and Technologies 10:2021–2032.*

2- **T.B. Djuitchou Yaleu**, E.R. Fankem, B.R. Nana Nbendjo, On the nonlinear thermo-mechanical analysis of a stayed-beam having fractional viscoelastic properties in complex environment, *Journal of Applied Nonlinear Dynamics,* ***(in press)***.

Collection of the published papers

Journal of Vibration Engineering & Technologies (2022) 10:2021–2032
https://doi.org/10.1007/s42417-021-00399-3

ORIGINAL PAPER

Effect of Thermal and High Static Low Dynamics Stiffness Isolator with the Auxiliary System on a Beam Subjected to Traffic Loads

T. B. Djuitchou Yaleu[1,2] · J. Metsebo[3] · B. R. Nana Nbendjo[1] · P. Woafo[1]

Received: 30 August 2021 / Revised: 5 October 2021 / Accepted: 7 October 2021 / Published online: 27 October 2021

Abstract

Purpose A high static low dynamic stiffness isolator with the auxiliary system (HSLDSAS) is used to control the vibrations characteristics of a hinged-hinged beam subjected to an axial and a constant moving load, taking into account the effect of the temperature on the structure.

Method HSLDS-AS is insert between a support and the beam; after obtaining the mathematical model via the newton second law of motion, the Galerkin discretization technique is used to derive the modals equations, which are solved by the harmonic balance method (HBM) coupled to averaging method for stability analysis.

Results and conclusion The results of this research reveals that, the isolator, reduces significantly peak amplitudes and force transmissibility of the structure. Furthemore, thermal variation can mask damage detection based on amplitude or natural frequency, and create additionnal stresses in the support or compromise the performance of isolation systems. These results will attract the attention of designers of damage detection and isolation systems.

Keywords High static low dynamic stiffness · Force transmissibility · Moving load · Thermal effect · Vibration control

Introduction

Most civil engineering structures are often subject to adverse environmental events, their exploitation loads and disasters [1–6]. For this reason, some studies were carried out for structures subjected in their various applications to combined actions of thermal and dynamic loadings. In fact, the temperature fluctuations create a thermal stress caused by contraction or dilatation of the materials (steel, concrete, etc..); this stress affects significantly the dynamics of the structure.

Although there are several research activities in the field of thermomechanical vibrations, we present here some works which have been done. The dynamics of a beam subjected to a magnetic field and thermal loads with the nonlinear deformation has been studied by Wu [7, 8]. Influences of the magnetic field parameters and temperature changes on the vibration characteristics of the beam have been discussed. The non-linear vibrations of moderately thick, curved and axially moving beams subjected to thermomechanical loads have been examined [9–11]. A spring-mass-beam system on the thermomechanical loading were investigated analytically [12]; the mass, spring and thermal effects on a hinged-hinged Euler Bernoulli beam have been analysed. Non-linear dynamics of a beam under the influence of thermal and mechanical loadings were analysed and discussed by Warminska et al. [13, 14].

In the reports mentioned above, most studies have shown that temperature varies inversely with natural frequencies and could increase the hardening non-linearity of the structure. As a result, durability and most of the structural damages detection techniques will not be optimal [15]. Faced with this, researchers and engineers have therefore carried out research to set up active, semi-active or passive control devices to increase the ability of structures to dissipate energy.

✉ B. R. Nana Nbendjo
nananbendjo@yahoo.com

[1] Laboratory of Modelling and Simulation in Engineering, Biomimetics and Prototypes, Faculty of Science, University of Yaounde I, P.O. Box 812, Yaoundè, Cameroon

[2] African Center of Excellence, National Advanced School of Engineering, University of Yaounde I, Yaoundè, Cameroon

[3] Department of Hydraulics and Water Management, National Advanced School of Engineering, University of Maroua, P.O Box 46, Maroua, Cameroon

A review literature on nonlinear passive vibration isolators have been made by Ibrahim [16]. Their pros and cons have been made. High static and low dynamics stiffness (HSLDS) are the main properties required to have an effective isolator which requires non-linearity. This principle was used by Shaw et al. [17] and Huang et al. [18, 19] to model this type of passive isolator. Recently, the HSLDS model isolators have gained more attention due to their strong conception and outstanding vibration isolation. Carrella et al. [20, 21] and Kovacic et al. [22] have carried out intensive theoretical work on HSLDS isolators having two horizontal spring providing negative stiffness and another one providing positive stiffness. Using planar springs, Lan et al. [23] have designed and experienced a quasi-zero stiffness (QZS) which is a special type of HSLDS isolator. To overcome the limitations of the HSLDS isolators, Liu et al. [24] modelled an HSLDS-AS by adding a linear auxiliary mass to the HSLDS isolator, to eliminate the jump phenomenon and improve therefore the reduction of the peak of transmissibility. In this later work, only displacement transmissibility has been studied. A passive vibration isolator integrated a dynamic vibration absorber with negative stiffness was developed by Thakadu et al. [26]. The isolator developed bear static load while limiting the static displacement and providing lower-even-zero dynamic stiffness, which are the qualities required for performant isolator. Taking into account various types of uncertainties, Bhowmik et al. [27] investigated on stochastic design of negative stiffness integrated tuned mass damper.

As a practical application of HSLDS isolators, Abbasi et al. [28] used a HSLDS for vibration control of a continuous rotating shaft and Sonfack et al. [29] investigated the performance of a quasi-zero stiffness isolator in vibration isolation of a multi-span continuous beam bridge under pier base vibrating excitation. The aims of this work are: to study the effects of HSLD-AS parameters and thermal variations on the natural frequencies, responses amplitude and force transmissibility of the system. To our knowledge, no work has been done yet for this purpose and specially for the force transmissibility of the HSDS-AS. For a good examination of the subject, in Sect. 2, an extent presentation of mathematical modelling is done, from this the HSLDS–AS mechanism are briefly explained, and the derivation of the dynamic equations of controlled beam has been done. Also, the equations of motion are discretized to second order ordinary differential equations using Galerkin's technique. The equations of amplitude and force transmissibility are derived in Sect. 3 by means of harmonic balance and averaging method, which permits to establish the stability of periodic solutions. Section 4 summarized the selected parameters used in this study. In Sect. 5, the results and discussion are given to illustrate the influences of HSLDS-AS parameters and temperature variations on natural frequencies, responses amplitude, and force transmissibility. A numerical method based on the fourth order Runge–Kutta method is used to validate the analytical result.

Mathematical Modelling

HSLDS-AS Mechanism

Figure 1a shows the structural model of HSLDS-AS carrying an isolation object which is in the present case a beam. Figure 1b presents the schematic model of HSLDS characteristic when a load is applied. In fact, HSLDS is a non-linear isolator which can induces in the isolated structure non-linear phenomenon like jump [20, 21]. Thus, including the auxiliary system contribute to eliminating the jump phenomenon due to the nonlinear stiffness of the isolator [24]. The advantages of HSLDS-AS are multiple tuned parameters and the elimination of jump phenomenon due to non-linear stiffness of the isolator.

A theoretical model of HSLDS-AS isolator consist of a vertical spring with stiffness k_1 and two oblique springs with same stiffness k_4 connected by two rods with the same length ℓ. The auxiliary mass m is added via two vertical springs with stiffness k_3 and k_2. The damping coefficients denoted by c_1, c_2 and c_3, are introduced regards to the energy dissipation.

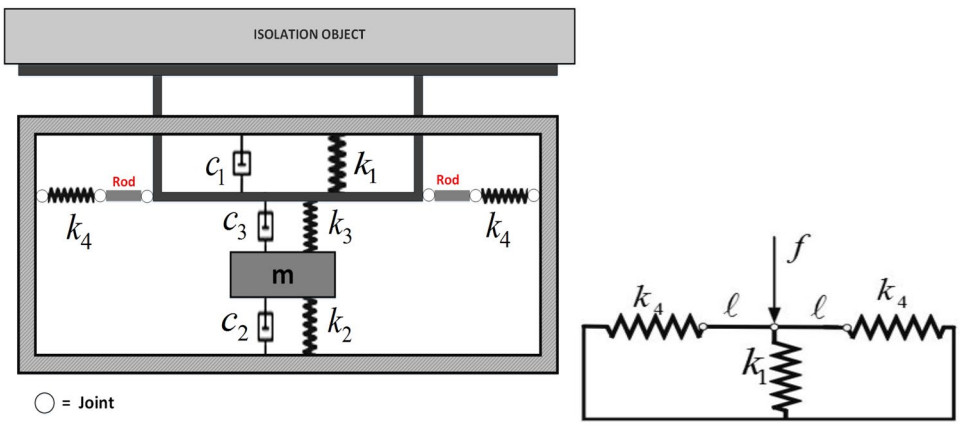

Fig. 1 **a** Structural model of HSLDS-AS and **b** schematic model of HSLDS characteristic

At the static position, springs k_4 have a compression δ_4 and the rods are horizontal; the pre-compressed horizontal spring and the rods realizes negative stiffness mechanism when a load is applied as shows Fig. 1b.

The corresponding force displacement relation of HSLDS is given by [24, 28]

$$F_{\text{HSLDS}}(W(X,T)) = 2k_4\left(\frac{\ell-\delta_4}{\sqrt{\ell^2-W(X,T)^2}}-1\right)W(X,t)+k_1W(X,T)\,. \tag{1}$$

$W = W(X,T)$ is the transversal displacement of the beam, X the coordinate measured along the length of the beam and T the time in second.

Setting $W^* = \frac{W}{\ell}$, the non-dimensional form of Eq. 1 is:

$$F^* = \frac{F_{\text{HSLDS}}}{k_1\ell} = 2\lambda_4\left(\frac{1-e}{\sqrt{1-W^{*2}}}-1\right)W^*+W^*, \tag{2}$$

differentiating Eq. 2 with respect of W^*, we obtain the non dimensional stiffness

$$K^* = 2\lambda_4\left(\frac{1-e}{(1-W^{*2})^{\frac{3}{2}}}-1\right)+1. \tag{3}$$

Considering that the system exhibits small displacement, Eqs. 2 and 3 can be approximated by using Taylor series expansion at third order and we obtain

$$F^* \simeq \alpha^2 W^* + \beta W^{*3}, \tag{4}$$

$$K^* \simeq \alpha^2 + 3\beta W^{*2}, \tag{5}$$

where

$$\alpha^2 = 1-2\lambda_4 e; \quad \beta = \lambda_4(1-e) \quad \lambda_4 = k_4/k_1 \quad \text{and} \quad e = \delta_4/\ell\,. \tag{6}$$

Figure 2a, b shows the comparative curves of F^* and K^*, for exact and approximate expressions. In case of small displacement, one can conclude a good correlation. Because of the satisfactory precision, the following approximate expression of force displacement are used for our study:

$$F_{\text{HSLDS}} \simeq k_1\ell\left(\alpha^2\frac{W}{\ell}+\beta\frac{W^3}{\ell^3}\right). \tag{7}$$

Equation of Motion

Figure 3 shows a hinged-hinged Euler Bernoulli beam isolated by a HSLDS-AS isolator. The simplified mechanical model of the studied system derived from Fig. 1a is shown in Fig. 4. The constituted system is placed in an environment where the temperature varies uniformly considering an axial compression load P [25]. The moving load expression used in this paper is given by Eq. 8. δ is the Dirac delta function and V the velocity of moving load.

$$F(X,T) = F\delta(X-VT). \tag{8}$$

The thermal stress due to the thermal change is given by Eq. 9 [7].

$$\theta = EK\Delta\Theta, \tag{9}$$

where $\Delta\Theta$ is the uniform temperature variation and K the thermal expansion coefficient of the material. Thus, the total stress in the structure is [34]

$$\sigma = E\varepsilon = E\left(\frac{\partial U}{\partial X}+\frac{1}{2}\left(\frac{\partial W}{\partial X}\right)^2-\frac{\theta}{E}\right), \tag{10}$$

where E denotes the Young's modulus of the material. Considering Eqs. 7, 8, and 10 and applying the Newton second law of motion [34–36], the equations of motion are

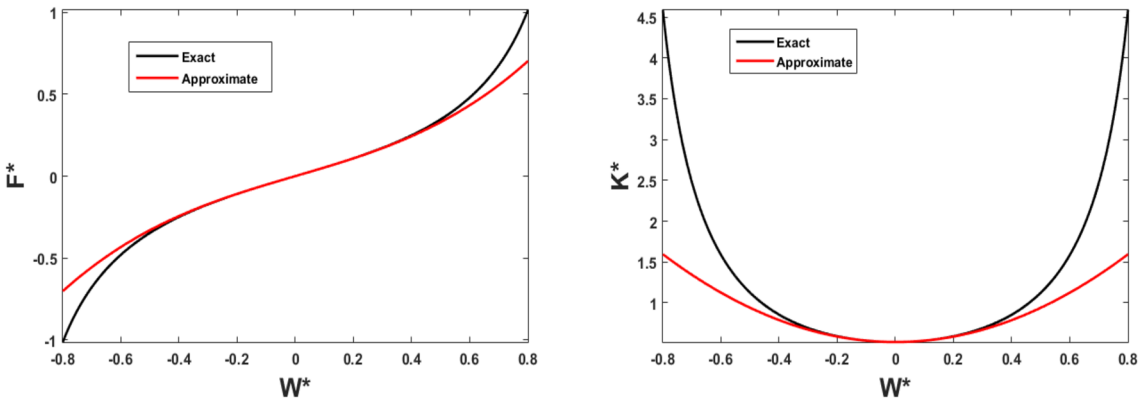

(a) (b)

Fig. 2 Comparison between the exact and approximate non-dimensional expressions: **a** force-displacement relationships and **b** stiffness of HSLDS system for $\lambda_4 = 1.0$ and $e = 0.5$

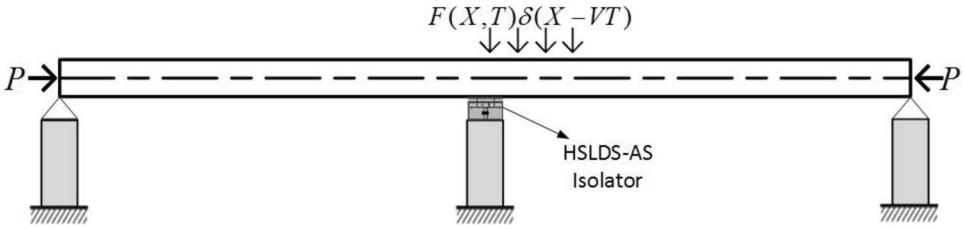

Fig. 3 Schematic mechanical model of a beam controlled by a HSLDS-AS

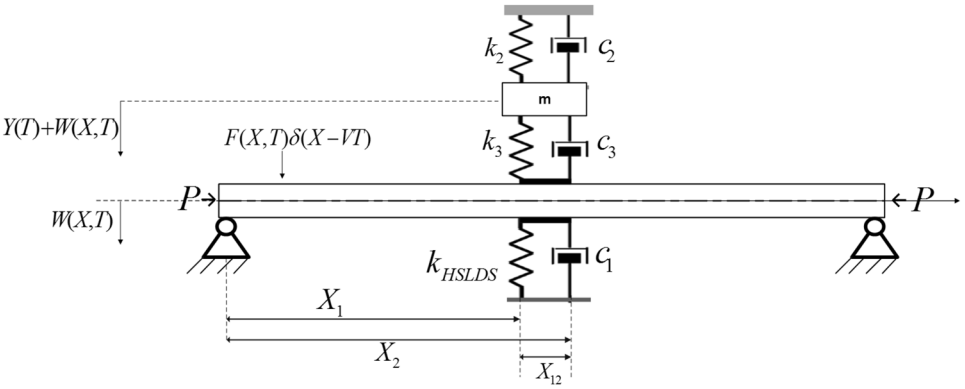

Fig. 4 Simplified mechanical model of the system

$$\begin{cases} \rho A\frac{\partial^2 W}{\partial T^2}+EI\frac{\partial^4 W}{\partial X^4}+\mathrm{c}\frac{\partial W}{\partial T}+(\mathrm{P}+\theta\mathrm{A})\frac{\partial^2 W}{\partial X^2}-\frac{EA}{2L}\frac{\partial^2 W}{\partial X^2}\int_0^L\left(\frac{\partial W}{\partial X}\right)^2\mathrm{d}X \\ +\frac{1}{X_{12}}\left(k_1\ell\left(\alpha^2\frac{W(X,T)}{\ell}+\beta\frac{\mathrm{W}^3}{\ell^3}\right)+c_1\frac{\mathrm{dW}}{\mathrm{d}T}-k_3Y-c_3\frac{\mathrm{dY}}{\mathrm{d}T}\right)G(X)=F\delta(X-VT)\ , \\ m\frac{\mathrm{d}^2Y}{\mathrm{d}T^2}+c_2\frac{\mathrm{dY}}{\mathrm{d}T}+m\frac{\partial^2 W}{\partial T^2}+c_2\frac{\partial W}{\partial T}+k_2W+k_2\mathrm{Y}+c_3\frac{\mathrm{dY}}{\mathrm{d}T}+k_3Y=0, \end{cases} \tag{11}$$

where $G(X)$ is defined by

$$G(X)=H\left(X-X_1\right)\ -H\left(X-X_2\right)=\begin{cases}0 & if \quad X\le X_1\\ 1 & if \quad X_1<X<X_2\\ 0 & if \quad X\ge X_2\end{cases}, \tag{12}$$

where $H(.)$ is a Heaviside function. $Y=Y(T)$ is the relative displacement of the auxiliary mass to the beam and T the time in second. Omitting the asterisk on V, the nondimensionalized equations of motion are

$$\begin{cases} \frac{\partial^2 w}{\partial t^2}+2\varepsilon\frac{\partial w}{\partial t}+v_f^2\frac{\partial^4 w}{\partial x^4}+(1+\theta_1)\frac{\partial^2 w}{\partial x^2}-\frac{v_1^2}{2}\frac{\partial^2 w}{\partial x^2}\int_0^1\left(\frac{\partial w}{\partial x}\right)^2\mathrm{d}x \\ +\frac{1}{x_{12}}\left(kw\ +\ \beta_0w^3+2\varepsilon_1\frac{\mathrm{dw}}{\mathrm{d}t}-\lambda_3y-2\varepsilon_3\frac{\mathrm{dy}}{\mathrm{d}t}\right)g(x)\ =\ f_0\delta(x-Vt)\ , \\ \mu\frac{\mathrm{d}^2y}{\mathrm{d}t^2}+\mu\frac{\partial^2 w}{\partial t^2}+2\varepsilon_2\frac{\partial w}{\partial t}+\lambda_2w+2(\varepsilon_2+\varepsilon_3)\frac{\mathrm{dy}}{\mathrm{d}t}+(\lambda_2+\lambda_3)y=\ 0 \end{cases} \tag{13}$$

where:

$$g(x)=H(x-x_1)\ -H(x-x_2)=\begin{cases}0 & If \quad x\le x_2\\ 1 & If \quad x_1<x<x_2\\ 0 & If \quad x\ge x_2\end{cases} \tag{14}$$

The dimensionless constants of these equations are

$$\begin{aligned} &t=T\sqrt{\frac{P}{\rho AL^2}};\quad v_f^2=\frac{EI}{PL^2};\quad v_1^2=\frac{EA}{P};\quad \theta_1=\frac{A\theta}{P};\\ &k=\frac{k_1L\alpha^2}{P}\quad;\beta_0=\frac{k_1L^3\beta}{P\ell^2};\quad \varepsilon=\frac{1}{2}c\sqrt{\frac{L^2}{\rho AP}}\\ &\varepsilon_1=\frac{c_1}{2}\sqrt{\frac{1}{\rho AP}};\quad \varepsilon_2=\frac{c_2}{2}\sqrt{\frac{1}{\rho AP}};\quad \varepsilon_3=\frac{c_3}{2}\sqrt{\frac{1}{\rho AP}};\\ &\lambda_2=\frac{k_2L}{P};\ \lambda_3=\frac{k_3L}{P};\quad \mu=\frac{m}{\rho AL}\\ &f_0=\frac{F}{P};\quad V^*=V\sqrt{\frac{P}{\rho A}};\quad x=\frac{X}{L};\quad y=\frac{Y}{L};\quad w=\frac{W}{L}\\ &x_1=\frac{X_1}{L}\ ;\quad x_2=\frac{X_2}{L}\ \text{and}\quad x_{12}=\frac{X_{12}}{L} \end{aligned} \tag{15}$$

Modal Equation

As indicated Wahrhaftig et al. [31, 32] the are many analytical procedures to solve this mathematical problem. To obtain the modal equations, Galerkin's technique is used. According to this method, the solution of the partial differential Eq. 13 for the hinged-hinged beam, is assumed to be in the form [33]

$$w(x,t) = \sum_{n=1}^{\infty} q_n(t)\sin(n\pi x). \tag{16}$$

With this, the modal equations are given by

$$\begin{cases} \ddot{q}_n(t) + 2\varepsilon_{cn}\dot{q}_n(t) + \omega_n^2 q_n(t) \\ +\Gamma_n q_n^3(t) - \alpha_{1n}y - \alpha_{2n}\dot{y} = 2f_0\sin(n\pi Vt) \\ \mu\ddot{y} + \beta_{2n}\dot{y} + \beta_{3n}y + \mu\ddot{q}_n(t) + 2\varepsilon_2\dot{q}_n(t) + \lambda_2 q_n(t) = 0 \end{cases}, \tag{17}$$

where

$$\begin{aligned} \alpha_{1n} &= \frac{2}{n\pi x_{12}}\left(\cos n\pi x_1 - \cos n\pi x_2\right)\lambda_3 \quad ; \\ \alpha_{2n} &= \frac{4}{n\pi x_{12}}\left(\cos n\pi x_1 - \cos n\pi x_2\right)\varepsilon_3 \\ \beta_{1n} &= \frac{2\left(1-(-1)^n\right)}{n\pi}\mu \quad ; \quad \beta_{2n} = 4(\varepsilon_2+\varepsilon_3)\frac{\left(1-(-1)^n\right)}{n\pi} \quad ; \\ \beta_{3n} &= \frac{2\left(1-(-1)^n\right)}{n\pi}\left(\lambda_2+\lambda_3\right) \end{aligned}$$

$$\begin{aligned} \omega_{bn}^2 &= (n\pi)^4 v_f^2 - (1+\theta_1)(n\pi)^2 \\ &\quad + \frac{k}{x_{12}}(x_2 - x_1 - \frac{1}{2\pi n}\left(\sin 2n\pi x_2 - \sin 2n\pi x_1\right)) \\ \Gamma_n &= \frac{1}{4}\Bigg(2(n\pi)^4 v_1^2 + \frac{\beta_0}{x_{12}}\left(3(x_2-x_1)\right. \\ &\quad \left. + \frac{\sin(4n\pi x_2) - \sin(4n\pi x_1)}{4n\pi} - 2\frac{\sin(2n\pi x_2) - \sin(2n\pi x_1)}{n\pi}\right) \\ \varepsilon_{cn} &= \varepsilon + \frac{\varepsilon_1}{x_{12}}\left(x_2 - x_1 - \frac{1}{2\pi n}\left(\sin 2\pi n x_2 - \sin 2\pi n x_1\right)\right). \end{aligned} \tag{18}$$

Dynamical Responses

Resonance Responses and Stability Analysis

The harmonic balance method offers an alternative for analysis of cases where steady state periodic solutions to the non-linear equation of motion are sought. Furthermore, due to the fact that simple HBM don't give the stability of the solution, the averaging method and the harmonic balance method [35, 36] are combined to analyse the stability of periodic solutions for the system at the first mode of vibration. According to this method we set

$$\begin{cases} q(t) = a_1(t)\cos\omega t + a_2(t)\sin\omega t \\ y(t) = b_1(t)\cos\omega t + b_2(t)\sin\omega t \end{cases}, \tag{19}$$

where $\omega = \pi v$ is the excitation frequency due to the moving load. Substituting Eq. 19 into Eq. 17 for $n = 1$, and equating the coefficients proportional to, $\cos\omega t$ and $\sin\omega t$ we obtain with the conditions $\ddot{a}_1 = \ddot{a}_2 = \ddot{b}_1 = \ddot{b}_2 = 0$,

$$\begin{aligned} &2\varepsilon_c\dot{a}_1 + 2\omega\dot{a}_2 - \alpha_2\dot{b}_1 + a_1\left(\omega_b^2 - \omega^2 + \tfrac{3}{4}\Gamma A^2\right) \\ &+2\varepsilon_c\omega a_2 - \alpha_1 b_1 - \alpha_2\omega b_2 = 0 \\ &2\omega\dot{a}_1 + 2\varepsilon_c\dot{a}_2 - \alpha_2\dot{b}_2 + a_2\left(\omega_b^2 - \omega^2 + \tfrac{3}{4}\Gamma A^2\right) \\ &-2\varepsilon_c\omega a_1 + \alpha_2\omega b_1 - \alpha_1 b_2 = 2f_0 \\ &2\varepsilon_2\dot{a}_1 + 2\mu\omega\dot{a}_2 + \beta_2\dot{b}_1 + 2\beta_1\omega\dot{b}_2 + \left(\lambda_1 - \mu\omega^2\right)a_1 \\ &+2\varepsilon_2\omega a_2 + \left(\beta_3 - \beta_1\omega^2\right)b_1 + \beta_2\omega b_2 = 0 \\ &-2\mu\omega\dot{a}_1 + 2\varepsilon_2\dot{a}_2 - 2\beta_1\omega\dot{b}_1 + \beta_2\dot{b}_2 - 2\varepsilon_2\omega a_1 \\ &+\left(\lambda_1 - \mu\omega^2\right)a_2 - \beta_2\omega b_1 + (\beta_3 - \beta_1\omega^2)b_2 = 0. \end{aligned} \tag{20}$$

To derive the amplitude responses equations let us set $a_1 = a\sin\varphi_1; a_2 = a\cos\varphi_1; b_1 = b\sin\varphi_2$ and $b_2 = b\cos\varphi_2$. Where a and φ_1 are amplitude and phase angle of $q(t)$. In the same way, b and φ_2 are amplitude and phase angle of $y(t)$. At the stationary state, we have $\dot{a}_1 = \dot{a}_2 = \dot{b}_1 = \dot{b}_2 = 0$, the amplitudes a and b satisfies the following non-linear equations:

$$\begin{cases} 4f_0^2 P_0(\omega) - a^2\left(P_1(\omega,a) + P_2(\omega,a) + P_3(\omega) + P_4(\omega) + P_5(\omega,a)\right) = 0 \\ a^2 P_6(\omega) = b^2 P_0(\omega) \end{cases} \tag{21}$$

$$tg(\varphi_1) = -\frac{\left(2\varepsilon_c(\beta_3 - \beta_1\omega^2) + \tau_{11}\right) + \chi_1\left(4\omega^2\varepsilon_c\beta_2 - \tau_{12}\right)}{\frac{1}{\omega}(\tau_{22} + \tau_{12}) + \chi_1\omega\left(2\beta_2\left(\omega_b^2 - \omega^2 - \frac{3}{4}\Gamma a^2\right) + \tau_{11}\right)} \tag{22}$$

$$tg(\varphi_2) = \frac{-\left(2\tau_{21} + \alpha_2\left(\lambda_2 - \mu\omega^2\right)\right) + \chi_2\left(\tau_{22} - 4\omega^2\varepsilon_c\beta_2 - 2\omega^2\alpha_2\varepsilon_2\right)}{\frac{1}{\omega}\left(\tau_{22} - 4\omega^2\varepsilon_c\beta_2 + \alpha_1\left(\lambda_2 - \mu\omega^2\right)\right) + 2\omega\chi_2\left(\tau_{21} + \varepsilon_2\alpha_1\right)}, \tag{23}$$

where:

$$\begin{aligned}
P_0(\omega) &= \left(\left(\beta_3 - \beta_1\omega^2\right)^2 + 4\omega^2\beta_2^2\right)\\
P_1(\omega, a) &= \left(\left(\omega_b^2 - \omega^2 + \frac{3}{4}\Gamma a^2\right)\left(\beta_3 - \beta_1\omega^2\right)\right.\\
&\quad \left.+\alpha_1\left(\lambda_2 - \mu\omega^2\right)\right)^2\\
P_2(\omega, a) &= 4\omega^2\left(\beta_2\left(\omega_b^2 - \omega^2 + \frac{3}{4}\Gamma a^2\right) + \alpha_1\varepsilon_2\right)^2\\
P_3(\omega) &= \omega^2\left(2\varepsilon_c\left(\beta_3 - \beta_1\omega^2\right) + \alpha_2\left(\lambda_2 - \mu\omega^2\right)\right)^2\\
P_4(\omega) &= 4\omega^4\left(2\varepsilon_c\beta_2 + \alpha_2\varepsilon_2\right)^2\\
P_5(\omega, a) &= 4\omega^2\left(\alpha_2\left(\omega_b^2 - \omega^2 + \frac{3}{4}\Gamma a^2\right) - 2\varepsilon_c\alpha_1\right)\\
&\quad \times\beta_2\left(\lambda_2 - \mu\omega^2\right) - \varepsilon_2\left(\beta_3 - \beta_1\omega^2\right)\Big)\\
P_6(\omega) &= \left(\lambda_2 - \mu\omega^2\right)^2 + 4\omega^2\varepsilon_2^2\\
\chi_1 &= \frac{2\beta_2}{\left(\beta_3 - \beta_1\omega^2\right)} \quad ; \quad \tau_{11} = 2\alpha_1\varepsilon_2 + \alpha_2\left(\lambda_2 - \mu\omega^2\right)\\
\tau_{12} &= -2\omega^2\alpha_2\varepsilon_2 + \alpha_1\left(\lambda_2 - \mu\omega^2\right) \quad ; \quad \chi_2 = \frac{2\varepsilon_2}{\left(\lambda_2 - \mu\omega^2\right)}\\
\tau_{21} &= \beta_2\left(\omega_b^2 - \omega^2 + \frac{3}{4}\Gamma a^2\right) + \varepsilon_c\left(\beta_3 - \beta_1\omega^2\right) \quad ;\\
\tau_{22} &= \left(\omega_b^2 - \omega^2 + \frac{3}{4}\Gamma a^2\right)\left(\beta_3 - \beta_1\omega^2\right).
\end{aligned} \tag{24}$$

Stability Analysis

For the stability analysis, we set $a_i = a_{i0} + \delta a_i$ and $b_i = b_{i0} + \delta b_i\,(i = 1, 2)$; where δa_i and δb_i are small perturbations. Expanding for this small perturbations and keeping linear terms, one obtains the following equations around the stationary harmonic oscillatory state amplitudes a_{i0} and b_{i0}

$$\delta\dot{r} = A\delta r, \tag{25}$$

where

$$\delta r = (\delta a_1; \delta a_2; \delta b_1; \delta b_2), \tag{26}$$

$$A = M.D, \tag{27}$$

$$M = \begin{bmatrix} 2\varepsilon_c & 2\omega & -\alpha_2 & 0\\ -2\omega & 2\varepsilon_c & 0 & -\alpha_2\\ 2\varepsilon_2 & 2\mu\omega & \beta_2 & 2\beta_1\omega\\ -2\mu\omega & 2\varepsilon_2 & -2\beta_1\omega & \beta_2 \end{bmatrix}^{-1}, \tag{28}$$

$$\begin{aligned}
D_{11} &= D_{22} = -\left(\omega_b^2 - \omega^2 + \frac{3}{2}\Gamma\left(2a_{20}^2 + A^2\right);\right.\\
D_{21} &= -\left(\frac{3}{2}\Gamma a_{10}a_{20} - 2\varepsilon_c\omega\right)\\
D_{12} &= -\left(\frac{3}{2}\Gamma a_{10}a_{20} + 2\varepsilon_c\omega\right);\\
D_{13} &= D_{24} = \alpha_1; D_{14} = -D_{23} = \alpha_2\omega\\
D_{31} &= D_{42} = -\left(\lambda_1 - \mu\omega^2\right); D_{41} = -D_{32} = 2\varepsilon_2\omega\\
D_{33} &= D_{44} = -\left(\beta_3 - \beta_1\omega^2\right); D_{43} = -D_{34} = \beta_2\omega.
\end{aligned} \tag{29}$$

The eigenvalues (s) is given by solving

$$\mathrm{Det}(A - s \times I) = 0. \tag{30}$$

The stability of the stationary oscillatory state solutions depends on the eigenvalues of the Jacobian matrix A. Then, the solution is stable if a eigenvalues have a negative real parts.

Force transmissibility

At the first mode vibration, the expression of the force transmitted to the isolator support is

$$f_t(t) = 2\varepsilon_c\dot{q}(t) + \omega^2 q(t) + \Gamma q^3(t) - \alpha_1 y - \alpha_2\dot{y}\,. \tag{31}$$

The force transmissibility when the dimensionless excitation force is $f_e(t) = 2f_0\sin(\pi\nu t)$ is given by [20]

$$T_f = \left|\frac{f_t(t)}{f_e(t)}\right|. \tag{32}$$

By inserting the analytical solution at first mode in Eq.32, T_f is given as follows

$$T_f = \frac{1}{2f_0}\sqrt{a^2\kappa_1 + b^2\kappa_2 + 2ab\sqrt{\kappa_1\kappa_2}\cos(\phi_2 - \phi_1)}, \tag{33}$$

with

$$\begin{aligned}
tg(\phi_1) &= \frac{-\left(\omega^2 + \frac{3}{4}\Gamma a^2\right) + 2\varepsilon_c\omega tg(\varphi_1)}{\left(\omega^2 + \frac{3}{4}\Gamma a^2\right)tg(\varphi_1) + 2\varepsilon_c\omega}\\
tg(\phi_2) &= \frac{-\alpha_1 + \alpha_2\omega tg(\varphi_2)}{\alpha_1 tg(\varphi_2) + \alpha_2\omega},
\end{aligned} \tag{34}$$

Table 1 Physical parameters and material properties

Parameters	Symbols	Values	Units
Density	ρ	7781.0	kg/m^3
Length	L	24.072	m
young's modulus	E	210.0	GPa
Area of cross section	A	0.03	m^2
Thermal expansion coefficient	K	10^{-5}	^{o}C^{-1}
Axial load	P	130.0	KN
Area moment of inertia	I	3.0×10^{-4}	m^4
HSLDS Rod length	l	0.35	m

$$\kappa_1 = \left(\left(\omega^2 + \frac{3}{4}\Gamma a^2\right)^2 + 4\varepsilon_c^2\omega^2\right),$$
$$\kappa_2 = \left(\alpha_1^2 + \omega^2\alpha_2^2\right). \tag{35}$$

The absolute force transmissibility of HSLDS-AS is defined as follow

$$T_{f_m} = 20\log(T_f). \tag{36}$$

Study Parameters Selection

In this study, the dimensionless material properties of the beam and fixed parameters of HSLDS-AS are chosen from Table 1. The current beam can be considered as a idealist modified deck beam [30] a cable stayed bridge. In the following analysis the non-dimensional transversal moving load magnitude is $f_0 = 0.05$ and the damping coefficient of the beam $\varepsilon = 0.05$. By using Eq. 15, we have the dimensionless values $v_f^2 = 0.8866$ and $v_1^2 = 50319.2308$. Taking into account Eq. 9 we have:

$$\beta_0 = \frac{L^2}{\ell^2}\frac{\lambda_4(1-e)}{1-2\lambda_4 e}k, \tag{37}$$

where k is the linear spring coefficient and β_0 the non-linear spring coefficient of the HSLDS isolator. For a fixed values of L, ℓ, λ_4 and e, Eq. 37 shows that β_0 and k are directly proportional and have the same influences on the system; therefore, the analysis of one of these parameters will be sufficient. Furthermore, for a performant control [24], $\lambda_4 e$ must be less than 0.5 so that the term α^2 is close to zero. In the present analysis, the default values of isolator parameters are $\varepsilon_1 = 2.5$; $\lambda_2 = 100.0$; $\lambda_3 = 10.0$; $\lambda_4 = 1.0$; $\varepsilon_2 = \varepsilon_3 = 1.0$; $e = 0.4$; $\mu = 0.003$; $k = 0.2$. For the localization of HSLDS-AS isolator the default values are $x_1 = 0.475$ and $x_2 = 0.525$. To study the performance of the isolator, we focused on the effect of ε_1, ε_2, ε_3, λ_2, λ_3, k, x_1, x_2 and x_{12} (thickness over which the isolator is in contact with the beam). In order to study the effect of temperature on the beam, with and without control, we set the variation of the non-dimensional thermal stress θ_1 in the interval [– 20.03; + 20.03], which corresponds to dimensional temperature change domain [−39.80 °C; + 39.80 °C].

Results and Discussion

We describe the effect of location, parameters of the HSLDS-AS and thermal variation on natural frequencies, amplitude curve and force transmissibility of the system.

Natural Frequency Study

In order to clarify the effect of the temperature rise on the dimensionless frequency, we consider a frequency variation factor as [34]

$$R_\omega = \frac{\omega_n(\theta_1 \neq 0) - \omega_n(\theta_1 = 0)}{\omega_n(\theta_1 = 0)}. \tag{38}$$

$\omega_n(\theta_1 \neq 0)$ and $\omega_n(\theta_1 = 0)$ are the natural frequencies when θ_1 is different from zero and equal to zero respectively.

In Fig. 5, we note that for the controlled beam, increase in the temperature causes the natural frequency to decrease and decreasing the temperature increases the natural frequency. Moreover, the thermal effect is more obvious at the first mode and the effect of thermal change on natural frequency becomes less with the increase of the order's mode. With the uncontrolled beam, the same result was found and the same conclusion is drawn. The same effects on natural frequencies was observed in other studies [12, 16]. The influence of the linear spring coefficient, thickness of control's force action

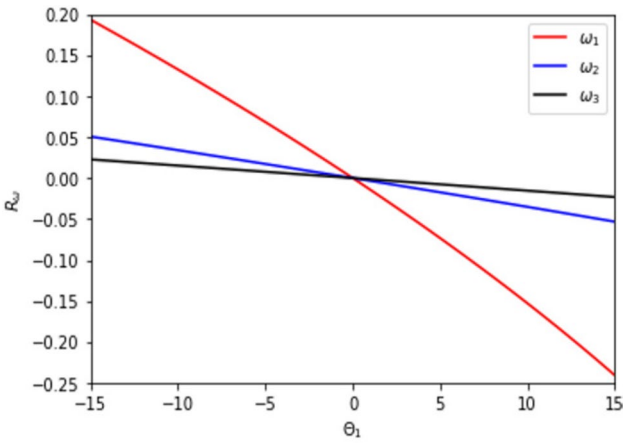

Fig. 5 Temperature effect on the first three natural frequencies of controlled and uncontrolled beam

x_{12} and the position of the HASLDS-AS Isolator on natural frequencies was investigated. By analysing the results in Table 2 with $\theta_1 = 0$, we conclude that:

(1) Changing the HSLDS-AS positions from the left-end to the mid-span of the beam results in an increase of the values of natural frequency of the system.
(2) Increasing the value of the thickness of action of the control, result in a decrease of the natural frequencies.
(3) Increasing of the linear spring coefficient increase the natural frequencies.

Amplitude Curves and Force Transmissibility

Numerical solutions are obtained by solving the equation Eq. 17 using the fourth order Runge–Kutta algorithm. Fig. 6 show the amplitude and force transmissibility curves for two types of solutions. by comparing these curves, we therefore end up with a validation of the results obtained with HBM.

Figure 7 illustrates the amplitude responses and force transmissibility curves for default parameters. The peak amplitude is reduced close to 33% and the peak transmissibility reduced close to 50%. Then, the isolator is very performant for amplitude control and absolute force transmissibility reduction.

Table 2 First natural frequencies for different values of location and linear spring coefficient of the HSLDS-AS Isolator

	ω_1					
k	$x_1 = 0.275$	$x_1 = 0.475$	$x_1 = 0.675$	$x_1 = 0.24$	$x_1 = 0.44$	$x_1 = 0.64$
	$x_2 = 0.325$	$x_2 = 0.525$	$x_2 = 0.725$	$x_2 = 0.36$	$x_2 = 0.56$	$x_2 = 0.76$
	$x_2 - x_1 = 0.05$	$x_2 - x_1 = 0.05$	$x_2 - x_1 = 0.05$	$x_2 - x_1 = 0.12$	$x_2 - x_1 = 0.12$	$x_2 - x_1 = 0.12$
0.02	8.746	8.746	8.746	8.746	8.7467	8.746
0.20	8.747	8.747	8.747	8.748	8.749	8.748
10.00	8.783	8.803	8.783	8.835	8,881	8,835
20.00	8.821	8.860	8.821	8.923	9.013	8.923
100.00	9.112	9.299	9.112	9.598	10.011	9.598

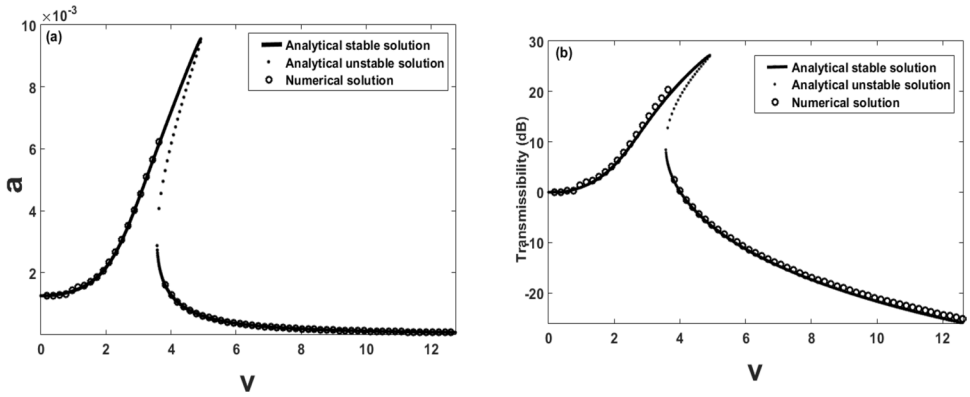

Fig. 6 **a** Analytical and numerical Amplitude responses of the structure with HSLDS-AS. **b** Analytical and numerical Absolute force transmissibility of the system with HSLDS-AS. Solid line denotes the stable responses and pointed line denotes the unstable responses for defaults parameters

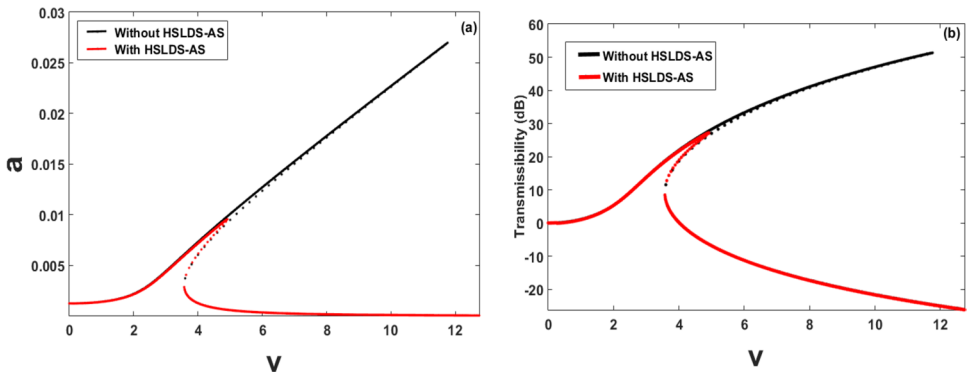

Fig. 7 **a** Amplitude responses of the beam without and with HSLDS-AS. **b** Absolute force transmissibility. Solid line denotes the stable responses and pointed line denotes the unstable responses for defaults parameters

Figure 8 describes the amplitude responses and force transmissibility curves with linear spring stiffness k. Theses two curves depend strongly on the values of k. Increasing of k causes the hardening behaviour and peak transmissibility to increase. This is justified By Eq. 37. The least values of this parameter are beneficial for a performant control or isolation. Especially the isolator can be ideal when the linear spring stiffness is set to zero and we have a quasi zero stiffness isolator with auxiliary system (QZS-AS).

Figure 9 shows the dynamics behaviors, by using nonlinear amplitude response and absolute force transmissibility curves with damping coefficient ε_1. It is pointed out that, at the low velocity, increasing the value of damping ratio causes the peak amplitude and transmissibility to decrease. But, this result is opposite at the high velocity. Then, the greatest values of this parameters is beneficial for a best isolation or control in case of low velocity.

Figure 10 explains the amplitude response and absolute force transmissibility curves with damping ratios ε_2 and ε_3. Increasing of these two parameters reduce the peak amplitude of the system. At the low velocity, increasing these parameters cause the force transmissibility to decrease, their effects are opposite at high velocity. It is convenient to use a practical value of these parameters. This result is opposite to the case of displacement transmissibility as studied by [24]; in the present case, effect of ε_3 is similar to that of ε_1 and is more notable than ε_2.

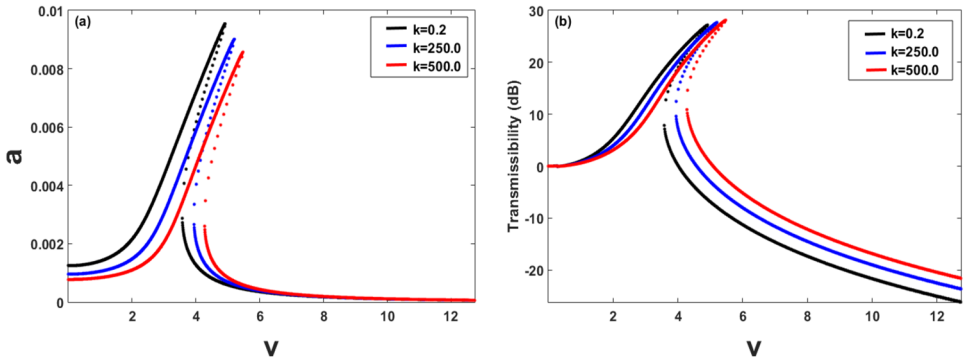

Fig. 8 Effect of k on: **a** amplitude responses of the isolated beam. **b** Absolute force transmissibility. Solid line denotes the stable responses and pointed line denotes the unstable responses for defaults parameters

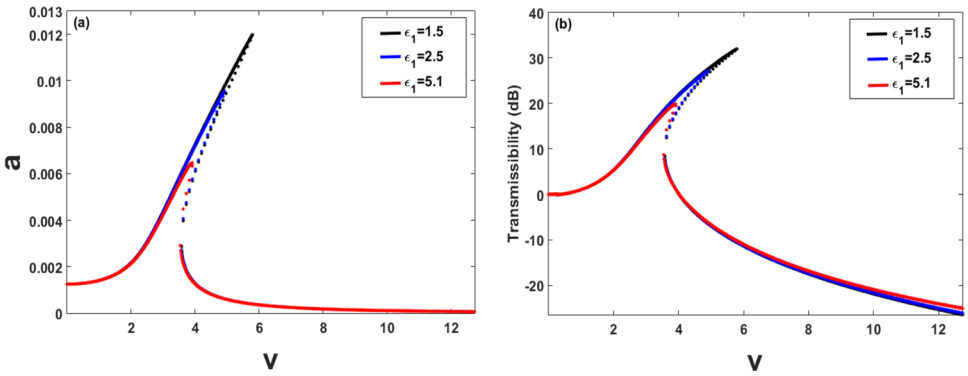

Fig. 9 Effect of ε_1 on: **a** Amplitude responses of the isolated beam. **b** Absolute force transmissibility. Solid line denotes the stable responses and pointed line denotes the unstable responses for defaults parameters

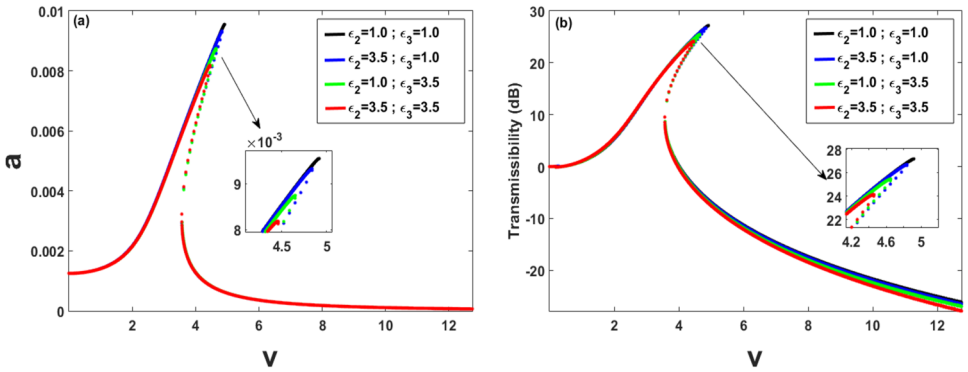

Fig. 10 Effect of ε_2 and ε_3 on: **a** amplitude responses of the isolated beam. **b** Absolute force transmissibility. Solid line denotes the stable responses and pointed line denotes the unstable responses for defaults parameters

The amplitude and absolute force transmissibility curves with different values of stiffness ratios λ_2 and λ_3 are presented in Fig. 11. For a smallest value of λ_3, increasing λ_2 reduce the peak amplitude and absolute force transmissibility. Also we remarks that, peak amplitude and transmissibility increase as λ_3 increase. Especially, when λ_2 is too great, increasing λ_3 may change the peak frequency and create a discontinuity in absolute force transmissibility as shown in Fig. 11b. This discontinuity is due to instability in dynamics of auxiliary mass. One can conclude that these last two stiffness must be moderate, great λ_2 and small λ_3 is recommended for a performant isolator. In another these effect are the same for low and high frequency.

Effect of x_{12} is depicted on Fig. 12. Since, at low velocity, increasing this value contribute to decrease the peak amplitude and absolute force transmissibility. Furthermore, at high velocity, the effect is opposite to the case of low amplitude. To be realistic for a practical application, a smallest value of x_{12} must be chosen.

Figures 13 and 14 displays the effect of thermal change in amplitude responses and absolute force transmissibility. It can be observed that, for the uncontrolled and controlled beam, decrease temperature increase the hardening behaviour and causes the amplitude curves to bend right. In another, the reduction of peak amplitude with temperature rise is more obvious for controlled beam (Fig. 13b). Besides, when the temperature increases, the transmissibility increase

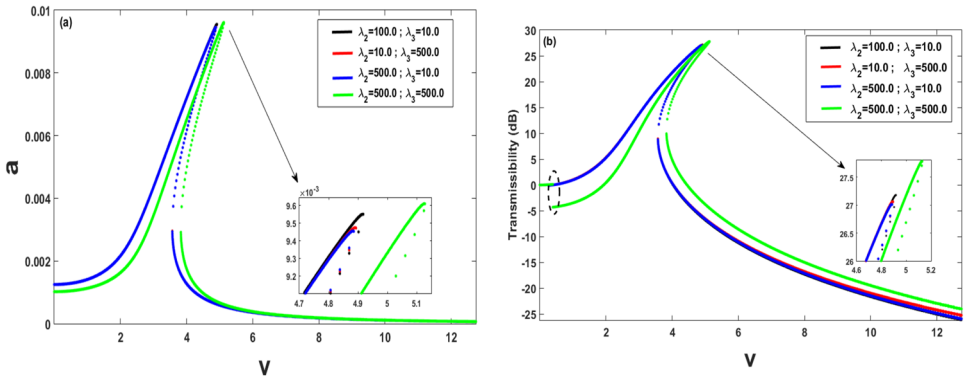

Fig. 11 Effect of λ_2 and λ_3 on: **a** amplitude responses of the isolated beam. **b** Absolute force transmissibility. Solid line denotes the stable responses and pointed line denotes the unstable responses for defaults parameters

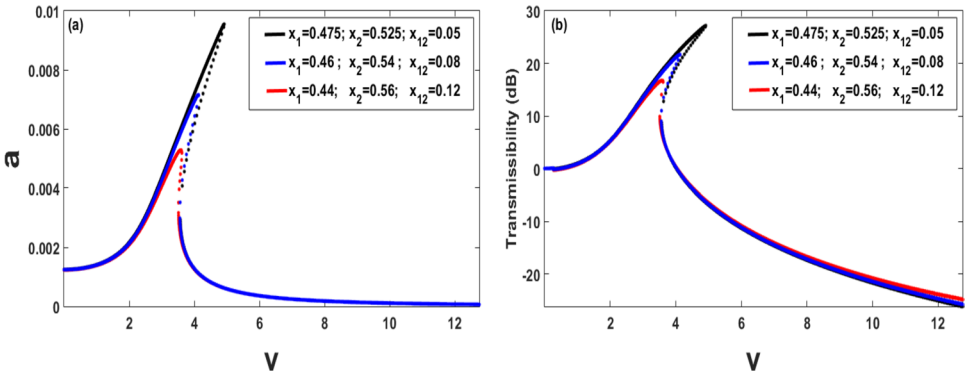

Fig. 12 Effect of x_{12} on: **a** Amplitude responses of the isolated beam. **b** Absolute force transmissibility. Solid line denotes the stable responses and pointed line denotes the unstable responses for defaults parameters

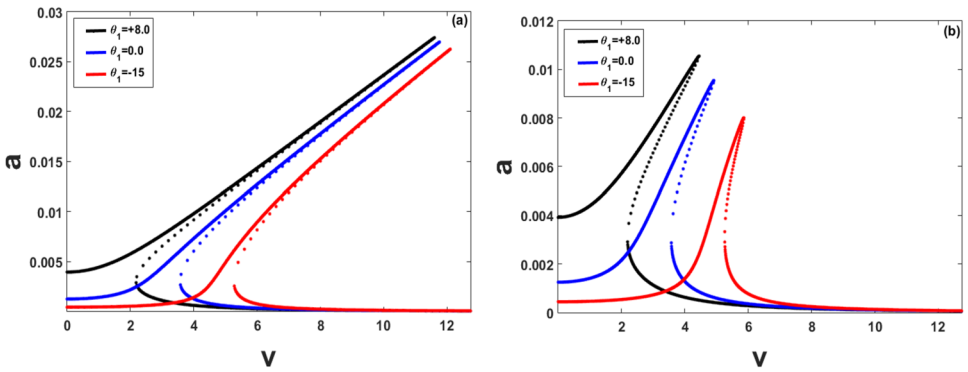

Fig. 13 Amplitude responses of the beam for different values of θ_1: **a** without HSLDS-AS **b** and With HSLDS-AS for default parameters. Solid line denotes the stable responses and pointed line denotes the unstable responses

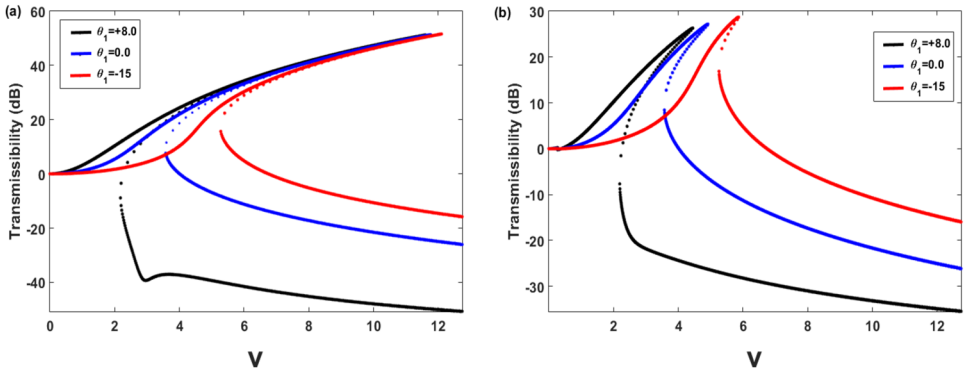

Fig. 14 Absolute force transmissibility for different values of θ_1: **a** Without HSLDS-AS **b** and With HSLDS-AS for default parameters. Solid line denotes the stable responses and pointed line denotes the unstable responses

at low velocity and decrease at high velocity. This means that the force transmitted to substructure increase with decreasing in temperature (Fig. 14). We concluded that, the temperature do not only reduce or increase the natural frequency or amplitude of a structure but, this variation affect consequently the transmissibility of the structure and can cause damage on the supports due to the redundant force transmitted due to temperature variation. This results must be taking on to account when designing isolator or supports.

Conclusion

The dynamic of a hinged-hinged beam controlled by an HSLDS-AS isolator under mechanical and thermal loads, has been investigated. The second laws of Newton with the laws of behaviour are used to establish the non-linear equations of the motion. The partial differential equations established via Garlekin method, are evaluated via the technique of balance harmonics coupled to average method and validate via RK4 method. The action of the isolator parameters and thermal effect on vibration characteristics of structure are analysed through a parametric study. It is shown that:

(1) The controller is efficient for a large value of the application thickness of the isolator force.
(2) The great values of vertical damping coefficient and low value of linear spring coefficient of the HSLDS isolator are advantageous for reducing the peak amplitude and transmissibility. In another, for a performant isolator the linear spring coefficient value must be very small and ideally set to zero.
(3) Some parameters attached to auxiliary mass can be benefit or not for a performant control, but a convenient choice is recommended.
(4) For the controlled and uncontrolled beam, a rise of temperature does decrease natural frequencies and increase the transmissibility (vice-versa).

Although, temperature effects are more appreciable at the first mode and can mask the failure detection base on natural frequencies and peak amplitude,thermal variations, have a very significant impact on the transmitted force, which can either create additional stresses in the supports or affect the performance of the isolation system. This results should be attract the attention of designers of damage detection and isolation systems.

Acknowledgements The authors thank the Foundation for financial support to this work which was completed partially throughout the research visit of Pr. Nana Nbendjo at the University of Kassel in Germany.

References

1. Chen Z, Xu Y, Wang X (2011) SHMS-based fatigue reliability analysis of multi loading suspension bridges. J Struct Eng 138:299–307
2. Chen Z, Xu Y-L, Li Q, Wu D-J (2011) Dynamic stress analysis of long suspension bridges under wind, railway, and highway loadings. Bridge Eng 16:383–391
3. Yi TH, Li HN, Gu M (2013) Wavelet based multi-step filtering method for bridge health monitoring using GPS and accelerometer. SSS 11:331–348
4. Maleki S, Maghsoudi-Barmi A (2016) Effects of concurrent earthquake and temperature loadings on cable stayed bridges. Int J Struct Stab Dyn 16:1550020
5. Anague Tabejieu LM, Nana Nbendjo BR, Filatrella G, Woafo P (2017) Amplitude stochastic response of Rayleigh beams to randomly moving loads. Nonlinear Dyn 89:925–937
6. Sahoo PR, Barik M (2021) Dynamic response of stiffened bridge decks subjected to moving loads. J Vib Eng Technol. https://doi.org/10.1007/s42417-021-00344-4
7. Wu GY (2005) The analysis of dynamic instability and vibration motions of a pinned beam with transverse magnetic fields and thermal loads. J Sound Vib 284:343–360
8. Wu GY (2007) The analysis of dynamic instability on the large amplitude vibrations of a beam with transverse magnetic fields and thermal loads. J Sound Vib 302:167–177
9. Manoach E, Ribeiro P (2004) Coupled, thermoelastic, large amplitude vibrations of Timoshenko beams. Int .J Mech Sci 46:1589–1606

10. Ribeiro P, Manoach E (2005) The effect of temperature on the large amplitude vibrations of curved beams. J Sound Vib 285:1093–1107
11. Guo XX, Wang ZM, Wang Y, Zhou YF (2009) Analysis of the coupled thermoelastic vibration for axially moving beam. J Sound Vib 325:597–608
12. Ghayesh MH, Kazemirad S, Darabi MA, Woo P (2020) Thermo-mechanical non-linear vibration analysis of a spring mass-beam system. Arch Appl Mech 82:317–331
13. Warminska A, Manoach E, Warminski J (2014) Nonlinear dynamics of a reduced multimodal Timoshenko beam subjected to thermal and mechanical loadings. Meccanica 49:1775–1793
14. Warminska A, Manoach E, Warminski J, Samborski S (2015) Regular and chaotic oscillations of a Timoshenko beam subjected to mechanical and thermal loadings. Cont. Mech Therm 27:719–737
15. Xia Y, Chen B, Weng S, Ni YQ, Xu YL (2012) Temperature effect on vibration properties of civil structures: a literature review and case studies. J Civ Struct Health Monit 2:29–46
16. Ibrahim RA (2008) Recent advances in nonlinear passive vibration isolators. J Sound Vib 314:71–452
17. Shaw AD, Neild SA, Wagg DJ, Weaver PM, Carrella A (2013) A nonlinear spring mechanism incorporating a bistable composite plate for vibration isolation. J Sound Vib 332:6265–6275
18. Huang XC, Liu XT, Hua HX (2014) On the characteristics of an ultra-low frequency nonlinear isolator using sliding beam as negative stiffness. J Mech Sci Technol 28:813–822
19. Huang XC, Liu XT, Sun JY, Zhang ZY, Hua HX (2014) Effect of the system imperfections on the dynamic response of a high-static-low-dynamic stiffness vibration isolator. Nonlinear Dyn 76:1157–1167
20. Carrella A, Brennan MJ, Kovacic I, Waters TP (2009) On the force transmissibility of a vibration isolator with quasi-zero stiffness. J Sound Vib 322:707–717
21. Carrella A, Friswell MI, Zotov A, Ewins DJ, Tichonov A (2009) Using nonlinear springs to reduce the whirling of a rotating shaft. Mech Syst Signal Process 23:2228–2235
22. Kovacic I, Brennan MJ, Waters TP (2008) A study of a nonlinear vibration isolator with a quasi-zero stiffness characteristic. J Sound Vib 315:700–711
23. Lan CC, Yang SA, Wu YS (2014) Design and experiment of a compact quasi-zero-stiffness isolator capable of a wide range of loads. J Sound Vib 333:4843–4858
24. Liu C, Yu K (2018) A high-static-low-dynamic-stiffness vibration isolator with the auxiliary system. Nonlinear Dyn 94:1549–1567
25. Wahrhaftig ADM, Brasil RMLRDF, Groba TB, Rocha LML, Balthazar JM, Nascimento LSMSC (2020) Resonance of a rotary machine support beam considering geometric stiffness. J Theoret Appl Mech 58(4):1023–1035. https://doi.org/10.15632/jtam-pl/126681
26. Thakadu K, Li KA (2021) Passive vibration isolator integrated a dynamic vibration absorber with negative stiffness spring. J Vib Eng Technol. https://doi.org/10.1007/s42417-021-00364-0
27. Bhowmik K, Debnath N (2021) On stochastic design of negative stiffness integrated tuned mass damper (NS-TMD). J Vib Eng Technol. https://doi.org/10.1007/s42417-021-00356-0
28. Abbasi A, Khadem SE, Bab Saeed (2016) Vibration control of a continuous rotating shaft employing high-static low-dynamic stiffness isolators. JVC 24:760–783
29. Sonfack Bouna H, Nana Nbendjo BR, Woafo P (2020) Isolation performance of a quasi-zero stiffness isolator in vibration isolation of a multi-span continuous beam bridge under pier base vibrating excitation. Nonlinear Dyn 100:1125–1141
30. Karoumi R (1998) Response of cable-stayed and suspension bridges to moving vehicles: analysis methods and practical modeling techniques. PhD dissertation, Royal institute of technology, SE 10044 Stockholm, Sweden
31. Wahrhaftig ADM, Magalhães KMM, Brasil RMLRF, Murawski Krzysztof (2021) Evaluation of mathematical solutions for the determination of buckling of columns under self-weight. J Vib Eng Technol 9:733–749. https://doi.org/10.1007/s42417-020-00258-7
32. Wahrhaftig ADM, Brasil RMLRF (2017) Vibration analysis of mobile phone mast system by Rayleigh method. Appl Math Model 42:330–345. https://doi.org/10.1016/j.apm.2016.10.020
33. Wahrhaftig ADM, Silva MAD, Brasil RMLRF (2019) Analytical determination of the vibration frequencies and buckling loads of slender reinforced concrete towers. Latin Am J Solids Struct 16:5. https://doi.org/10.1590/1679-78255374
34. Zhao Y, Huang C (2018) Temperature effects on nonlinear vibration behaviors of euler-bernoulli beams with different boundary conditions. Shock Vib 6:1–11
35. Nayfeh AH, Mook DT (1979) Nonlinear oscillations. Wiley, New York
36. Hayashi C (1964) Nonlinear oscillations in physical systems. Mc Graw-Hill Inc, New York